Max-Planck-Institut
für Meteorologie

MAX-PLANCK-GESELLSCHAFT

International Max Planck Research School
on Earth System Modelling

The influence of plant nitrogen availability on the global carbon cycle and N_2O emissions

Bikash Ranjan Parida

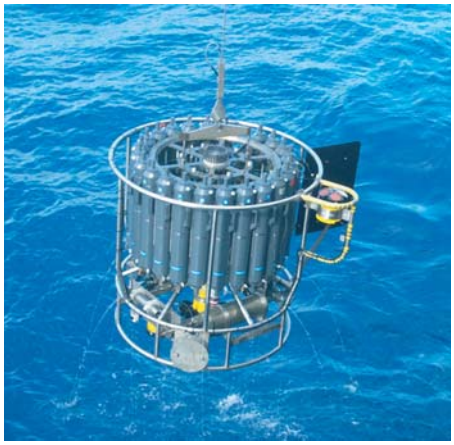

Berichte zur Erdsystemforschung 92/2011

Reports on Earth System Science

Hinweis

Die Berichte zur Erdsystemforschung werden vom Max-Planck-Institut für Meteorologie in Hamburg in unregelmäßiger Abfolge herausgegeben.

Sie enthalten wissenschaftliche und technische Beiträge, inklusive Dissertationen.

Die Beiträge geben nicht notwendigerweise die Auffassung des Instituts wieder.

Die "Berichte zur Erdsystemforschung" führen die vorherigen Reihen "Reports" und "Examensarbeiten" weiter.

Notice

The Reports on Earth System Science are published by the Max Planck Institute for Meteorology in Hamburg. They appear in irregular intervals.

They contain scientific and technical contributions, including Ph. D. theses.

The Reports do not necessarily reflect the opinion of the Institute.

The "Reports on Earth System Science" continue the former "Reports" and "Examensarbeiten" of the Max Planck Institute.

Anschrift / Address

Max-Planck-Institut für Meteorologie
Bundesstrasse 53
20146 Hamburg
Deutschland

Tel.: +49-(0)40-4 11 73-0
Fax: +49-(0)40-4 11 73-298
Web: www.mpimet.mpg.de

Layout:

Bettina Diallo, PR & Grafik

Titelfotos:
vorne:
Christian Klepp - Jochem Marotzke - Christian Klepp
hinten:
Clotilde Dubois - Christian Klepp - Katsumasa Tanaka

Berichte zur Erdsystemforschung 92/2011

The influence of plant nitrogen availability on the global carbon cycle and N_2O emissions

Bikash Ranjan Parida

aus Bhadrak, India

Hamburg 2011

Reports on Earth System Science 92/2011

ISSN 1614-1199

Bikash Ranjan Parida
Max-Planck-Institut für Meteorologie
Bundesstrasse 53
20146 Hamburg
Germany

Als Dissertation angenommen
vom Department Geowissenschaften der Universität Hamburg

auf Grund der Gutachten von
Prof. Dr. Martin Claussen
und
Dr. Jens Kattge

Hamburg, den 7. Juni 2011
Prof. Dr. Jürgen Oßenbrügge
Leiter des Departments für Geowissenschaften

ISSN 1614-1199

The influence of plant nitrogen availability on the global carbon cycle and N_2O emissions

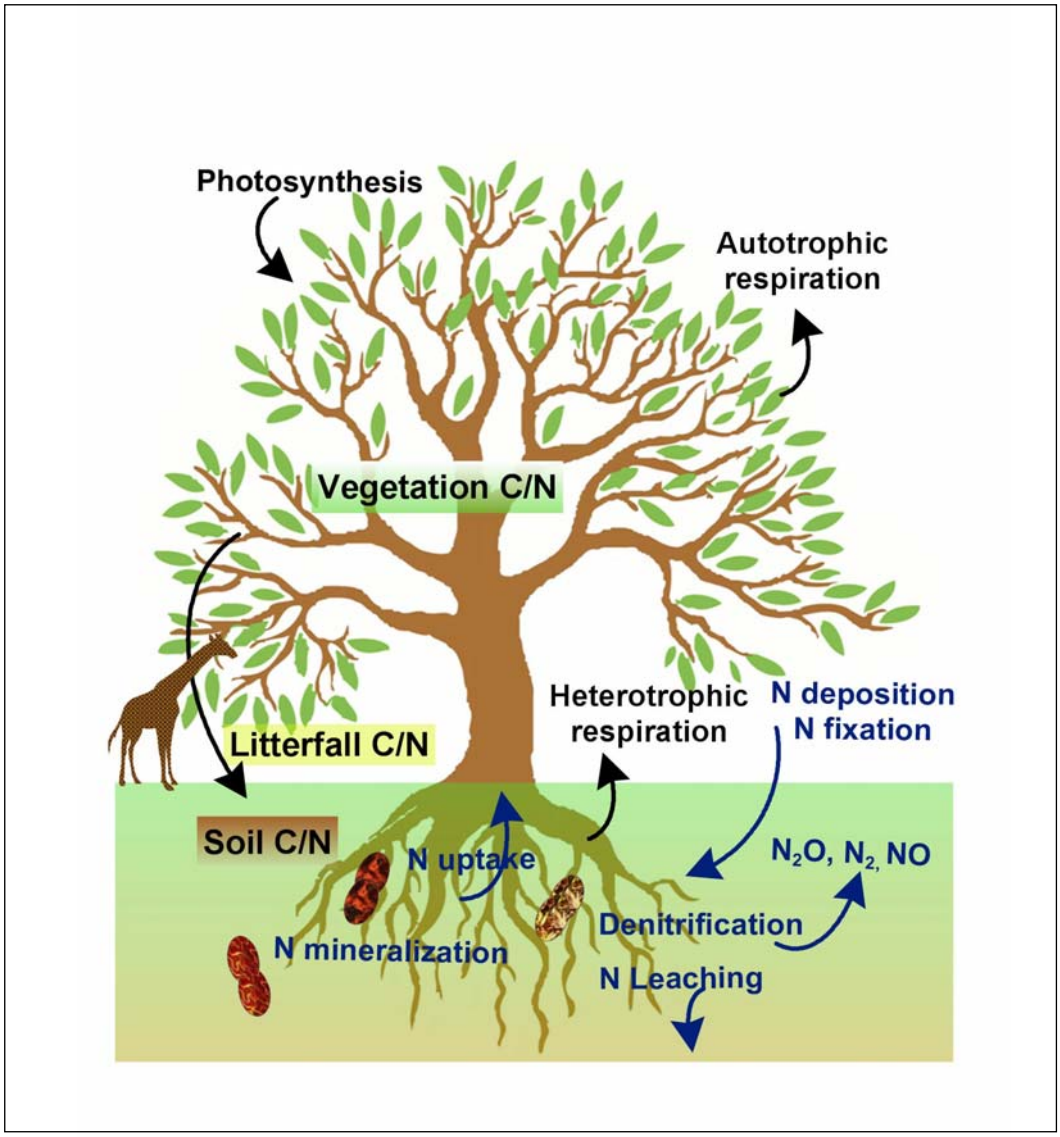

Bikash Ranjan Parida

Hamburg 2011

Table of Contents

Abstract

During the last two centuries, increasing atmospheric CO_2 concentration and climate change have altered the land carbon (C) cycling and the availability of nitrogen (N) for plants. Despite the cycling of C and N in the terrestrial ecosystems is tightly coupled, many modeling studies have ignored the interactions of land N cycle with the C cycle. In this thesis, their interactions are studied by incorporating a new and simple scheme for the terrestrial N cycling in the process-based land C cycle model JSBACH. The present study also investigates: Nitrous oxide (N_2O) emissions from natural soils under climate change and climate-N_2O feedback; N_2O emissions that arise from both land use change and fertilized agricultural soils; and the role of long-lived wood products for climate change mitigation.

To study the C-N cycle interaction, two main simulations are performed: carbon-only (C) and coupled carbon and nitrogen cycle (CN). The simulation results show that the coupling of C and N cycles leads to a lowering of the projected global land C uptake by 16% as compared to the C simulation during the 21st century in response to increasing atmospheric CO_2 concentration and climate change under the SRES A1B scenario. The results show that the inclusion of the land N cycle in the model leads to a significant reduction of positive climate-carbon cycle feedback by 21%. The development of Progressive Nitrogen Limitation (PNL) in forests and grasslands ecosystem is also analyzed. In forest ecosystems, the soil N availability decreases during the first half of the 21st century under increased CO_2 concentration and climate change. This results support the hypothesis "PNL" that soil mineral N availability decreases under elevated CO_2 as N is locked in long-lived woody biomass and soil organic matter. However, starting from roughly the second half of the 21st century, the PNL starts alleviating because of the relaxation of N scarcity due to global warming. In grasslands, the occurrence of PNL is much stronger than forests. Aside from this, to study the robustness of occurrence of PNL additional sensitivity experiments have been performed. Since doubling of N fixation is quite unrealistic, these experiments show that the appearance of PNL for grasslands during the 21st century is a very robust simulation result, whereas occurrence of PNL in forests is much less robust.

N_2O is produced in soils as a byproduct during nitrification and denitrification. This is a greenhouse gas and contributes significantly to global climate change. Simulations are performed to investigate N_2O emissions from natural soils under climate change and climate-N_2O feedback. The simulation results show that emissions from natural soils contribute 8.0 Tg N yr^{-1} to the global N_2O budget by the end of the 21st century. By including all N_2O emission sources (e.g., soil, ocean, fossil fuel, fertilizer, etc.) it is found that rise in atmospheric N_2O concentration is consistent with observations over the period 1860-2005 (a rise from 276 to 320 ppb). Under the A1B scenario, the atmospheric N_2O concentration increases up to 469 ppb by the end of the 21st century. Globally, a radiative forcing from N_2O emissions is about 0.6 Wm^{-2}, which equates to a projected increase in temperature by 0.46^0C by the end of the 21st century. According to this study, it is inferred that the climate-N_2O feedback is negligible because the value of feedback factor is very small (ca. 0.0003).

The results described in the previous paragraph were without agriculture. Human-induced land cover change (e.g., deforestation) and use of synthetic N fertilizers have released N_2O into the atmosphere. The simulated global N_2O emissions due to land use change are 0.75 Tg N yr^{-1} for the 1990s; this contributes about 5% of the global N_2O budget. N_2O emissions from fertilized agricultural soils are 4.9 Tg N yr^{-1} for the 2050s; a significant amount, namely 60% of these emissions is a direct consequence of the application of synthetic N fertilizers. In addition, the results show that agricultural N_2O emissions are highest in Asia, followed by North America, and Europe, that is, 46, 18, and 14%, respectively.

Wood products from forests are important in the context of climate change mitigation by curbing the land use emissions. The simulation results show that globally, long-lived wood products store 7.2 Pg C. The carbon sink from wood products lowers the land use carbon emissions by 6% over the period 1860-2000. As compared to fossil fuel emissions, this carbon sink has only a minor role to play in helping to mitigate the effects of climate change.

List of abbreviations

AR4	fourth assessment report
C	carbon
C^4MIP	Coupled Climate-Carbon Cycle Model Intercomparison Project
FAO	Food and Agriculture Organization of the United Nations
FACE	free air carbon dioxide enrichment
GO	global orchestration scenario
GHGs	greenhouse gases
GWP	global warming potential
HR	heterotrophic respiration
IPCC	Intergovernmental Panel on Climate Change
JSBACH-CN	land surface scheme applied in this study with carbon and nitrogen
LAI	leaf area index
NPP	net primary productivity
N	nitrogen
N_2O	nitrous oxide
PFT	plant functional type
P	phosphorus
PNL	progressive nitrogen limitation
RF	radiative forcing
SAR	second assessment report
SOM	soil organic matter
SRES	special report on emissions scenarios
TAR	third assessment report

Chapter 1

1. General introduction

1.1. Nitrogen cycle in terrestrial ecosystems

Nitrogen (N) is an abundant element in the atmosphere (ca. 78%) but it exists in unreactive form that cannot be used directly by plants. In general, available N is cycled from soil to plants through plant assimilation. Subsequently, plant releases organic N into soil through litter. This organic N is further decomposed by microorganisms and during decomposition organic N is converted into inorganic N. Moreover, by an additional pathway plants directly can take up N from plant litter through symbiotic associations with mycorrhizal fungi (Smith and Read, 1997). This process is most efficient under nutrient deficient conditions (Näsholm et al., 1998; Wallenda and Read, 1999).

The processes of microbial decomposition are: N mineralization, nitrification, and denitrification (Figure 1.1). The additional N cycle processes that make N available for plants are N fixation and N deposition. The details of these processes are explained as follows.

Assimilation:

By this process both ammonium (NH_4^+) and nitrate (NO_3^-) are absorbed by plants via their roots (Pidwirny, 2006). These compounds are incorporated in the plants in the form of various plant proteins and nucleic acids.

N Mineralization: [Organic N $\rightarrow NH_4^+$]

Conversion of organic N into NH_4^+ by soil microorganisms is called mineralization or ammonification (Pidwirny, 2006).

Nitrification: [$NH_4^+ \rightarrow NO_3^-$]

The NH_4^+ from N mineralization is further converted to nitrate NO_3^- by nitrifying bacteria (e.g., *Nitrosomonas sp.*, *Nitrolobus sp., and Nitrospira sp.*) (Pidwirny, 2006). This process is called nitrification. In addition, nitrous oxide (N_2O) is produced as a byproduct of the nitrification pathway (Farquharson et al., 2008) (Figure 1.2a).

Denitrification: [$NO_3^- \rightarrow N_2 + N_2O$]

By this process NO_3^- is converted into N_2 by denitrifying bacteria (e.g., *Pseudomonas sp.* and *Clostridium sp.*) (Pidwirny, 2006). This process occurs commonly under anaerobic conditions. N_2O is produced as a byproduct of the denitrification pathway (Farquharson et al., 2008) (Figure 1.2b).

N Fixation: [$N_2 \rightarrow NH_4^+$]

Conversion of N_2 into NH_4^+ by N fixing bacteria (e.g., *Rhizobium, Azotobacter*) is called N fixation (Pidwirny, 2006). Other processes responsible for N fixation are:

- atmospheric fixation by lightning
- industrial fixation (Haber-Bosch process)

N deposition:

N deposition is the input of various atmospheric N containing pollutants to the biosphere. These pollutants are generally N oxides (NO_X) and ammonia (NH_3).

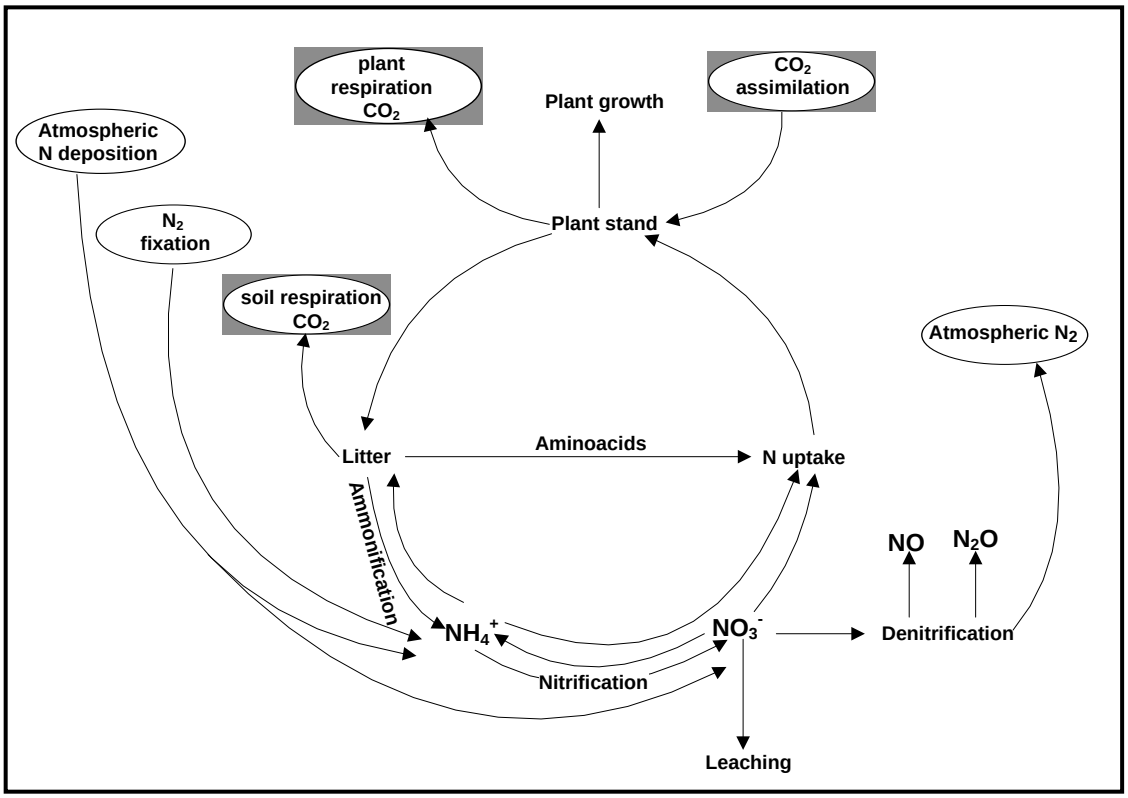

Figure 1.1: The schematic diagram depicts the terrestrial ecosystem N cycle and the major pathways of N (Source: Schulze, 2000). Gray boxes indicate C fluxes.

a) Nitrification

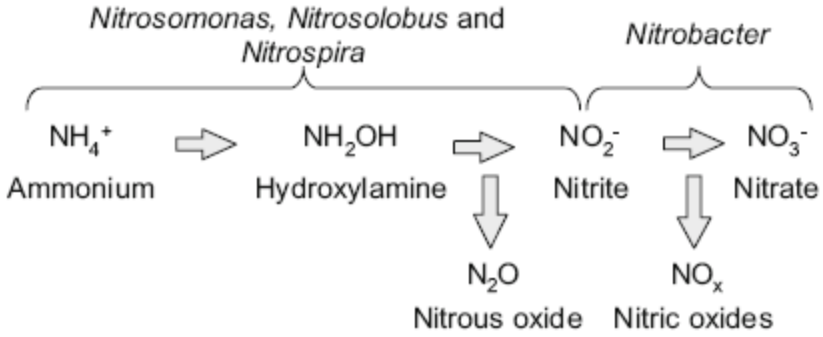

b) Denitrification

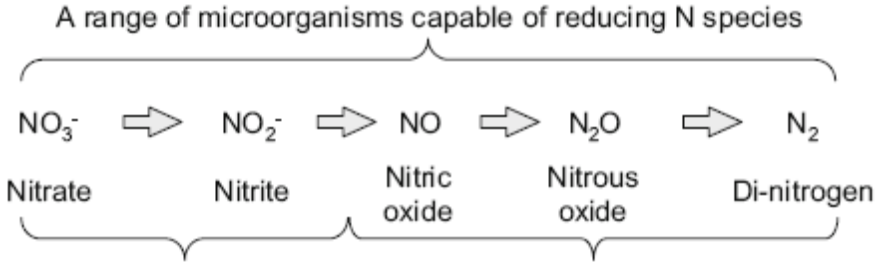

Figure 1.2: The microbial N transformation in the process of (a) nitrification and (b) denitrification (Source: Farquharson et al., 2008).

1.2. Motivation of this study

Nitrogen is an essential nutrient for plant growth because plant photosynthesis is strongly linked with the leaf N content (Wright et al., 2004; Grassi et al., 2005). Approximately 25-30% of leaf N is invested in Rubisco (ribulose-1,5-bisphosphate carboxylase oxygenase) (Jensen, 2000). This enzyme is generally responsible for catalyzing the first step of carbon assimilation (Lu and Zhang, 2000; Warren et al., 2003). Therefore, N deficiency in leaves decreases carbon assimilation.

During the last two centuries, atmospheric CO_2 concentration has increased strongly due to the worldwide deforestration and fossil fuel burning. Under rising atmospheric CO_2 concentration, plant photosynthesis is getting more effiecient ("CO_2 fertilization"). On the

other hand, N availability for plants is not increasing as CO_2 is growing in the atmosphere. Thus, over a longer time N deficiency may influence gross primary production (GPP) and net primary production (NPP) by down-regulating the plant photosynthetic capacity (Grassi et al., 2005).

Despite the importance of N during plant photosynthesis many terrestrial ecosystem models have ignored the explicit land N cycle dynamics while estimating the terrestrial biosphere C sink as well as the development of future land C storages. For example, the models used in the Coupled Climate-Carbon Cycle Model Intercomparison Project (C^4MIP) experiments (Friedlingstein et al., 2006) have ignored the N cycle dynamics. However, the situation is now rapidly changing, since some of the existing land C cycle models have integrated the N cycle dynamics into climate models (Thornton et al., 2007; Sokolov et al., 2008; Jain et al., 2009; Zaehle et al., 2010a). In the above mentioned C-N cycle models, the key N cycling processes substantially depend on many model parameters. For instance, the variable C-to-N ratios are hardly controllable in previous models and hence they may propagate the uncertainty. Many of the relevant N cycling processes are not well understood to address the C-N cycle interaction under rising CO_2 concentration and climate change. In order to address their interactions, this study incorporates a new, simple scheme for terrestrial N cycling into the existing land carbon cycle model (JSBACH). The newly developed C-N cycle model (called here as JSBACH-CN) is based on only a small number of basic principles, namely mass conservation, a supply-demand ansatz, and fixed C-to-N ratios. Moreover, this modeling approach needs only a very limited number of additional state variables and model parameters as compared to the original JSBACH-C model.

In the present study, N_2O emissions from the terrestrial biosphere under climate change are also investigated. N_2O is a greenhouse gas and contributes 6-7% to global climate change (Xu et al., 2008). Its atmospheric concentration is increasing at the rate of 0.6-0.9 ppb/yr (Albritton and Meira Filho, 2001). N_2O has a life-time of about 114 years (Albritton and Meira Filho, 2001) and may play important role in global warming in the near future due to its higher global warming potential (ca. 296 times) than CO_2. Increase in temperature due to climate change may cause a rise in N_2O emissions by inducing N mineralization rates (Prinn et al., 1999; Grant et al., 2008). N_2O emissions can be further enhanced by climate-N_2O feedback. Additionally, N_2O emissions are influenced by

human-induced land cover change (e.g., deforestration). Therefore, it is important to study N_2O emissions that arising from climate and land use change.

1.3. Scientific questions of the study

This thesis is focused to understand the atmosphere-plant-soil nitrogen cycling processes and to investigate the response of terrestrial ecosystems to future climate change. To investigate the complex interactions among atmosphere, plant, and soil C-N cycling, this study attempts to address the following key questions:

1. Does the land N cycling constraint the global future land C uptake?
2. Does the progressive N limitation (PNL) develop in response to increasing CO_2 and climate change?
3. Are N_2O emissions from natural soil a significant source for the global N_2O budget for the 21st century?
4. Is the climate-N_2O feedback so strong that it will lead to additional global warming?
5. How large N_2O emissions are from anthropogenic land cover change that contribute to global N_2O budget?
6. Do N_2O emissions from fertilized agricultural soils increasing for the 21st century and how much of N_2O is contributed by use of synthetic N fertilizers?
7. Can wood products be used for mitigating climate change?

In order to achieve the above mentioned research questions a sets of simulations are performed with the JSBACH-CN model. These research questions are separated into three Chapters and the details are as below.

1.4. Outline of the thesis

Chapter 2 deals with the construction of the new JSBACH-CN model starting with a description of the existing JSBACH-C model. The key N cycle processes newly implemented are described in this chapter. The additional carbon cycle processes and model parameters to improve carbon allocation are also described but the details are kept in the appendix. By using the newly developed JSBACH-CN model, this Chapter

addresses main research questions of nitrogen constraints on the global land carbon cycle and PNL hypothesis (see questions 1 and 2). To accomplish this several simulations are performed.

Chapter 3 deals with N_2O emissions and climate-N_2O feedback (see questions 3 and 4). To study this, the processes controlling N_2O emissions are implemented in the JSBACH-CN model. Simulations are performed in order to obtain the emissions from natural soils under climate change. In particular, to address the question 4, the simulated N_2O emissions from natural soils need to be combined with the other emission sources data, for instance, emissions from fossil fuel and biomass burning, synthetic fertilizers, etc. The later mentioned emission sources are obtained from the recent study by Davidson (2009). The combined emission sources are used to construct atmospheric N_2O concentrations by employing a calculation of Höhne and Blok (2005). Further, the constructed atmospheric N_2O concentration is converted to radiative forcing (RF) and temperature increases.

Chapter 4 deals with N_2O emissions from anthropogenic land cover change and fertilized agricultural soils (see questions 5 and 6). To address these questions, the anthropogenic C and N pools are implemented in the JSBACH-CN model. These anthropogenic pools are called: annual, decadal, and centennial with 1 year, 10 year, and 100 year turnover time. The above anthropogenic C pools are modelled in accordance with the Grand Slam Protocol proposed by Houghton et al. (1983). Moreover, the anthropogenic C pools store some amount of carbon in the form of wood products (e.g., fuel wood, paper products, building, furniture, etc.) and thereby the present study analyzes the role of long-lived wood products in mitigating climate change (see question 7). In particular, N_2O emissions from fertilized agricultural soils are studied by including synthetic N fertilizer application to agricultural ecosystems. Several simulations are performed in order to address the questions pertaining to this Chapter.

Finally, in Chapter 5, the main findings and conclusions of this thesis are synthesized and discussed.

Chapter 2

2. Coupled nitrogen-carbon cycle simulations for the 21st century with JSBACH-CN and progressive nitrogen limitation

Abstract

The global Carbon (C) and Nitrogen (N) cycles are strongly linked in the terrestrial ecosystems. In the present study, their interactions are studied by incorporating a new and simple scheme for the terrestrial N cycling in the process-based land C cycle model JSBACH. This Chapter describes the processes and the model structure that are incorporated in the JSBACH-CN model. To study the C-N cycle interaction, two main simulations are performed: carbon-only (C) and coupled carbon and nitrogen cycle (CN). The C and CN simulations show that the simulated contemporary land carbon sink and carbon stocks are consistent with the observational estimates. The simulated global N storages are consistent with those obtained by various other models and also with published observational estimates.

The coupling of C-N cycle in the terrestrial biosphere leads to a lowering of the global land C uptake by 8% as compared to the C simulation for present-day conditions. N availability decreases during the 21st century and causes a significant reduction of the projected land C uptake by 16% in response to increasing atmospheric CO_2 concentration and climate change under the SRES A1B scenario. The results show that the inclusion of the land N cycle in the model leads to a significant reduction of positive climate-carbon cycle feedback by 21%. To check the robustness of certain model assumptions two sensitivity experiments are designed, assuming quite drastic modifications of the model. Even with these modifications today's land carbon sink is well within the uncertainty range from observational estimates. However, the assumption "plant N uptake first" makes a significant difference for the future development of the C cycle in the model. The assumption "microbial N uptake first" does not change significantly the land carbon uptake. Since soil microorganisms are superior competitors to plants, the standard model

setup (i.e. equal competition between plants and soil microorganisms) turned out to be most appropriate setup but the assumption "plant N uptake first" can be ruled out as unrealistic.

The development of Progressive Nitrogen Limitation (PNL) in forests and grasslands ecosystem is analyzed. The results show that in forest ecosystems, the soil N availability decreases during the first half of the 21st century under increased CO_2 concentration and climate change. This results support the hypothesis "PNL" that soil mineral N availability decreases under elevated CO_2 as N is locked in long-lived woody biomass and soil organic matter. However, starting from roughly the second half of the 21st century, the PNL starts alleviating because of the relaxation of N scarcity due to global warming. In grasslands, the occurrence of PNL is much stronger than forests. Aside from this, to study the robustness of occurrence of PNL additional sensitivity experiments have been performed. Since doubling of N fixation is quite unrealistic, these experiments show that the appearance of PNL for grasslands during the 21st century is a very robust simulation result, whereas occurrence of PNL in forests is much less robust.

2.1. Introduction

During the last 200 years, emissions from worldwide deforestation and fossil fuel burning have increased atmospheric carbon dioxide (CO_2) concentrations and surface temperature significantly (IPCC, 2001; Hungate et al., 2003). The resulting green house warming changes global climate, whose future extent will not only depend on the size of future emissions, but also on the development of future carbon (C) sinks of the terrestrial biosphere and ocean. During the last few decades, land and ocean have accounted for a sink of C of 1.7-2.6 and 1.7-2.2 Gt C yr^{-1} respectively, which is together about 50% of today's fossil fuel emissions (IPCC, 2007), but the future trend of the C sink largely depends on the responses of land and ocean to increasing CO_2 concentrations and climate change. However, besides the uncertainty of climate scenarios themselves, predicting future atmospheric CO_2 concentrations is also hampered by the uncertainties of terrestrial biospheric responses to elevated CO_2 concentration and availability of nitrogen (N) in soil (Oren et al., 2001). Although under optimal water and nutrient conditions an elevated CO_2 concentrations typically increases net primary productivity (NPP) in short-term

experiments (Norby et al., 2005; Reich et al., 2006), and modeling studies suggest that limited N availability will constrain productivity responses of the global vegetation to elevated atmospheric CO_2 over the long term (Reich et al., 2006; Finzi et al., 2007).

The cycling of C and N in the terrestrial ecosystems is tightly coupled and the response of the terrestrial C sink to increased atmospheric CO_2 can be understood only by accounting for the complex interactions among leaf N concentration, plant growth, C allocation, C decomposition, and N mineralization in soils (McGuire et al., 1997; Körner, 2000). Plant photosynthesis is strongly influenced by leaf N content (Chen et al., 1993; Reich et al., 1999; Wright et al., 2004), approximately 25-30% of leaf N is invested in Rubisco (ribulose-1,5-bisphosphate carboxylase oxygenase) (Jensen, 2000), that catalyzes the first step of C assimilation (Lu and Zhang, 2000; Warren et al., 2003). Therefore, N deficiency in leaves significantly decreases C assimilation. N regulates not only plant metabolic rates (e.g., photosynthesis, respiration) but also the turnover of soil organic matter (SOM) (Anderson, 1973; Flanagan and van Cleve, 1983; Sprugel et al., 1996). The supply of mineral N is mostly controlled by soil microbial activity that in turn depends on the supply of organic C from plant litter (Hungate et al., 2003; Luo et al., 2004). During decomposition of SOM, soil microbes mineralize the organic N. Once mineralized, plants and soil microbes (immobilization) can take up this N as nutrient. The rate of decomposition depends on climate conditions, litter quality, soil microbial activity, and N input (e.g., deposition and fixation) (Kirschbaum and Paul, 2002) so that changes in these conditions influence plant N availability as well as plant productivity.

Despite the importance of N in regulating both plant and soil processes, in many modeling studies of the future climate-carbon-cycle dynamics, interactions with the N cycle have been ignored (e.g., Friedlingstein et al., 2006). Notable exceptions are the studies by Sokolov et al. (2008), Thornton et al. (2007, 2009), and Zaehle et al. (2010a), who integrated the N cycle dynamics into existing climate-C cycle models. They consistently found that coupled climate-carbon-cycle models without N cycle significantly overestimate the C sequestration and its future trend under a changing climate. As a result, the C-N interaction might significantly reduce the net terrestrial C uptake and may possibly change the sign of the C cycle-climate feedback during the 21st century under rising CO_2 concentration and climate change (Hungate et al., 2003; Sokolov et al., 2008; Thornton et al., 2009). The models used in the Coupled Climate-Carbon Cycle Model

Intercomparison Project (C^4MIP) experiments consistently show a positive feedback between the C cycle and climate (Friedlingstein et al., 2006), but none of the models included the restrictions arising from the N cycle. Future warming will increase both plant and soil respiration, and cause additional soil N to be available to the vegetation as it increases SOM decomposition (Melillo et al., 2002) and N mineralization. The additional soil N may stimulate plant growth and thus leads to enhanced C sequestration, resulting in a negative feedback between the C cycle and climate (Sokolov et al., 2008; Thornton et al., 2009). Despite the plausibility of such considerations, quantitatively the N cycle and its interactions with the C cycle are only poorly understood. Uncertainties are quite large (Luo et al., 2006a) and accordingly the question to which extent N deficiency may constrain the future land C uptake is an ongoing debate (Hungate et al., 2003; Luo et al., 2004; Reich et al., 2006).

Indeed, in the ecological community a second, very different scenario is discussed. Under increasing atmospheric CO_2 concentration photosynthesis is getting more efficient ("CO_2 fertilization") so that ecosystems may develop a shortness of N, usually called "N limitation". This expectation leads to the so called "progressive nitrogen limitation (PNL)" hypothesis (Luo et al., 2004; Reich et al., 2006) where elevated CO_2 enhances plant N uptake and thereby sequestration of N into long-lived biomass (e.g., wood in forests) and SOM pools, resulting in a decrease of soil N availability for plant growth and consequently, a reduction of plant productivity over time due to the reduced N availability (Luo et al., 2004; De Graaff et al., 2006). A faster depletion of available N is observed under elevated CO_2 by young trees (Finzi and Schlesinger, 2002; De Graaff et al., 2006). Experimental studies show that PNL is observed in scrub oak woodland (Hungate et al., 2006), loblolly pine forest (Luo et al., 2004) and grassland ecosystems (Gill et al., 2006; Hovenden et al., 2008) following the stimulation of biomass under elevated CO_2. Observations from open top chamber (OTC), greenhouse and free air carbon dioxide enrichment (FACE) experiments suggest that indeed terrestrial ecosystems require more N to support enhanced plant growth under elevated CO_2 concentration (Luo et al., 2006a). In addition, most of the studies discussed that soil N availability commonly limits the enhancement of plant biomass accumulation under elevated CO_2 (Luo et al., 1994; Oren et al., 2001; Reich et al., 2006).

However, there is an ongoing discussion whether PNL indeed exists, or whether other processes could delay or alleviate PNL. A number of experimental studies have reported an increase in the N use efficiency (NUE) under elevated CO_2 concentration in forest ecosystems (Johnson et al., 2003; Hungate et al., 2006). This process decreases the quantity of N required to support high rates of NPP (Finzi et al., 2002) and reduces the N concentration in plant tissues (increases C-N ratio) (Johnson et al., 2003) and thus leads to an alleviation of PNL. Experimental studies show that stimulation of SOM decomposition caused by additional rhizodeposition of labile substrates under elevated CO_2 ("priming") may alleviate PNL as well (Jenkinson et al., 1985; De Graaff et al., 2009). A faster rate of internal N cycling by an enhanced rate of mineralization of SOM may also counteract PNL by reducing N deficiency in soils (Barnard et al., 2006; Van Groenigen et al., 2006; Müller et al., 2009). The latter mechanism is probably responsible for the lack of PNL in a grassland ecosystem studied by Rütting et al. (2009) at the New Zealand-FACE site. Similarly, Hovenden et al. (2008) found for another grassland site in Tasmania alleviation of PNL because of enhanced N mineralization under global warming conditions. In other studies it was reported that elevated CO_2 stimulated root production (Pregitzer et al., 2000; Finzi et al., 2007; Stover et al., 2007) which leads to greater acquisition of N from the deep soils. The development of this additional access to deep soil N sources is another process that was observed to lead to an alleviation of PNL (McKinley et al., 2009). Additionally, some authors speculate that a PNL could be delayed by stimulating an additional gain of N through biotic N fixation or decreasing N losses (Hungate et al., 1999; Johnson et al., 2004; Luo et al., 2006a).

Although in the above mentioned studies various mechanisms to alleviate PNL have been proposed, in none of these studies, PNL is discussed especially for the large warming expected during the 21st century. Furthermore, the above stated studies on PNL occurrence or absence are mainly based on short-term experimental field studies (e.g., < 10 year), and are thus not fully conclusive yet with respect to the occurrence of PNL in future (Norby et al., 2006). In this regard, models are particularly useful because they allow to simulate the occurrence of PNL at much longer time scales.

The aim of the present study is to analyze the global development of PNL during the 21st century and the sign of the feedback between climate and C cycle in relation to N availability. To address these questions, this study developed a model for coupled

terrestrial C and N cycles (JSBACH-CN). Particular emphasis is given to differences between forests and grasslands ecosystem, because there are indications that these two ecosystems behave differently with respect to PNL (see above). In view of the complexity of the N-cycle and the lack of detailed process understanding, the model development is based on only a small number of basic principles (mass conservation, supply-demand ansatz, fixed C-to-N-ratios), that can clearly be overseen and tested in sensitivity experiments.

The newly developed JSBACH-CN model builds upon the land surface C cycle model JSBACH, which is based on the biosphere model BETHY (Knorr, 2000) and the ECHAM5 soil scheme (Roeckner et al., 2003). JSBACH includes a photosynthesis scheme following Collatz et al. (1992) for C_4 and Farquhar et al. (1980) for C_3 plants comprising an explicit dependence of productivity on atmospheric CO_2 concentration (Raddatz et al., 2007). Heterotrophic respiration increases linearly with soil moisture and exponentially with soil temperature (Q_{10}) (Raich and Potter, 1995). To obtain from this a CN-cycle model this study assumes (i) fixed C-to-N-ratios for the various plant and soil compartments, and (ii) follow a supply-demand ansatz. As will be shown below, by these assumptions the extension of the existing C-cycle model in JSBACH into a coupled CN-model, is thereby an almost necessary consequence of the mass conservation of nitrogen in the system. In addition to the prescribed C-to-N-ratios, only a few additional parameters are needed to describe the exchange fluxes with the atmosphere and water cycle. Beyond the parameters of the existing C-cycle model, the N-model has in total 3 additional parameters (fixed C-to-N-ratios, denitrification loss rate, leaching rate) and 3 additional state variables (litter green pool, mobile plant pool, and soil mineral pool).

It may be objected that by such a simple approach this model is more unrealistic than other models. But in view of the lack of quantitative understanding of the dynamics of the N-cycle, more model parameters or degrees of freedom would not necessary by implicit increased realism. For instance, the variable C-N ratios were hardly controllable in previous models (Xu-Ri and Prentice, 2008; Yang et al., 2009; Zaehle et al., 2010a) and thus the assumptions with respect to the variable C-N ratios for different plant and soil compartments may propagate uncertainty. Another simplification of this approach is that this study does not distinguish between ammonia (NH_4^+) and nitrate (NO_3^-) and accordingly employs only a single pool for soil mineral N because it is unclear under what

circumstances plants favor one type of mineral N above the other (Falkengren-Grerup, 1995; Nordin et al., 2001; Jones et al., 2005). Moreover, to which extent plants prefer NH_4^+ versus NO_3^- for N uptake via their roots generally varies over seasons, locations, and plant species (Epstein and Bloom, 2005); trying to include mechanistic models for such preferences would introduce additional uncertainty into the model. However, models have been developed (Xu-Ri and Prentice, 2008; Zaehle et al., 2010a) to estimate nitrification (i.e. NH_4^+ availability) and denitrification (i.e. NO_3^- availability) in soils by explicitly representing microbial dynamics (Li et al., 2000) using an empirical function for the dependence on soil water, temperature, and pH (Parton et al., 1996, 2001). To compensate for the lack of detail, this study systematically checks the robustness of the results by performing sensitivity experiments where parameters are varied in reasonable bounds, and by additional simulations experiments that address the question of robustness with respect to certain design decisions for the model.

The chapter is structured as follows. In Section 2.2, this study describes the construction of the CN-cycle model starting with a description of the existing JSBACH C-cycle model. This will make the design decisions for the new combined CN-model transparent. In Section 2.3, a number of experiments are performed to study the robustness of model results with respect to certain model parameters and design decisions. In Section 2.4.1, the improvement of carbon allocation is discussed. In Section 2.4.2, simulated contemporary land carbon sink and C stocks are compared with observational estimates. In Section 2.4.3, the model results are compared with site-scale observations. The effect of N limitation on the global land C and certain design decisions for the model are presented in Section 2.4.4 and 2.4.5, respectively. In Section 2.4.6, this study presents N availability and feedback between climate and carbon cycle. The hypothesis PNL and how robust is the PNL in forests and grasslands ecosystem are presented in Section 2.4.7 and 2.4.8, respectively. Finally, in Section 2.5, the model assumptions and the effect of N availability on the global C cycle including feedback are discussed. Besides, the PNL under climate change is discussed.

2.2. From JSBACH-C to JSBACH-CN

JSBACH (Raddatz et al., 2007) has been developed as land component for the model of atmospheric circulation ECHAM (Roeckner et al., 2003). Accordingly, it incorporates all processes relevant to provide the boundary conditions for simulations of atmospheric dynamics like the balances of radiation, heat, and water fluxes, as well as surface temperature, albedo, and roughness length. In addition JSBACH describes the uptake and release of CO_2 by vegetation and soils so that JSBACH can be used in combined climate and carbon cycle simulations (see e.g., Friedlingstein et al., 2006; Jungclaus et al., 2006).

This latter part of the model on the cycling of land carbon consists of several subprocesses for photosynthesis, phenology, carbon allocation, and auto- and heterotrophic respiration. In addition, it includes implicit limitation by N availability due to the parameter values of maximum rates of carboxylation (V_{cmax}), which implicitly describes N availability. – Please note that throughout the thesis, if not otherwise stated, the term "N limitation" is used as a shortcut for "additional" N limitation beyond the limitation arising from V_{cmax}.

To incorporate nitrogen cycling into JSBACH-C – as it is called in the following to distinguish it from the new JSBACH-CN model – only the (combined) submodel for carbon allocation and heterotrophic respiration has been modified. To understand how the nitrogen processes were incorporated, this study first describes in the following the existing carbon cycling model of JSBACH-C and in a second step how nitrogen cycling is included. Figure 2.1 gives an overview of the resulting model for C and N cycling in JSBACH-CN.

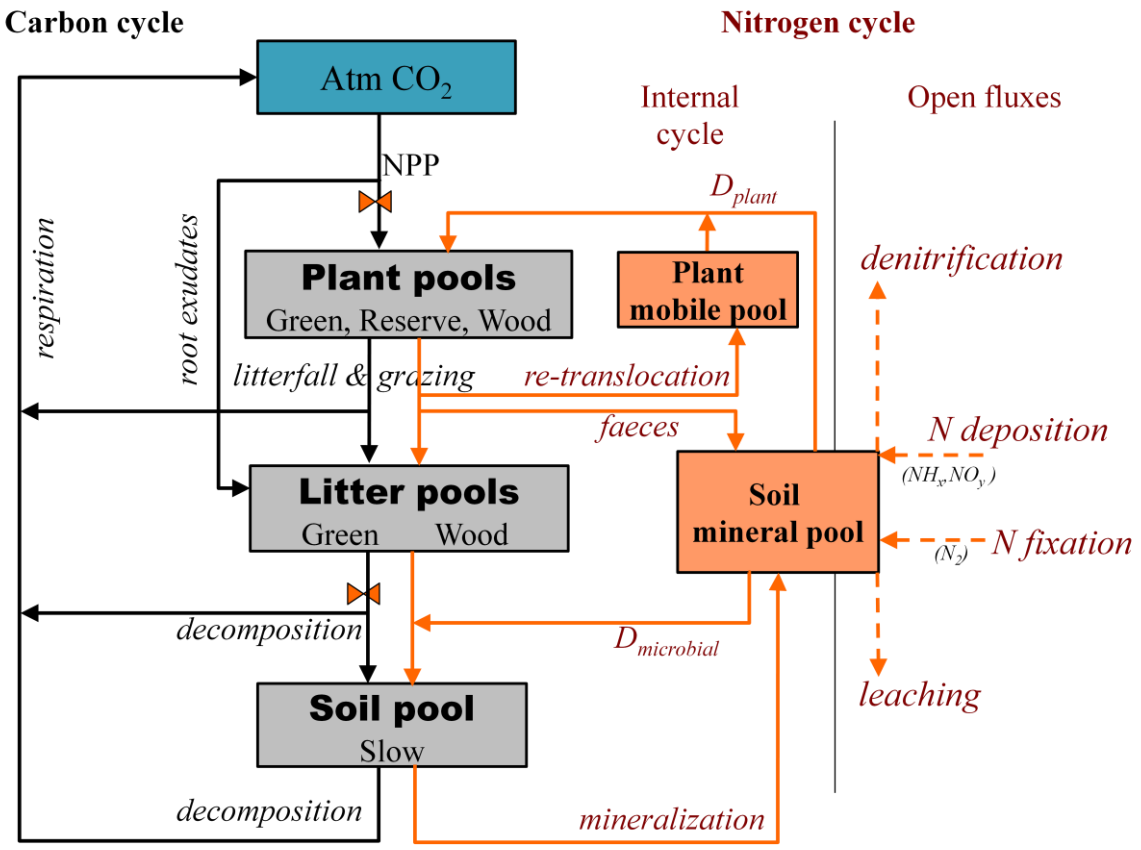

Figure 2.1: Flux diagram depicting the coupling of C and N cycling in JSBACH-CN. The black arrows indicate C fluxes, solid orange arrows indicate N fluxes and the dashed orange arrows depict N exchange fluxes with the environment (for shortness called "open" fluxes here). The opposing orange triangles at certain C fluxes indicate a control by N related processes. The allocation of carbon is driven by net primary productivity (NPP). NPP is allocated to the three pools representing vegetation in JSBACH-C, the green, reserve, and wood pool. In addition, a small fraction of NPP is transferred as root exudate to the pool for green litter. C enters the pools for green and woody litter by litterfall and grazing. Grazers respire and C is lost to the atmosphere. Decomposition of litter (green & wood) and soil organic matter (slow pool) causes soil respiration (HR), and returns CO_2 to the atmosphere. By decomposition of soil organic matter, mineral N is released to the soil mineral pool. Mineralized N can be immobilized by soil microbes and is also available for plant N uptake. Grazing causes a transfer of N through animal faeces, which contribute to the soil mineral N. Other N-fluxes are leaf re-translocation of N preceding leaf shedding, animal faeces N following grazing, plant N uptake (D_{plant}) and microbial N uptake ($D_{microbial}$). The soil mineral pool receives N from N fixation and deposition, while it looses N via leaching and denitrification.

2.2.1. Cycling of carbon

JSBACH distinguishes between different types of vegetation (so called "plant functional types", PFTs). In the setup used for the present study these are six tree PFTs (tropical, extratropical, and coniferous, each subdivided into deciduous and evergreen), two shrub PFTs (deciduous and evergreen), two grass PFTs (C_3 and C_4 pathways), and two crop PFTs (tropical and extratropical). Each of these PFTs is associated with six C pools to describe the storage of organic C on land (Figure 2.1). The sizes of these pools are the state variables of the model. Tissues of living plants are represented by the three pools called green pool (leaves, fine roots, and sap wood), wood pool (stems, branches, and coarse roots) and reserve pool. In the latter, C is stored in the form of sugars and starches that the plants use as an energy reserve. Soil C is divided into two pools for decomposing green and woody litter, and a pool ("slow") for organic material decomposing at long time scales (50-100 years).

Table 2.1: Notations used in description of the JSBACH-CN model.
Abbreviations for pools: G: green; W: wood; R: reserve; LG: litter green; LW: litter wood; S: slow; M: mobile; SM: soil mineral. X, A: any of the foregoing pools, atmosphere. Throughout, fluxes are denoted by F and fractions by f.

Notation	Meaning
C_X	$size\ of\ C\ \ pool\ for\ type\ X\ [mol(C)/m^2]$
N_X	$size\ of\ N\ pool\ for\ type\ X\ [mol(N)/m^2]$
nc_X	$N\ to\ C\ ratio\ for\ type\ X$
$f_{NPP\rightarrow X}$	$fraction\ of\ potential\ NPP\ allocated\ to\ X$
$f_{X\rightarrow A}$	$fraction\ of\ C\ flux\ lost\ from\ X\ to\ A$
$f_{X\rightarrow S}$	$fraction\ of\ C\ flux\ lost\ from\ X\ to\ slow$
NPP^{pot}	$potential\ NPP$
NPP_X^{pot}	$part\ of\ potential\ NPP\ allocated\ to\ X$
NPP^{dir}	$part\ of\ NPP\ that\ can\ be\ directly\ allocated\ without\ uptake\ of\ soil\ mineral\ N\ by\ using\ N\ from\ the\ mobile\ pool$
NPP_X^{dir}	$part\ of\ NPP\ direct\ allocated\ to\ X$
$F_{exudates}$	$C\ fluxes\ due\ to\ root\ exudates$

$F_{grazing}$	$C\ fluxes\ due\ to\ grazing$
R_X^{pot}	$potential\ C\ decomposition\ respiration\ fluxes\ from\ X$
R_S	$C\ decomposition\ respiration\ flux\ from\ slow\ pool$
τ_X	$turnover\ time\ of\ X$
f_{limit}	$factor\ descrbing\ the\ strength\ of\ N\ limitation$

In the following the equations are written down for the temporal development of the six carbon pools of JSBACH-C such that they are also valid for JSBACH-CN. This makes the equations a bit more complicated than necessary for understanding the carbon-only model, but prevents unnecessary doubling of equations when introducing nitrogen below. The carbon-only case is obtained from these equations for

$f_{limit} = 1$.

The two other nitrogen specific variables showing up in the following (NPP_G^{dir} and NPP_W^{dir}) drop out in this case. The meaning of these objects is described in detail when introducing the nitrogen dynamics in the next section. At the moment it is sufficient to notice that f_{limit} quantifies the strength of nitrogen limitation, such that $f_{limit} = 1$ represents optimal nitrogen availability, and $f_{limit} = 0$ the case of severe nitrogen limitation.

The model is driven by NPP. NPP itself is computed in other parts of JSBACH, following the implementation of the BETHY model (Knorr, 2000) assuming optimal N availability therefore it is called *potential* NPP here (NPP^{pot}). As described in detail in Appendix 2.1, NPP^{pot} is splitted into separate influxes NPP_G^{pot}, NPP_W^{pot}, and NPP_R to the three vegetation pools plus a certain part $F_{exudates}$that is reserved for root exudates (see Table 2.1 for the notation), i.e.

$$NPP^{pot} = NPP_G^{pot} + NPP_W^{pot} + NPP_R + F_{exudates} \quad (1)$$

The reason why only NPP_G^{pot} and NPP_W^{pot} are equipped with the index "pot" but not NPP_R will also get clear when introducing N limitation in the next section.

The three vegetation pools develop in time according to the following rate equations:

$$\frac{dC_G}{dt} = f_{limit}\,(NPP_G^{pot} - NPP_G^{dir}) + NPP_G^{dir} - F_{litter} - F_{grazing} \quad (2)$$

$$\frac{dC_W}{dt} = f_{limit}\,(NPP_W^{pot} - NPP_W^{dir}) + NPP_W^{dir} - \frac{C_W}{\tau_W} \quad (3)$$

$$\frac{dC_R}{dt} = NPP_R - \frac{C_R}{\tau_R} \quad (4)$$

The first terms on the right hand side describe the NPP flux into the pools, the following terms the carbon losses. These losses are as follows: All plants loose carbon because of aging, diseases, pests, windbreak etc. For the green and reserve pool these losses are modelled as an exponential decay with life times τ_W and τ_R, ignoring any seasonality in such losses. For the green pool seasonality must be taken into account because of active leaf shedding especially in deciduous species. Accordingly, the litter loss term F_{litter}, which depends on the temporal development of the leaf area index, has a more complicated form, described in Appendix 2.1. In addition losses by grazing ($F_{grazing}$) are explicitly accounted for in this scheme, because such losses can be large especially in grassland ecosystems (see Appendix 2.1 for details).

The dynamics of the two litter pools (litter green and litter wood) is modeled as:

$$\frac{dC_{LG}}{dt} = \frac{C_R}{\tau_R} + F_{litter} + F_{grazing}\, f_{grazing\rightarrow LG} + F_{exudates} - f_{limit}\; R_{LG}^{pot} \quad (5)$$

$$\frac{dC_{LW}}{dt} = \frac{C_W}{\tau_W} - f_{limit}\; R_{LW}^{pot} \quad (6)$$

The losses from the green and reserve pool are fed into the litter green pool; accordingly the loss terms in equations (2), (3), and (4) are gain terms in (5), although with a slight modification: only a fraction ($f_{grazing\rightarrow LG}$) of the grazing flux is transferred to the litter green pool, the remaining C is lost as CO_2 and CH_4 directly to the atmosphere via the metabolism of the grazers or herbivores. Similarly, the losses from the wood pool enter the

litter wood pool (compare equations (3) and (6)). Both litter pools loose carbon by heterotrophic respiration; these are the last terms on the right hand side. These decomposition fluxes (R_{LG}^{pot}, R_{LW}^{pot}) are determined by a Q_{10} model (Raich and Potter, 1995) which accounts for temperature and moisture, while it ignores the pH value. The time scale of decomposition is about one to two years for the litter green and 30 years for the litter wood pool.

The last pool to be considered is the slow pool. Its dynamics is described by:

$$\frac{dC_S}{dt} = f_{limit}\left(f_{LG\to S}\, R_{LG}^{pot} + f_{LW\to S}\, R_{LW}^{pot}\right) - R_S \qquad (7)$$

It is fed by those parts of the litter pools, that could not be fully respired at the short turnover time of those pools (e.g., lignins). Accordingly, only a fraction $f_{LG\to S}$ and $f_{LW\to S}$ of the decomposition fluxes R_{LG}^{pot} and R_{LW}^{pot} from equations (5) and (6) enter the slow pool. Finally, also the slow pool looses carbon by heterotrophic decomposition to the atmosphere (R_S) which is once more described by a temperature and moisture dependent Q_{10} model (Raich and Potter, 1995), although with an effective turnover time in the range 50-100 years.

To complete the carbon balance, the losses to the atmosphere have to be tracked; for details see Appendix 2.1.

2.2.2. Cycling of nitrogen

The cycling of N is closely coupled to that of C – and vice versa. Since many details of this interrelationship are uncertain, in this study the modelling approach to incorporate N dynamics into JSBACH-C aims at a transparent representation with a minimum of additional assumptions and parameters.

It is clear that the carbon in the JSBACH allocation scheme refers to carbon that is bound in organic molecules. And except for the carbon in the reserve pool (sugar, starches), such molecules typically also contain nitrogen. Accordingly, to add the cycling of N to this scheme – except for the reserve pool – all other C pools have to be associated with a partner N pool that describes the N content of the respective organic molecules. To

complement the existing C pools, this makes together 5 nitrogen pools; the obvious notation for them is N_G, N_W, N_{LG}, N_{LW} and N_S. In addition, for building organic molecules in all types of tissues and organs, there are forms of N flexibly available in plants that make it necessary to introduce a sixth pool for such mobile N in plants, called N_M. And finally, the processes in the soils crucially depend on the availability of mineral N, i.e. nitrate and ammonia, so that a seventh pool called "soil mineral N pool" (SM) is introduced, and denoted as N_{SM}. A simpler pool structure compatible with JSBACH-C is hardly conceivable.

But not all of these pools need to be dynamic, in the sense that they are independent state variables of the model. Indeed, to prevent uncontrollable complexity the ratio between the N and C content – the so called N-to-C ratio nc – is kept fixed for each pair of partner pools, except for the green litter:

$$N_X = nc_X \, C_X \text{ , for pools X = G, W, LW, and S.} \qquad (8)$$

As will get clear below, the green litter pool cannot be endowed with a fixed N-to-C ratio because of the very structure of the JSBACH-C allocation scheme. – Because of Eq. (8) only the dynamics of the three remaining nitrogen pools, namely N_M, N_{LG}, and N_{SM}, which are the necessary additional state variables, needs to be specified.

For extending the JSBACH C-allocation scheme into a CN-allocation scheme, not only the C pools, but also the C fluxes have to be associated with N partners, because the exchange of organic molecules between pools typically carries also a N flux (compare Fig. 2.1). Important for the modelling of these fluxes – and in particular for the question of N limitation – are the proportions between the nc–values in the chain of N cycling: A flux from a pool with high nc to a pool with lower nc is associated with a gain of freely available N in the plants or soils filling the pools for mobile N or the SM pool. Only processes associated with fluxes where the receiving pool has a higher nc–value than the source pool can be limited by N availability because already for the tiniest flux to happen, additional N must be available from the mobile and SM pools. This mechanism is the source for N limitation in the model described here. Table 2.2 shows typical nc–values together with those used in JSBACH-CN. Contemplating the flux diagram with these values in mind, the locations where N availability may limit C fluxes can be identified (see

the orange bow tie symbols in Fig. 2.1). This association of C fluxes with N fluxes leads also to the explanation why the litter green pool in the present flux scheme cannot be endowed with a fixed N-to-C ratio: According to Eq. (5) fluxes with two different nc–values enter the litter green pool, namely a flux with N-to-C ratio nc_G from the green pool, and a fluxes with N-to-C ratio zero from the reserve pool and via exudates. These two types of fluxes mix during the year into the litter green pool at different proportions. Hence, during the year, the N-to-C ratio of the litter green pool must vary, because these two fluxes have different nc–values.

Table 2.2: nc_X values.

Pool X	nc_X (values in JSBACH-CN)	References	nc_X (literature range)
G	1/35	White et al., 2000	1/25 – 1/58 †
W	1/150	Cole and Rapp, 1981	1/50† – 1/250 #
LG	<= 1/75 (variable)	White et al., 2000	1/45 – 1/120 †
LW	1/550	White et al., 2000	1/550 – 1/730 †
S	1/15	Cleveland and Liptzin, 2000	1/8 – 1/30 ¶

† White et al., 2000 ¶ Zinke et al., 1984; McGuire et al., 1992; Melillo et al., 1993

Cole and Rapp, 1981; Vitousek et al., 1988; Esser et al., 2011; Yang et al., 2009

A first major design decision for constructing the coupled CN allocation model concerns the mathematical representation of N-limitation. A demand-supply ansatz is chosen, i.e. the N demand from the vegetation and soil processes are compared with the N flexibly available from the mobile and soil mineral pools, and reduce the carbon turnover accordingly. The demand by vegetation is computed by assuming that the NPP that drives the C allocation scheme (see Eq. (1)) in absence of limited N availability can be interpreted as a *potential* NPP that in absence of N limitation could be fully allocated. Hence, concerning the plants, this study does not embark into modelling N limitation from the side of photosynthetic production, e.g. via an explicit model for Rubisco availability. Instead, the problem is tackled indirectly: If there is not enough N available to perform the allocation of potential NPP, this is interpreted as a lack of Rubisco so that photosynthetic must happen at a reduced rate. The demand-supply ansatz is also applied to the soil part of

the model. Here, an alternative could be an explicit modelling of soil microbial dynamics depending on N availability. In view of today's very limited knowledge on this microbial dynamics (Zak et al., 2000; Gärdenäs et al., 2011) this would introduce additional large uncertainties. Instead, this study sticks to the implicit representation of microbial activity by the Q_{10} model already present in the C-only allocation scheme, interpreting the resulting turnover rates as maximally possible, i.e. as *potential* turnover rates that need to be limited by N availability.

A second major design decision concerns the question on the relative use of N from the two pools with rapidly available N to satisfy the plant and soil N demand. This study assumes here that the plants first use the N from the mobile N pool, before they make use of the content of the soil mineral N pool. Therefore, "demand" means here the demand of N to be supplied by the SM pool only. To obtain this demand, first that part of potential NPP has to be determined for whose allocation the vegetation itself can provide sufficient N in the mobile pool. This part will be called "direct" (NPP^{dir}), because it can be directly allocated without further use of soil mineral N. Accounting for allocation to the green and wood pools at equal proportions this is straightforwardly given by:

$$NPP_X^{dir} = \min\left(NPP_X, \frac{NPP_X^{pot}}{NPP_G^{pot} + NPP_W^{pot}} \left[\frac{dN_M}{dt}\right]^{max} {nc_X}^{-1}\right) \; for\; pools\; X = G, W \quad (9)$$

where the term in square brackets denotes the maximum rate at which the mobile N pool can supply N. In the discrete formulation used to solve the differential equations of the CN-allocation model numerically this maximum rate is set to $N_M/\Delta t$, where Δt is the time step of the discretization (1 day) so that during one time step the mobile pool can be at most fully depleted. The minimum of the two terms in (9) is taken to assure that the direct part does not surmount the intended allocation to the particular pool. With (9) the plant N demand that additionally needs to be satisfied by the SM pool is thus obtained as:

$$D_{plant} = nc_G\left(NPP_G^{pot} - NPP_G^{dir}\right) + nc_W\left(NPP_W^{pot} - NPP_W^{dir}\right) \quad (10)$$

Note that here only the potential NPP influx to the green and wood pool has to be considered, because the NPP influx to the reserve pool is not associated with a partner N-flux.

Next the N demand by the microbial decomposition of litter has to be determined. The two C fluxes that may be N limited are those from the litter green and litter wood pools to the slow soil pool. The potential C fluxes were called R_{LG}^{pot} and R_{LW}^{pot} in the previous section. Taking into account that during decomposition certain fractions $f_{LG\to A}$ and $f_{LW\to A}$ of the decomposition flux are lost as CO_2 to the atmosphere, the soil microbial N demand is given as:

$$D_{microbial} = (nc_S - \frac{N_{LG}}{C_{LG}})\left(f_{LG\to S}\, R_{LG}^{pot}\right) + (nc_S - nc_{LW})\left(f_{LW\to S}\, R_{LW}^{pot}\right) + f_{LG\to A}\frac{N_{LG}}{C_{LG}}\, R_{LG}^{pot} + f_{LW\to A}\, nc_{LW}\, R_{LW}^{pot} \quad (11)$$

Here the first line describes the N demand by microbes from the litter green and litter wood pools. The second line describes part of the soil microbial N demand that is fulfilled by the N gain associated with the release of CO_2 to the atmosphere by heterotrophic respiration from the two litter pools.

Therefore, the total demand to be satisfied by the SM pool is

$$D_{total} = D_{plant} + D_{microbial} \quad (12)$$

Having determined the N demand, the N limitation factor f_{limit}, that formally was already introduced in the previous section, can now be given a precise meaning:

$$f_{limit} = \begin{cases} \left[\frac{dN_{SM}}{dt}\right]^{max}/D_{total} & for\ D_{total} > \left[\frac{dN_{SM}}{dt}\right]^{max} \\ 1 & otherwise \end{cases} \quad (13)$$

The term in square brackets is the maximum rate at which the soil mineral N pool (SM) can supply N. Accordingly, N limitation appears when the maximum N supply rate is smaller than the demand, in which case f_{limit} is the ratio between the maximum supply rate and the demand. Hence for severe N limitation f_{limit} is close to zero. In the second case ($f_{limit} = 1$) the SM pool can satisfy the demand. – Please note that in the discretized formulation the SM pool can be depleted only once during a model time step (1 day). Thus this maximum rate is set to $N_{SM}/\Delta t$.

Having now fully introduced f_{limit}, the cycling of C in the presence of N limitation ($f_{limit} < 1$) as given by equations (2) to (6) can be explained. The total N-demand can formally be written as:

$$D_{total} = \sum_{n=1}^{4} nc_n \, F_n^{pot} \qquad (14)$$

Where the F_n^{pot} are the potential C fluxes showing up in Eqs. (10) and (11) whose realization demands for a certain amount of N according to the respective nc–values. Under conditions of N-limitation not the full demand (D_{total}) can be realized, but according to (13) only the N-flux

$$D_{limited} = f_{limit} \, D_{total} = \sum_{n=1}^{4} nc_n \, f_{limit} \, F_n^{pot} \qquad (15)$$

where (14) has been inserted. This shows that consistency between the limited N flux and C fluxes can be achieved by reducing all potential C fluxes F_n^{pot} by the factor f_{limit}. And indeed, everywhere where one of the C fluxes potentially limited by N availability shows up in equations (2) to (6), the factor f_{limit} has been inserted. Alternatively, one could think about distributing the N limitation in a more complicated way to the particular C fluxes. But without any good argument to do so, the most transparent way without need for further model parameters is to distribute the limitations according to this simple rule. It may be remarked that this in particular means that both, soil microorganisms and plants, compete equally effective for soil mineral N. And because plants live in symbiosis with mycorrhiza by which the access to mineral N is improved, this seems a reasonable assumption. – Please note that (15) contains no NPP influx to the reserve pool (compare equation (10)) because this is not limited by N availability. This is the reason why NPP_R had not been equipped with an upper index "pot", as already remarked in the previous section; in this case potential and actual flux are identical.

It remains to write down the equations for the three dynamic N pools. First the mobile N pool is considered. Although the litter green pool has a varying nc–ratio, a kind of "target" nc–ratio is needed for it to determine the amount of N re-translocated from the leaves into the mobile N pool before leaf shedding. This value is called nc_{LG}. The amount of re-translocated N is determined from the difference between the N content $nc_G F_{litter}$ of the

dropped leaves before re-translocation, and the N content $nc_{LG}F_{litter}$, the litter should have when the leaves enter the litter green pool; this is what the target nc–value nc_{LG} is needed for. Recalling that the mobile N pool not only receives N from re-translocation, but also looses N to satisfy the direct parts of NPP allocation, the equation for the dynamics of the mobile N pool can now be written as:

$$\frac{dN_M}{dt} = (nc_G - nc_{LG})\, F_{litter} - \; nc_G NPP_G^{dir} - nc_W NPP_W^{dir} \qquad (16)$$

Next the litter green pool is considered. Here a glance at the partner equation (5) for the C fluxes is helpful: At its right hand side only the influx by litter and the loss flux to the slow pool are accompanied by N fluxes, because the carbon gain from the reserve pool and the exudate flux are by definition free of N, and the N from the grazing flux is assumed to enter via dung the SM pool directly. Hence, because the litter flux was constructed to have the nc–value of the receiving slow pool, one obtains

$$\frac{dN_{LG}}{dt} = nc_{LG}\, F_{litter} - \; f_{limit}\, f_{LG\to S}\, nc_S R_{LG}^{pot} \qquad (17)$$

Finally, the dynamics for the SM pool is obtained by collecting all soil mineral N fluxes implied by the foregoing model formulation. This gives:

$$\begin{aligned}\frac{dN_{SM}}{dt} = \;& nc_S\, R_S \\ & + (nc_W - nc_{LW})\frac{C_W}{\tau_W} + \; (nc_G - nc_{LG})\, F_{grazing} \\ & - f_{limit}\, D_{total} \\ & + F_{depo} + \; F_{fix} - \; F_{leach} - F_{denit}\end{aligned} \qquad (18)$$

The right hand side term in the first line represents N gain associated with the release of CO_2 to the atmosphere by heterotrophic decomposition (R_S) from the slow soil pool. The second line describes the N gain from the decay of the wood pool and by transfer of N from the green pool to the green litter pool through grazing. The term in the third line accounts for the N losses needed by soil microbial activity and plants. Finally, the fourth line collects all N exchange fluxes with the environment, namely gains from athmospheric N deposition F_{depo} and biotic N fixation F_{fix}, as well as N losses by leaching F_{leach} and denitrification F_{denit}. All these exchange fluxes are described in detail in Appendix 2.2.

Finally, it may be noted that because of the linear downscaling of the uptake of C in presence of N limitation, the *actual* NPP (NPP^{act}) is obtained from the *potential* NPP (NPP^{pot}) by

$$NPP^{act} = f_{limit}\left(NPP_G^{pot} - NPP_G^{dir} + NPP_W^{pot} - NPP_W^{dir}\right) + NPP_G^{dir} + NPP_W^{dir} + NPP_R + F_{exudates} \quad (19)$$

(compare Eqs. (1), (10) and (15)) although one may debate whether or not to include exudate fluxes into the definition of NPP.

2.3. Setup of model experiments and driving data

Starting point for the present study are simulations performed by Roeckner et al. (2011). The simulations were performed to investigate consistently climate and carbon cycle for the historical period and into the future using a coupled climate-carbon cycle model. The authors employed a kind of reverse approach to derive for given development of atmospheric CO_2 concentration the "implied" fossil fuel emissions from the simulated land-atmosphere and ocean-atmosphere carbon exchange fluxes. These implied fossil fuel emissions were in reasonable agreement with estimates of fossil fuel emissions from economic data. For the land carbon dynamics the JSBACH-C model (as this named it here) was used, i.e. the results were obtained without considering possible changes in nutrient availability. The simulations by Roeckner et al. (2011) are – partly – repeated in the present study, but now include the cycling of terrestrial nitrogen. The term "partly" means here that only the simulations for the cycling of land carbon (plus nitrogen) are repeated, but do not run the other parts of the coupled climate-carbon cycle model used by Roeckner et al. (2011).

Such a "reduced" simulation is possible because the JSBACH-C model, as well as the JSBACH-CN model, need only a very few inputs (compare Section 2.2). The necessary inputs for JSBACH-C are Net Primary Productivity (NPP), Leaf Area Index (LAI), soil temperature, and soil moisture, for JSBACH-CN in addition runoff is needed. These inputs are taken from the published data of the study by Roeckner et al. (2011) found in the CERA database (Roeckner, 2009). Data are retrieved for the period (1860-2100). Concerning the future climate development, Roeckner et al. (2011) performed simulations

following several different scenarios. In the present study, only simulation results obtained for the SRES A1B scenario are used (for a description see Nakicenovic et al., 2000).

To prepare the transient simulations with JSBACH, first the carbon and nitrogen pools were brought into equilibrium by performing two successive spin-up simulations, using a repeated 30 years cycle obtained from the above forcing data (data used from 1860-1890). By running JSBACH-C, first the carbon pools are brought into equilibrium. They typically reach their pre-industrial steady state after 5000 years of simulations. To find also the pre-industrial steady state for the combined set of carbon and nitrogen pools, JSBACH-CN is initialized with the carbon pool obtained in the first spin-up, and nitrogen pools estimated from typical N-to-C values. The obtained equilibrium pool values are then used to initialize the transient simulations 1860-2100 explained below.

In addition to the forcing data needed to run JSBACH-C, for JSBACH-CN also atmospheric N deposition data are needed: For the pre-industrial simulations the data set are used from Galloway et al. (2004). To generate N deposition maps for the whole period 1860-2100 the snapshot maps for years 1860, 2000, and 2030 by Galloway et al. (2004) and Dentener et al. (2006) were linearly interpolated/extrapolated proportionally to the development in atmospheric CO_2 concentrations for the historical period and the subsequent CO_2 development under the A1B scenario (see Appendix 2.2 for details).

The questions addressed in this study are investigated by performing a series of transient simulations experiments (Table 2.3), all covering the years 1860-2100. The first transient experiment, called C is performed with JSBACH-C, i.e. without any nitrogen dynamics. Because the simulation is forced with data from the Roeckner et al. (2011) study, this simulation simply reproduces the development of the land carbon dynamics found there. The second experiment (called CN) is the main experiment in this study, where the full JSBACH-CN model is used as described in Section 2.2. All other experiments summarized in Table 2.3 are either setup to check the robustness of the assumptions behind particular design decisions for the model (CN-mi and CN-pl) or to analyze special aspects showing up in the CN-simulation (CN-ct, CN-fd, CN-lz, and CN-ns). Details of the setup of these experiments will be explained in subsequent sections. – Please note that, if not otherwise stated, throughout the simulations a constant land cover map (1860 A.D) is used.

Table 2.3: List of experiments to study the C-N interactions during 1860-2100.

Experiments	Remarks and modifications
C	C - only simulation
CN	C-N reference simulation
C-u	Like C experiment, but "uncoupled"
CN-u	Like CN experiment, but "uncoupled"
CN-mi	microbes 1st priority for soil mineral N
CN-pl	plants 1st priority for soil mineral N
CN-ct	constant temperature
CN-fd	fixation doubled
CN-lz	leaching zero
CN-ns	nc-value of soil pool reduced

Notes: transient CO_2 forcing is same in all experiments; transient temperature forcing is same in all experiments except CN1; transient F_{depo} forcing is same in all experiments when N cycle is active.

2.4. Results

2.4.1. Improvement of excess carbon

The term "excess carbon" means the amount of carbon or NPP that can't be allocated in any of the three vegetation carbon pools, i.e. green, reserve, and wood, due to the structural limit of the pool size (see Appendix 2.1 for details). This means that the excess amount of carbon is a carbon allocation problem in the JSBACH-C model. In addition, if the explicit N cycle is added to the existing JSBACH-C model, the excess carbon leads to an additional problem of N mass conservation. This is simply because the N-containing organic compounds associated with this amount of excess carbon are unknown. In order to reduce the excess amount of carbon, this study thus implements additional carbon cycle processes as well as it improves model parameters (see Appendix 2.3 and 2.4 for details). The above mentioned improvements are incorporated in the JSBACH-CN model.

In Table 2.4, the excess carbon is compared between the JSBACH-C and JSBACH-CN model. More precisely, the comparison is done with the JSBACH-C model version that

was used by Pongratz et al. (2009) and Roeckner et al. (2011). From this JSBACH-C model version, the total excess C is found to be around 41 Pg C (or 58% of total NPP) from all PFTs (Table 2.4). This is mostly because of the missing carbon cycle processes in the JSBACH-C model, for example, root exudates, grazing, fire, harvesting, etc. As a consequence, these amounts of excess C was simply allocated in the fast soil pool without passing the carbon from the vegetation pools.

Table 2.4: Comparison of excess C between the JSBACH-C and JSBACH-CN model for present-day conditions (means for 1970-99). Excess C in % is with respect to total NPP.

		JSBACH-C		**JSBACH-CN**	
PFTs	**NPP (Pg C)**	**Excess C**	**% Excess C**	**Excess C**	**% Excess C**
TrBE	25.8	15.37	21.65	0.94	1.3
TrBD	8.72	5.96	8.39	1.0	1.4
TempBE	0.67	0.35	0.49	0.0	0.0
TempBD	2.79	0.72	1.01	0.0	0.0
EC	5.25	0.37	0.52	0.0	0.0
DC	0.63	0.005	0.01	0.0	0.0
ES	5.2	3.02	4.25	0.42	0.6
DS	0.02	0.014	0.02	0.0	0.0
C_3G	6.83	5.13	7.23	0.18	0.2
C_4G	8.9	7.38	10.39	0.0	0.0
Tundra	0.22	0.04	0.06	0.0	0.0
Crop	6.05	3.42	4.82	0.5	0.7
Total	71.0	41.7	**58.8**	3.0	**4.2**

Abbreviations:

TrBE: Tropical broadleaf evergreen trees; TrBD: Tropical broadleaf deciduous trees
TemBE: Temperate broadleaf evergreen trees; TemBD: Temperate broadleaf deciduous trees; EC: Evergreen coniferous trees; DC: Deciduous coniferous trees; ES: Evergreen shrubs; DS: Deciduous shrubs; $C_{3/4}$ G: $C_{3/4}$ grasses

More amounts of excess C are mainly from grasslands (i.e. C_3 and C_4 grasses) and tropical forests as compared to the other PFTs in the JSBACH-C model (Table 2.4). Tropical forests contribute around 30% excess C, whereas grasslands account for around 18%. The remaining 10% excess C is from the evergreen shrubs and crops. In contrast, the simulation results of the C experiment obtained from the JSBACH-CN model show that the added processes, especially grazing, lead to a substantial reduction of the excess C

from grasslands as compared to forests (tropical, temperate, and coniferous) and shrubs. The reason for this is that higher grazing rates are accounted in grasslands than for forests and shrubs. In addition, root exudates reduce the excess C to some extent from all PFTs.

The model parameters that are improved are leaf shedding (or leaf longevity) and green carbon to leaf carbon ($f_{G/L}$); the later parameter determines the structural limit of the green pool (see Appendix 2.1 for details). The leaf shedding is mostly computed from LAI drops but in evergreen species the leaf turnover by aging is fully compensated by leaf growth so that for this case a constant shedding rate is assumed. The results show that the improved leaf shed constant in grasslands and evergreen forests indeed reduces the amount of excess C. The parameter, $f_{G/L}$ determines the amount of litter carbon (F_{litter}). By improving this parameter it also reduces the excess C from all PFTs.

By incorporating the above carbon cycle processes and improving model parameters, the amount of excess C is reduced considerably in the JSBACH-CN model, which is around 4% (or 3 Pg C) of total NPP. For tropical forests, the amount of excess C is reduced to 2.7% from 30%. For grasslands, 18% excess C by JSBACH-C model is allocated completely in the JSBACH-CN model. Nevertheless, there are still some missing processes in the model and because of that around 4% excess C is still not allocated and it needs to be improved in future. Moreover, these added processes and model parameters not only reduce the amount of excess C from the model but also improve the C allocation in a most reasonable way.

2.4.2. Contemporary land carbon cycle

2.4.2.1. Today's land carbon sink

To demonstrate that at global scale the simulated cycling of carbon in the C and CN simulations is consistent with observations, in Table 2.5 observed and simulated land uptake is compared for the 80s and 90s. CO_2 concentration in the atmosphere fertilizes the land vegetation so strongly that despite C losses from land use changes (deforestation) the continents act as a C sink. In order to compare the C sink fairly with observational estimates, the C and CN simulations are performed explicitly with land use change. The simulations show that the C sink is about 2.55 and 3.1 Pg C/yr by the C experiment for

1980s and 1990s, respectively. This is about 0.75-1.1 Pg C/yr larger than the sink found by Roeckner et al. (2011), who used an earlier version of JSBACH-C. The inclusion of the land N cycle reduces the land C sink in the CN experiment by about 0.1 Pg C/yr for 1980s and 1990s. All these values are well within the uncertainty range from observational estimates (Roedenbeck et al., 2003; IPCC AR4).

Table 2.5: Comparison of simulated land carbon sink (Pg C/yr) for 1980-89 and 1990-99 with observational estimates.

	1980s	**1990s**
C	2.55	3.1
CN	2.45	3.0
Roeckner et al. (2011)	1.8 [a]	2.0
IPCC AR4	1.9±1.1 [b]	2.6±1.1 [b]
Roedenbeck et al. (2003)	2.2±0.9	2.6±0.9
CN-mi	2.45	2.8
CN-pl	2.60	3.2

[a] Personal communication by Traute Crueger.

[b] Assuming emissions due to land use change as in IPCC Special Report on Land Use, Land-use Change and Forestry (2000).

2.4.2.2. Today's land carbon stock

In Table 2.6, the simulated global land C stocks of vegetation, litter, and soil are presented that is obtained in the C and CN experiments (i.e. with land use change) for the last three decades of the 20th century. The simulations results show that the simulated vegetation C stock is around 472 Pg C or 18% of the total C (Table 2.6) of which around 122 Pg C is lost by land use emissions over the period 1860-2000. Thus, the total vegetation C stock is around 594 Pg C and is in general agreement with inventory based estimates (ca. 560-652 Pg C) by Saugier and Roy (2001). The simulated litter C stock is found to be around 204 Pg C (ca. 8% of total C). This includes in the model below ground litter. Assuming that above ground litter makes about half of the total litter, it ends up with about 102 Pg C for above ground litter, which is comparable with estimates based on observations (68-97 Pg C) by Matthews (1997) or models (47-196 Pg C) (Matthews, 1997; Wang et al., 2010).

The simulated soil C stock is around 1980 Pg C (ca. 74% of total C), which is higher than the estimate of 1500 Pg C for the top 1 meter depth of soil by by Post et al. (1982), but lower than the estimate of 2300 Pg C for the top 3 meters by Batjes (1996).

Table 2.6: Global land C stocks obtained by the C and CN experiments (means for 1970-99).

Pool sizes: Pg C	**C**	**CN**
Vegetation C	473.7	471.3
Litter C	202.6	207.1
Soil C	1992.2	1969.8
Total C	2668.5	2648.2

As expected, due to the additional constraint of N availability, the global C stored at land is slightly lower in the CN experiment than in the C experiment. Besides a slightly lower value for vegetation C, this reduction arises mainly from the C in soils, whereas the litter C stock is even slightly larger in the CN experiment. This counter intuitive behaviour arises because in contrast to the soil decomposition fluxes, the C-influxes from the litter pool to the soil C pool are limited by N availability.

2.4.3. Comparison with site-scale observations

In this section the simulated fluxes and N stocks are compared with observations from the so-called 'calibration sites' from Raich et al. (1991) and McGuire et al. (1992) covering various PFTs (see Appendix 2.5 for details about sites). The sites data consist of NPP, plant N uptake rate, plant N content, and soil organic N content.

Unfortunately, such a comparison of simulation results with data obtained at site scale (meters) cannot be considered as a fair test of the quality of the model because it has been developed for a quite different scale, namely the scale of several grid boxes of Earth system models, which are hundreds of kilometres. Nevertheless, this comparison here is presented, to demonstrate that in an order-of-magnitude sense the model behaves as should be expected.

The simulation data used for comparison are the mean values from 1970 to 1999 obtained from the CN simulation. In Figure 2.2a simulated actual annual NPP is compared (see Eqs. (1) and (19)) with observations. Simulated NPP is well correlated (r=0.90, n=12, $p < 0.001$) with the observations. Equally good correlations are found for plant N content (Figure 2.2b), and the plant N uptake (Figure 2.2c). Outliers in these latter two figures are mostly from tropical forest sites. For these sites simulated plant N content and also plant N uptake is smaller than observed. These differences may be explained by differences in the nc–value for woody biomass: In this model, a global average value $nc = 1/150$ is used for all vegetation types (see Table 2.2) that is smaller than the value $nc = 1/75$ at the tropical observation sites (see Raich et al., 1991). Moreover, it is well known that for large parts of the tropics plant growth is limited by lack of phosphorus (P) (Tanner et al., 1998; D'Antonio et al., 2006), so that from this point of view the model should in the tropics overestimate NPP, and underestimate plant N content and plant N uptake, which is partially seen in Figs. 2a-2c, although this tendency is not fully consistent for all tropical sites.

For simulated soil organic N content the correlation with observations turns out to be much weaker (Figure 2.2d) (r=0.58, n=12, $p < 0.05$). This could actually be expected since the decomposition of organic material very much depends on the particular local community of microorganisms, that surely cannot be represented on a model like this. Nevertheless, it should be recognized that simulated values are in the proper range of observation values. And once more here, three tropical sites are involved in overestimations.

Besides this comparison with site scale observation, in Appendix 2.6 simulated global N storages as simulated by the JSBACH-CN model are compared with those obtained by various other models (Xu-Ri and Prentice, 2008; Wang et al., 2010; Zaehle et al., 2010b). The vegetation and the litter N are simulated to be 4.9 and 1.2 Pg N, respectively. The simulated soil organic N and inorganic N storage are around 139.5 and 1.2 Pg N, respectively. These results are consistent with those obtained by various other models and also with published observational estimates (see Appendix 2.6 for details).

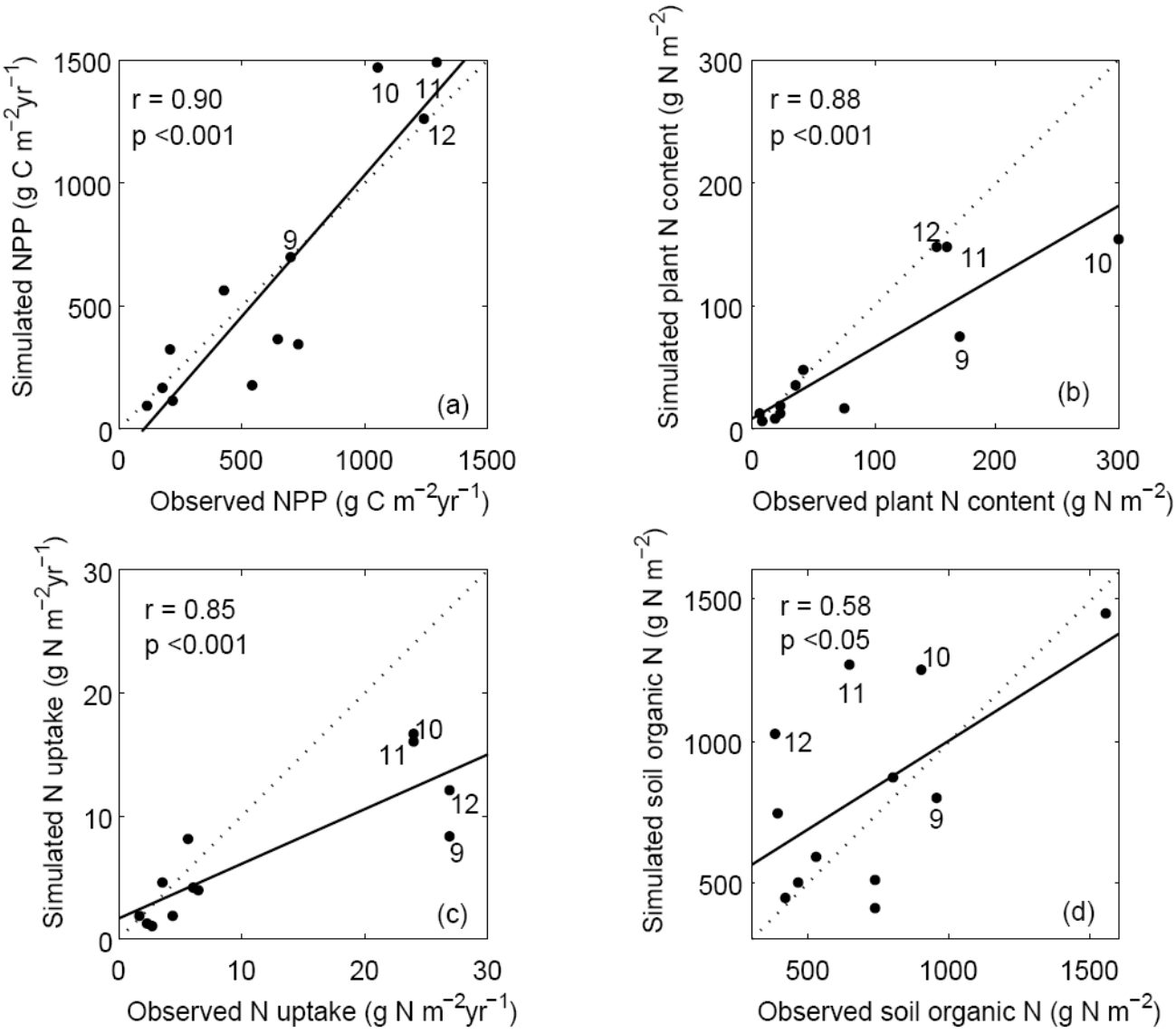

Figure 2.2: Comparison of simulated actual annual NPP (a), plant N content (b), plant N uptake (c), and soil organic N content (d) with observations (n = 12). The diagonal dotted lines are the 1:1 line and the solid line represents the least square regression line. The numbers 9 to 12 are the tropical forest sites (Appendix 2.5).

2.4.4. Effect of N limitation on the global land carbon

Here the C and CN experiments are analyzed with respect to nitrogen constraints on the global land carbon cycle in response to increasing atmospheric CO_2 concentration (SRES A1B scenario) and climate change. For this principal study: Henceforth, the simulated data are analyzed only from natural vegetations in order to prevent the complications that will arise from land use change. The simulations results show that the change in total land carbon uptake is around 107 Pg C and 98 Pg C over the period 1860 to 2000 for the C and CN experiments, respectively (Figure 2.3). So the land carbon uptake until 2000 differs only by about 9 Pg C (or 8%) by accounting for changes in N availability. For the period 2000-2100, the land carbon uptake projected by the C experiment is 366 Pg C, but in the CN experiment it is projected as 308 Pg C. Thus, N limitation causes a reduction of the total land carbon uptake by about 58 Pg C (or 16%).

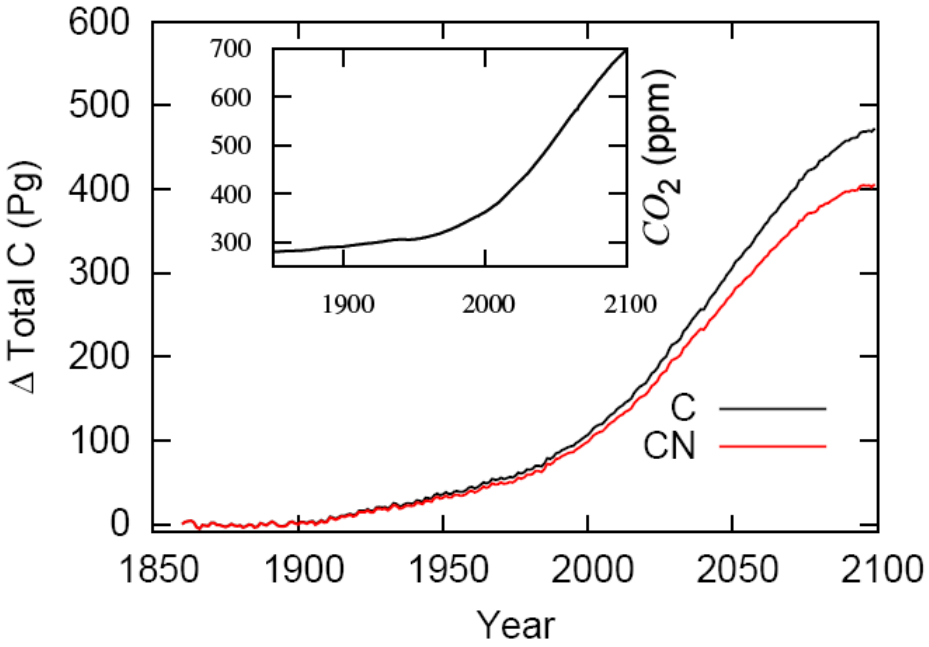

Figure 2.3: Change in the total land carbon uptake over the period 1860-2100 in the C and CN experiments. The inset shows the atmospheric CO_2 concentration (ppm) underlying the simulations for the historical period and the SRES A1B emission scenario.

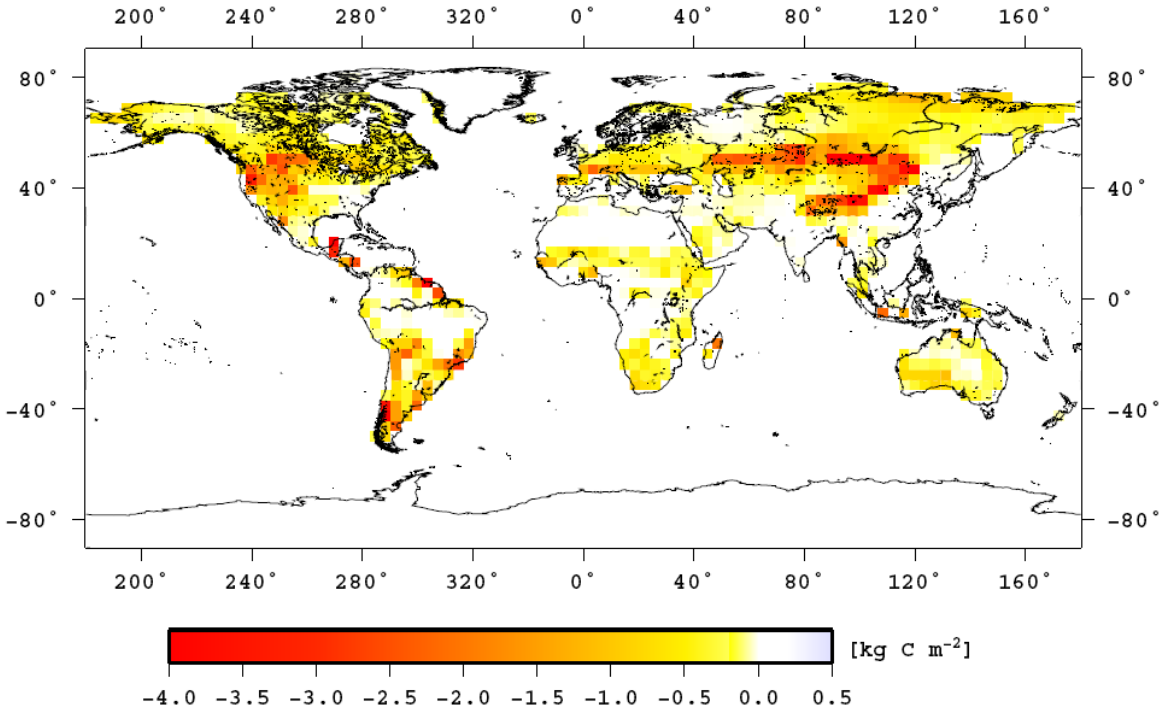

Figure 2.4: Spatial distribution of change in 30 years means (2070-99) of the total global land C storage (CN – C experiments).

To see which vegetation is constrained by N availability, Figure 2.4 shows the spatial distribution of change in total land carbon storage (i.e. CN minus C) for the last three decades of the 21st century, where negative values indicate a reduction of the land carbon storage due to N limitation. The strongest limitation is found in temperate regions where a reduction up to 4 kg C m^{-2} is seen. Further analysis shows that in these regions mostly grasslands rather than forests ecosystem are affected (the steppes of Asia and North America). The same is true for subtropical grasslands especially at some regions of Southern America. N affects mostly the C_3 grasses in temperate and boreal regions due to high microbial N demand. This in turn, leads to less mineral N availability. Additionally, lower temperature in this region also leads to slow mineralization rate and thereby less mineral N availability. Although tropical and subtropical forests are highly productive, which implies a particularly high plant N demand, the results show that they are almost everywhere unconstrained by N availability except for some small regions. N availability doesn't limit especially tropical and subtropical forests because of high mineralization rate induced by warming.

Table 2.7: Global land C stocks at the end of the 21st century obtained in C and CN experiments (means for 2070-99). ΔC denotes change in land C stocks (CN minus C) and parenthesis values are change in percent.

Pool sizes: Pg C	**C**	**CN**	**ΔC**
Vegetation C	783	767	-16 (-2.0%)
Litter C	240	246	6 (+2.5%)
Soil C	1938	1887	-51 (-2.6%)
Total C	2961	2900	-61 (-2.0%)

Comparing for the two experiments the carbon stocks at the end of the 21st century (see Table 2.7), it is seen that N availability mostly affects carbon storage in soils (51 Pg C difference) as compared to vegetation and litter carbon storage. For the absolute values of stored C this is simply a mass effect: in a linear rate model changes in throughout affect the largest pools strongest, which is here the soil C stock. But also in a relative sense soil C storage is affected most: The reason for this is that N availability limits in this model the turnover rate of litter carbon but not that of soil carbon. Accordingly, for the litter pool the ratio between in- and outfluxes increases during the 21st century, whereas for the soil pool this ratio decreases, to the consequence that there is a relative increase in litter carbon of 2.5%, but a relative decrease in soil carbon of 2.6%.

There is some evidence in the literature for a reduction of soil carbon stocks by limited N availability: Knops et al. (2009) reported for a grassland site that the accumulation of soil carbon tended to be limited by N inputs, which potentially can be constrained by soil mineral N availability (Wedin and Tilman, 1996; Knops and Tilman, 2000). The results are also consistent with simulations performed with the ISAM-CN model that also shows a reduction of the soil carbon storage due to N limitation (Jain et al., 2009). Generally, it would be interesting to see whether observations could confirm the relative increase in litter carbon and the relative decrease in soil carbon following a reduction in N availability that is seen in the simulations.

2.4.5. Competition between plants and soil microorganisms for soil mineral N

To check the robustness of the assumptions behind the major design decisions for the model (see Section 2.2.2) two additional experiments are performed called CN-mi and CN-pl (Table 2.3). In these experiments, f_{limit} is distributed in a more complicated way to the particular C-fluxes by giving a different priority to the soil microorganisms and plants in their competition for soil mineral N. In the standard CN experiment soil mineral N is distributed to microorganisms and plants proportional to their demand (see equation 12 and 13). Instead, in the CN-mi experiment, soil microorganisms are allowed to tap first into the soil mineral N pool to satisfy their N demand (i.e. $D_{microbial}$), and plants are allowed to use only the remaining soil mineral N. In the other experiment, called CN-pl, the converse rule is used: plants are allowed to use the soil mineral N first to satisfy their N demand (i.e. D_{plant}), and only the rest is allowed to be used by soil microorganisms.

By giving priority to soil microorganisms (CN-mi) for soil mineral N, the results show that the carbon decomposition rates (i.e. C turnover) are enhanced substantially in the litter pool as well as in the slow soil pool. As a result, the litter C and the soil C storage are reduced in the CN-mi experiment as compared to the CN experiment (with equal priority between plants and microorganisms). Results also show that the left over soil mineral N is still sufficient to satisfy plant demand (D_{plant}) so that productivity is not affected. Overall, by the end of the 21st century the total land C uptake is reduced by about 30 Pg C (ca. 7%) as compared to the CN experiment (Figure 2.5), which suggests a minor effect of this model assumption on the total global land C uptake. Generalizing this result, the simulation experiments suggest that an increased N availability to soil microorganisms not necessarily translates into increased ecosystems C storage because increased N availability can stimulate the C decomposition rate. This is in line with studies by Körner and Arnone (1992) and Hu et al. (2001) who reported that increased N availability leads to a faster C turnover rate and thereby limits ecosystem C storage.

Conversely, by giving priority to plants (CN-pl), the results show that in this case the soil mineral N availability limits the litter C decomposition rate substantially. As a consequence, more carbon remains in the litter pool. The total land C uptake is enhanced substantially by about 81 Pg C (ca. 20%) by the end of the 21st century as compared to the CN experiment (Figure 2.5), which results in a substantially larger accumulation of C in

the terrestrial ecosystems. Further analysis shows that the litter C decomposition rate is constrained strongest in temperate and boreal C_3 grasses as compared to forest ecosystems.

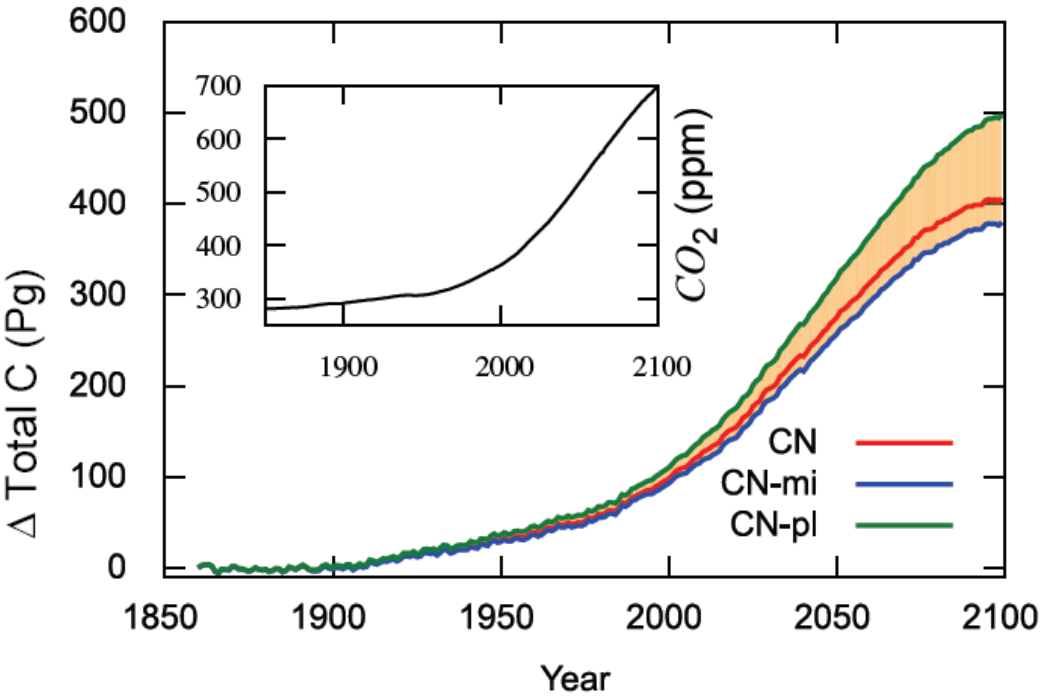

Figure 2.5: Sensitivity check of the competition between plants and soil microorganisms for accessing the soil mineral N. The shaded region depicts the sensitivity of total land carbon uptake to the way soil microbial and plant access to soil mineral N is modelled.

Furthermore, the carbon sinks for the 1980s and 1990s obtained by the CN-pl experiment differ only slightly from the values obtained in the C experiment for these decades (compare Table 2.5). In the CN-mi experiment, the carbon sink obtained for 1980s almost equals the sink found in the CN experiment, but it is less by about 0.2 Pg C/yr for 1990s. This difference is well within the uncertainty of observations (compare Table 2.5).

Comparing Fig. 2.3 and Fig. 2.5, it shows that despite N limitation the CN-pl experiment accumulates more carbon than the C experiment. The overall effect is not large: By the end of the 21st century the total land C stock is enhanced by about 19 Pg C (ca. 1%) in the CN-pl experiment as compared to C experiment. Nevertheless, to understand why this larger C stock arises in Table 2.8 the global land C stocks are compared that obtained in the C and CN-pl experiments for the last three decades of the 21st century. The results show that the difference comes mainly from the litter C stock which is about 32% larger than in the C experiment. The reason for the higher litter C stock is that in the CN-pl

experiment soil microorganisms have only reduced access to soil mineral N which severely limits the decomposition of litter carbon (see Section 2.4.4). This result in a relatively larger accumulation of litter C stocks, which in turn, leads to larger accumulation of C in the terrestrial ecosystems.

Table 2.8: Global land C stocks at the end of the 21st century obtained in C and CN-pl experiments (means for 2070-99). ΔC denotes change in land C stocks (CN-pl minus C) and parenthesis values are change in percent.

Pool sizes: Pg C	**C**	**CN-pl**	**ΔC**
Vegetation C	783.0	776.5	-6.5 (-1.0%)
Litter C	240.0	318.5	78.5 (+32%)
Soil C	1938.0	1885.0	-53.0 (-2.7%)
Total C	2961.0	2980.0	19.0 (+1.0%)

2.4.6. Nitrogen availability and feedback between climate and carbon cycle

The term climate-carbon cycle feedback was introduced by Friedlingstein et al. (2006) which refers to "an increase in CO_2 leads to climatic change, and climatic change in turn affects the CO_2 concentration, the climate, atmospheric CO_2, and the carbon cycle form a feedback loop" (Friedlingstein et al., 2006). To study the effect of nitrogen on the climate-carbon cycle feedback two additional experiments are performed similar to the previous C and CN experiments but without CO_2 induced climate change. These additional C and CN experiments (called C-u and CN-u in Table 2.3) are referred here as "uncoupled" simulations, a terminology that was introduced by Friedlingstein et al. (2006). Accordingly, the standard C and CN experiments are called here "coupled". Technically, the difference between the coupled and the uncoupled experiments is that in the former case JSBACH is driven by climate data from simulations by Roeckner et al. (2011) obtained with the full coupled version of the MPI-ESM (see Section 2.3), whereas for the additional simulations the driver data are taken from the "uncoupled" MPI-ESM simulation by Roeckner et al. (2011). In this latter uncoupled simulation the CO_2 concentration was kept fixed in the radiation code at its pre-industrial value 282 ppm, so that no greenhouse warming appeared, although the land biosphere still had to react to the increasing atmospheric CO_2.

For global land C uptake the simulations give 567.5 and 362 Pg C over the period 2001-2100 for the uncoupled and coupled C experiments, respectively (Table 2.9). Thus, the land C uptake is largely reduced by 205.5 Pg C in the coupled simulations. This is caused by the positive climate-carbon cycle feedback (see also Friedlingstein et al., 2006; Raddatz et al., 2007; Roeckner et al., 2011). With N cycle, the land C uptake is reduced only by 162 Pg C. Accordingly, the climate-carbon cycle feedback is still positive but 21% smaller than without nitrogen. To address the uncertainty arising from the handling of N in the model the feedback has also been analyzed for CN-pl experiment: Here the inclusion of the N has the opposite effect, namely an increase of the magnitude of the positive climate-carbon cycle feedback by 33% as measured by the difference in carbon uptake.

Table 2.9: Global land carbon uptake (Pg C) in coupled and uncoupled simulations (SRES A1B scenario) over the period 2001-2100 for the C, CN, and CN-pl experiments.

	uncoupled	**coupled**	**coupled-uncoupled**
C	567.5	362.0	-205.5
CN	466.0	304.0	-162.0
CN-pl	656.5	383.0	-273.5

The reason for the smaller feedback with nitrogen in the standard CN experiment is that nitrogen limitation is stronger for the uncoupled simulation than the coupled simulation due to a smaller mineralization rate. Thereby, NPP is strongly affected by nitrogen availability in the uncoupled simulation. This leads to less vegetation C uptake as well as soil C uptake. As a consequence, the difference of land carbon uptake between the coupled and uncoupled simulations is lowered by nitrogen availability, leading to a smaller feedback.

However, for the CN-pl simulation the situation is different: Here NPP in the uncoupled simulation is behaving almost like in the uncoupled C simulation, i.e. it isn't significantly affected by nitrogen availability. But nitrogen availability severely reduces the turnover rate of litter carbon in the uncoupled simulation and thus, stores more carbon in the ecosystems. Although in the coupled simulation mineral N availability is increased by global warming this effect cannot compensate for the retention of litter carbon seen in the uncoupled simulation. As a result, the difference of land carbon uptake between the

coupled and uncoupled simulations is larger in the CN-pl experiments than in the CN leading to a stronger positive feedback.

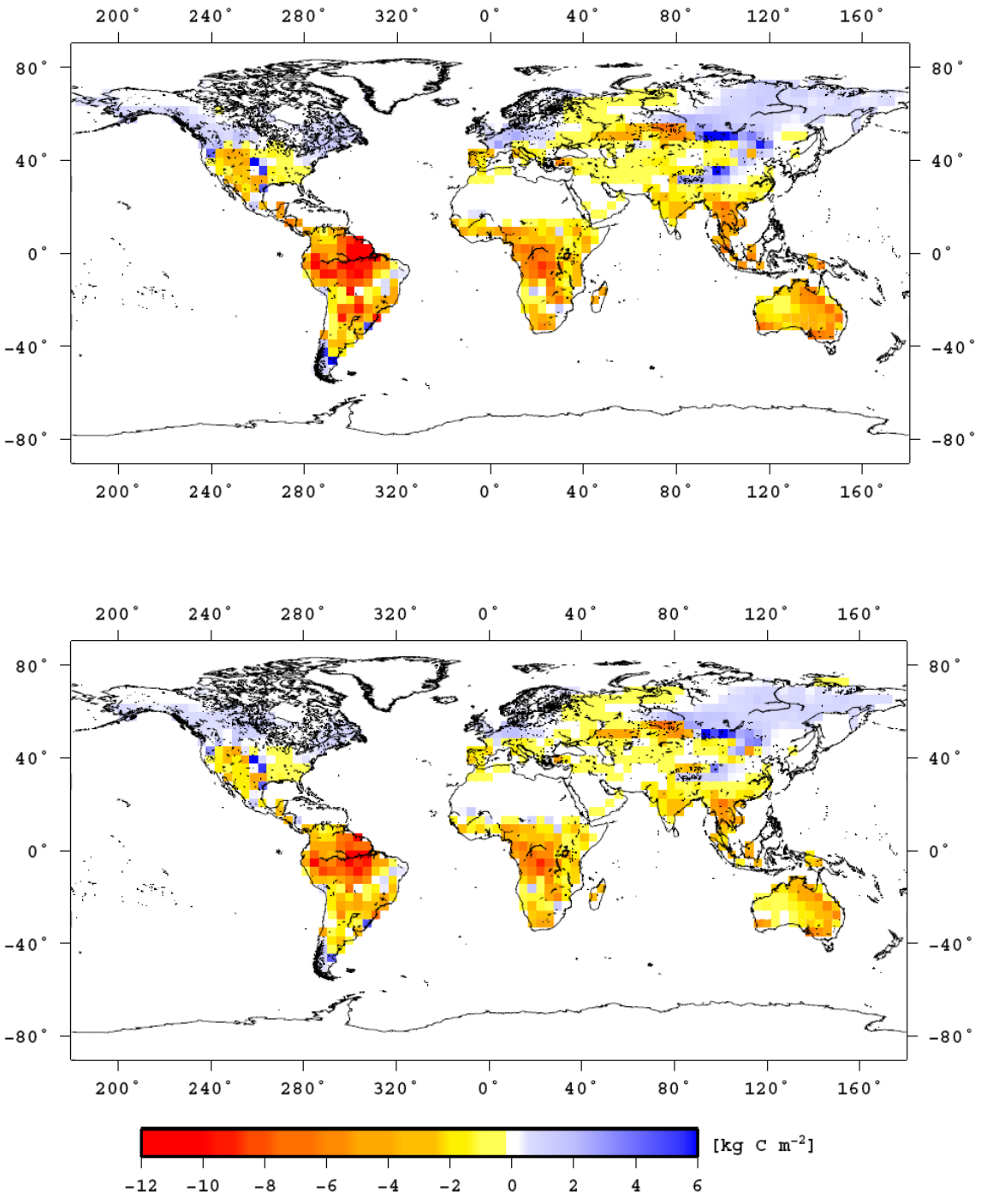

Figure 2.6: Difference in land C uptake between the coupled and the uncoupled simulations in the period 2070-2100. Top: C simulations; bottom: CN simulations. Regions with negative (positive) values take up less (more) carbon under global warming conditions and contribute to a positive (negative) climate-carbon cycle feedback.

The regional contribution to the global climate-carbon cycle feedback is shown in Figure 2.6 (means for 2070-99) for the C experiment (top) and the CN (bottom). In both cases the tropical regions are the main contributors to the positive climate-carbon cycle feedback. In contrast, the contribution of the low-latitude boreal regions is negative. This opposing behaviour has already been discovered and explained by Raddatz et al. (2007), where an almost identical simulation setup was used. Hence, by accounting for nitrogen availability, the geographic signature of the feedback is not changed, only its magnitude is affected. Further ananlysis shows that forests and grasslands ecosystem behave similar with respect to the climate-carbon cycle feedback.

2.4.7. Progressive nitrogen limitation

As discussed in the previous sections, the simulations show for the 21st century a significant reduction of C storage in the CN experiment as compared to the C experiment, and this happens predominantly in grasslands. In the present section this study investigates whether this reduction can be explained by the progressive nitrogen limitation hypothesis (PNL), claiming that under increased atmospheric CO_2 concentrations the associated enhanced plant productivity leads to enhanced sequestration of organic N in long-lived wood and SOM that subsequently leads to a lack of N availability (see the discussion in the introduction). To this end this study further analyzes the CN experiment, but complements it by an additional experiment CN-ct, which is identical to the CN experiment, except that the soil temperatures are kept at their pre-industrial values. By this additional experiment the effect of increasing CO_2 is isolated.

An obvious radical question in model simulations is: How PNL can be detected. For example, an indicator of PNL could be whether the fraction of ecosystem N content locked up in organic molecules is increasing under increased atmospheric CO_2 concentrations. Decrease in N mineralization or increase in microbial N immobilization could be also an indicator of PNL (Luo et al. 2004; de Graaff et al. 2006). They subsequently can reduce the soil mineral N availability through high plant N uptake and N immobilization by soil microorganisms under increased CO_2 concentrations. Here the soil mineral N availability is taken as an indicator to detect the PNL.

Figure 2.7 shows the simulation results for soil mineral N storage, separately for forests (tropical/subtropical and temperate/boreal) and grasslands (tropical/subtropical and temperate/boreal). At first tropical and subtropical forest ecosystems (including shrubs) are considered. For these Figure 2.7a shows that the simulated soil mineral N availability in the CN experiment decreases from 1950 to 2040 (Like PNL), followed by a relaxation thereafter (Not PNL). In contrast, in the CN-ct experiment, the soil mineral N availability decreases from 1950 and remains almost constant throughout the 21st century (Like PNL). This shows that the two contrasting effects (Like PNL / Not PNL) of soil mineral N availability are largely controlled by warming effects. More precisely: The warming enhances N mineralization and thus leads to additional releases of mineral N to the soil. If this effect gets larger than the sequestration of N following raising CO_2 concentrations, the system overcomes PNL. This explains the change around 2040 seen in the CN experiment.

This soil mineral N availability leaves its traces in NPP (Figure 2.7, right panel): In the CN experiment relative NPP difference is reduced up to 1.6% until 2040 (compared to the C experiment), whereas in the CN-ct experiment, around 3.6% reduction of relative NPP difference is found until 2040. The relative NPP difference is reduced less in the CN experiment as compared to the CN-ct experiment, which indicates the importance of PNL. Indeed, the CN experiment shows that the relative NPP difference starts recovering after 2040 which is in line with increased availability of soil mineral N (compare Figure 2.7a). In contrast, the CN-ct experiment shows that the relative NPP difference reduction is still increasing until 2100. The reason for this is that although soil mineral N availability remains almost constant from 2040 to 2100, NPP is increasing due to CO_2 fertilization and thus leads to higher plant N demand. This causes nitrogen limitation and leads to a reduction in relative NPP difference. Accordingly, for forests and shrubs (tropical and subtropical) the relative reduction in productivity is indeed a result of PNL.

But this behaviour depends on the forest type: It is even stronger for temperate and boreal forests. For these Figure 2.7b shows that the simulated soil mineral N availability in the CN experiment decreases well into the 21st century (Like PNL), followed by a relaxation thereafter (Not PNL). In contrast, in the CN-ct experiment, the soil mineral N availability is not recovering from the decrease (Like PNL). As a result, in the CN experiment relative NPP difference is reduced up to 5% until 2070, whereas in the CN-ct experiment, around 14% reduction of relative NPP difference is found until 2070 (Figure 2.7b, right panel).

After 2070, a slight recovery of relative NPP difference in the CN experiment is seen (compare Figure 2.7b, right panel) that follows the enhanced soil mineral N availability. In contrast, the CN-ct experiment shows that the relative NPP difference reduction is still increasing until 2100 because of high plant N demand as discussed above. Besides, less soil mineral N availability in the CN-ct experiment can even lead to threefold higher relative NPP difference reduction as compared to the CN experiment. In summary, the results show that temperate/boreal forests are strongly affected by N availability.

For grassland ecosystems (Figure 2.7c), only C_3 grasses are considered because C_4 grasses are unaffected by increasing CO_2 because of their particular metabolism. First tropical and subtropical C_3 grasses will be considered (Figure 2.7c). Here N availability in the CN experiment decreases continuously from the 19th century until the first half of the 21st century and recovers thereafter. In the CN-ct experiment the same behaviour is seen, but the recovery is much weaker. As a result, in the CN experiment the relative NPP difference is reduced up to 10% until 2050, whereas in the CN-ct experiment, 15% reduction of relative NPP difference is found until 2050 (Figure 2.7c, right panel). After 2050, the recovery in soil mineral N leads to a stabilization of relative NPP difference in the CN experiment (compare Figure 2.7c, right panel). Accordingly, for tropical and subtropical C_3 grasses, the reduction in productivity is indeed a result of PNL.

This PNL behaviour is even stronger for temperate and boreal C_3 grasses. Figure 2.7d shows that soil mineral N availability decreases continuously throughout the whole simulation for the CN and CN-ct experiments. As a result, the relative NPP difference is reduced up to 20% and 35% until end of the 21st century for the CN and CN-ct experiments, respectively (Figure 2.7d, right panel). Overall, the results show that temperate and boreal C_3 grasses are severely limited by N availability causing as a result of PNL a strong reduction in relative NPP difference.

In forests ecosystem, PNL develops mostly at the beginning of the 21st century and continued until first half of the 21st century but thereafter the PNL is alleviated due to the relaxation of soil mineral N availability. Conversely, in grasslands, PNL develops much earlier than forests. They develop mostly at the beginning of the 19th century and continued until first half of the 21st century. However, thereafter the occurrence of PNL is also relaxed because of the relaxation of N scarcity from climate warming.

Further analysis shows that the soil mineral N availability substantially decreases for the 21st century in the Northern high latitude boreal regions as compared to tropical and subtropical regions. This is due to climate warming that induces higher annual NPP by prolonging the growing season of vegetation in the boreal regions. Accordingly, the enhanced NPP leads to higher plant N uptake, which in turn, leads to a less soil mineral N availability. Thus, these mechanisms lead to PNL in both forests and grasslands ecosystem in the Northern high latitude boreal regions. On the other hand, tropical and subtropical vegetations are already adapted to climate warming and thereby warming does not have any influence on the growing season of vegetation (i.e. stabilization of NPP). Thus, these mechanisms lead to an avoidance of PNL in tropical and subtropical ecosystems. Therefore, the recovery of PNL is much stronger in tropical and subtropical ecosystems than the temperate and boreal ecosystems.

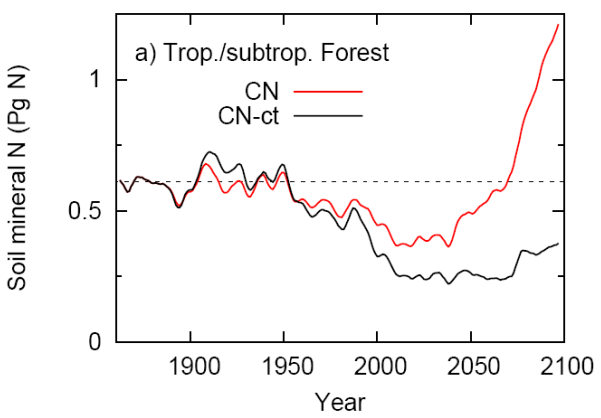
a) Trop./subtrop. Forest
CN
CN-ct
Soil mineral N (Pg N)
Year

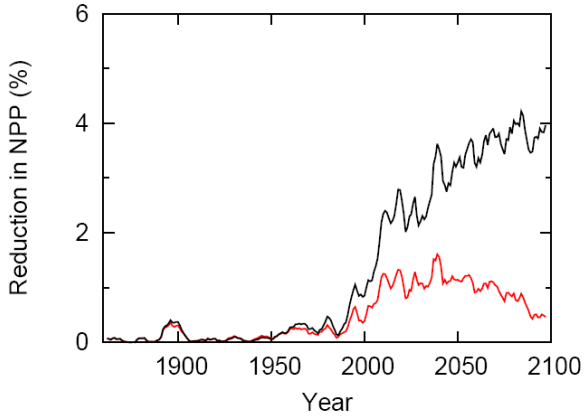
Reduction in NPP (%)
Year

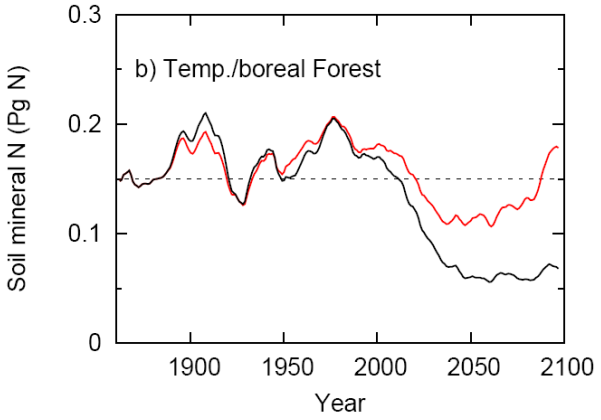
b) Temp./boreal Forest
Soil mineral N (Pg N)
Year

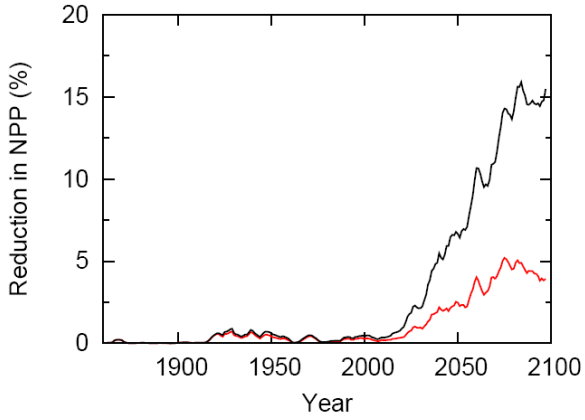
Reduction in NPP (%)
Year

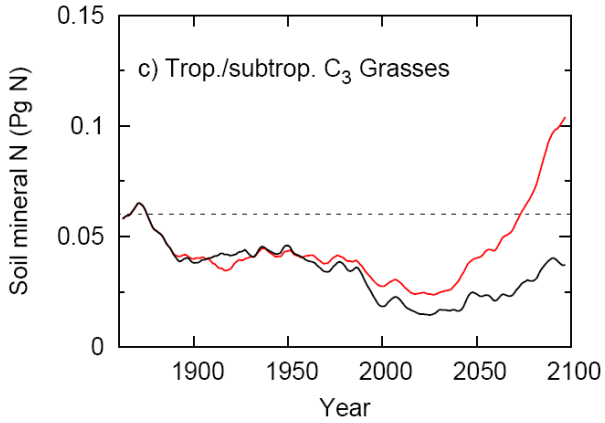
c) Trop./subtrop. C3 Grasses
Soil mineral N (Pg N)
Year

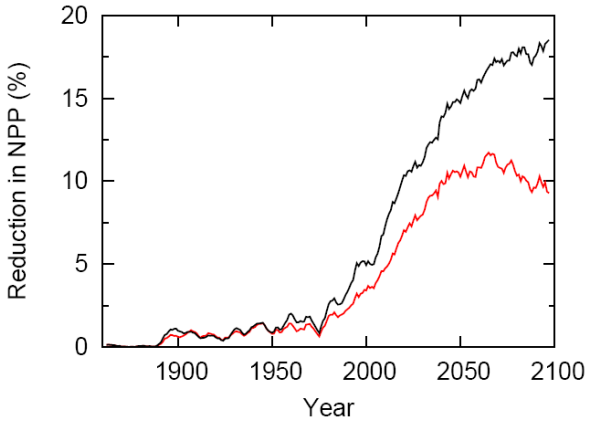
Reduction in NPP (%)
Year

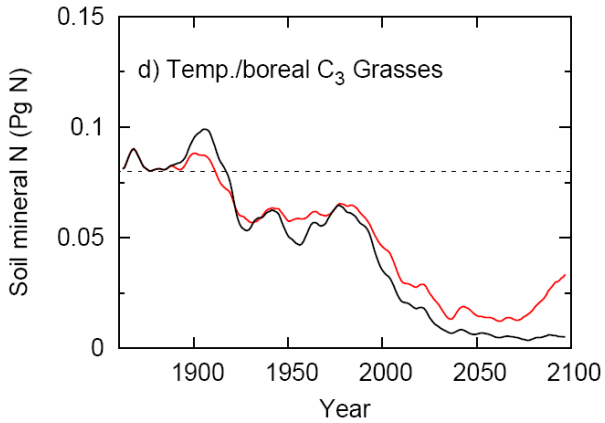
d) Temp./boreal C3 Grasses
Soil mineral N (Pg N)
Year

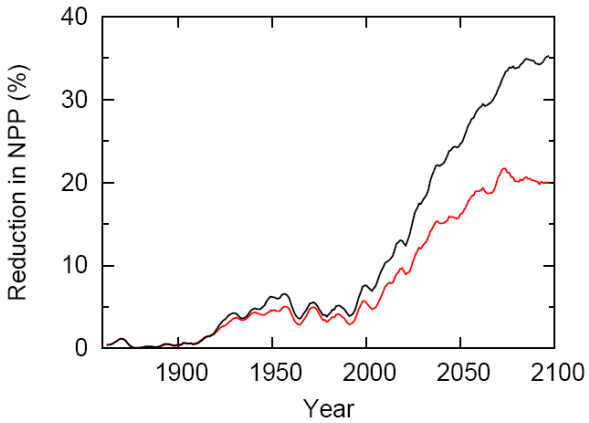
Reduction in NPP (%)
Year

Figure 2.7: Globally simulated soil mineral N (Pg N) availability in forests (a, b) and grasslands (c, d) ecosystem in the CN and CN-ct experiments. The right panel shows the corresponding global reduction in NPP: Plotted is the relative difference of NPP between the C and CN (or CN-ct) experiments with respect to NPP in the C experiment in % (more precisely: 100*(NPP(C)-NPP(CN))/NPP(C)). The dotted lines represent the mean value of first 30 years (1860-89) of soil mineral N.

2.4.8. How robust is the occurrence of PNL

In this section the robustness of the foregoing results are investigated for the occurrence of PNL in forest and grassland ecosystems. To this end, three additional sensitivity experiments (named CN-fd, CN-lz, and CN-ns) are performed. The design of these experiments is led by the more radical question whether the occurrence of PNL can be suppressed in the model by choosing different model parameters. More precisely, the model parameters tested to alleviate PNL are the biotic N fixation rate, the leaching factor (sf), and the nc–value of the slow soil pool. These are the parameters that most likely have a strong influence on the availability of soil mineral N.

In the CN experiment, the global N fixation F_{fix} for the present-day turned out to be 148 Tg N/y, which is at the lower end of the uncertainty range (ca. 100-290 Tg N/y) estimated by Cleveland et al. (1999). Therefore in the CN-fd experiment the N fixation rate is doubled (see Appendix 2 for details). As a result, the global N fixation turned out to be 296 Tg N/y, which is still within the observational uncertainty. Thereby, the additional exogenous N may alleviate the PNL. Another way to increase soil mineral N availability is to reduce the leaching. To study the extreme case, F_{leach} is set to zero in the CN-lz experiment. Finally, in the CN-ns experiment, the nc–value of the slow soil pool is reduced about one quarter (from 0.066 to 0.05). This also should increase the availability of soil mineral N because thereby less N is organically bound in the soils.

The results from these additional experiments are as follows. By doubling biotic N fixation (CN-fd), the soil mineral N availability indeed increased as compared to the CN experiment. As a result, in the CN-fd experiment relative NPP difference reduction is less throughout the whole simulation as compared to the CN experiment (Figure 2.8a and 2.8b). Thereby the occurrence of PNL is almost completely suppressed especially in

forests ecosystem. For grasslands, more available mineral N also leads to a less reduction of relative NPP difference of about 10% (CN experiment) to 5% (CN-fd) especially in the tropical and subtropical C_3 grasses by the end of the 21st century (Figure 2.8c). In temperate and boreal C_3 grasses, more available mineral N leads to a lowering of the relative NPP difference reduction from 20 to 12% (Figure 2.8d). Thereby the occurrence of PNL is also alleviated substantially in grasslands ecosystem. The simulation results show that the global leaching is turned out to be around 58 Tg N/y in the CN experiment, which is 2.5 times smaller than the today's global N fixation. By setting this flux into zero in the CN-lz experiment, this does not really help to alleviate the PNL (Figure 2.8). Finally, by lowering the nc–value of the slow soil pool, the strength of PNL is indeed alleviated but still present (Figure 2.8).

By doubling biotic N fixation, the PNL is almost suppressed especially for the forests ecosystem but not for the grasslands. This is because the PNL occurrence is much stronger in grasslands (see Figure 2.7, right panel) and hence they need more amounts of exogenous N inputs than the forests. Overall, the CN-lz and CN-ns experiments suggest that the PNL is alleviated to some extent for both forests and grasslands. However, none of the experiments completely remove N limitation from grasslands ecosystems and indicates like a permanent PNL. Moreover, the CN-fd experiment is turned out to be significant for alleviating PNL because of its larger fluxes as compared to leaching. In addition, the parameters nc–value of the slow soil pool and leaching seem not to be a significant model parameter to suppress the PNL.

In summary, since doubling of N fixation is quite unrealistic, this sensitivity experiment (CN-fd) shows that the appearance of PNL for grasslands during the 21st century is a very robust simulation result, whereas occurrence of PNL in forests is much less robust. In addition, other model parameters chosen to test the robustness of the simulation results (i.e. nc–value) suggest that the appearance of PNL for forests and grasslands during the 21st century is also a robust simulation result.

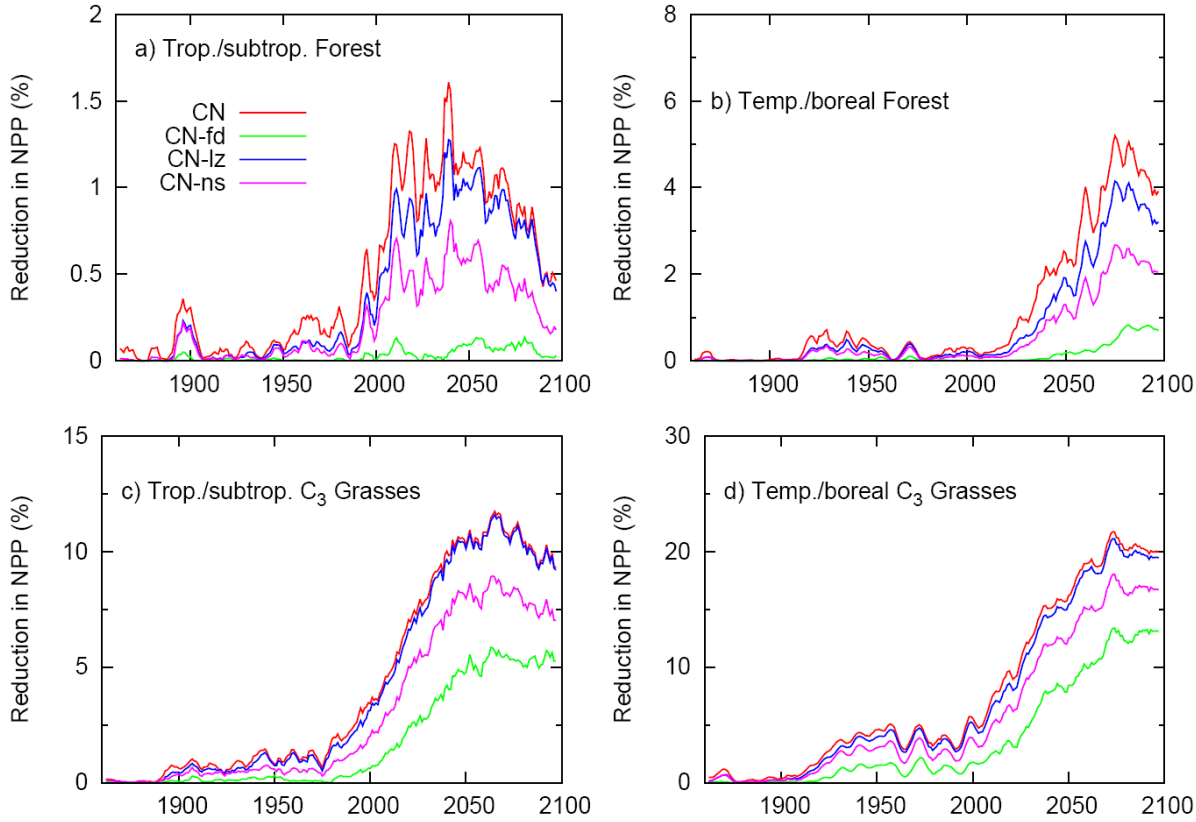

Figure 2.8: Globally reduction in relative NPP difference (see caption of Fig. 2.7 for definition) in the CN, CN-fd, CN-lz, and CN-ns experiments.

2.5. Discussions

2.5.1. Competition between plants and soil microorganisms

Commonly, soil microorganisms are considered as competitors superior to plants for accessing mineral N from soils (Rosswall, 1982; Hodge et al., 2000; Schimel and Bennett, 2004). However, by an additional pathway plants directly can use nitrogen through symbiotic associations with mycorrhizal fungi (Read, 1996; Näsholm et al., 1998). To check the robustness of the model results with respect to one of the key design decisions, namely to distribute available soil mineral N to the soil microorganisms and plants proportional to their demand (see section 2.2.2), two alternative ways of distributing soil mineral N were analyzed: soil microorganisms access the soil mineral N first and then plants use the left over N (experiment CN-mi), and vice versa (experiment CN-pl).

Simulation results show that the assumption of CN-mi does not change significantly the model results with respect to the total land C uptake by the end of the 21st century. In contrast, the assumption of plants first (CN-pl) has a significant effect on the global total land C uptake because it leads to about 20% more C accumulation in the terrestrial ecosystems. This is mostly a result of a reduction in litter decomposition because of reduced N availability to soil microorganisms. The effect is expressed strongest in grasslands because of high microbial N demand under rising CO_2 concentration. Moreover, the plant growth is enhanced because they are allowed to use soil mineral N first to satisfy their N demand. As a result, this leads to larger N uptake from soils in response to increasing CO_2 concentration. These results are consistent with an experimental study by Hu et al. (2001) who reported that under increased CO_2, plant N uptake is enhanced in grasslands and thus it leads to less soil mineral N availability for soil microorganisms. Thereby, when the soil microorganisms are limited by N (Kaye and Hart, 1997; Wang and Bakken, 1997), a decrease in soil mineral N availability can further decrease carbon decomposition and at the same time it can enhance the ecosystems carbon storage (Hu et al., 2001).

The carbon sink obtained by employing the "plant N uptake first" assumption almost equals to that obtained in the C experiment despite the inclusion of the N cycle. Conversely, the carbon sink obtained by CN-mi experiment almost equals that from the CN experiment. Nevertheless, all values obtained for today's land carbon sink are well within the uncertainty range of observational estimates so that from an observational point of view the particular model assumptions are cannot be discriminated. However, as mentioned above the "plant N uptake first" assumption makes a significant difference for the future development of the C cycle in the model. Since microbes are generally considered to be more competitive for soil N as compared to plants, the "plant N uptake first" assumption can be ruled out as unrealistic. Therefore it is interesting that the alternative extreme assumption "microbial N uptake first" does not change significantly the land carbon uptake so that the standard model setup (experiment CN) where soil N is divided into the plant and microbial demand turns out to be the most appropriate setup. Thus, in the following sections, the results particularly from the standard experiment CN are discussed.

2.5.2. N limitation of terrestrial land C uptake and climate-C cycle feedback

The experiments show that the inclusion of the land N cycle leads to a lowering of the total global land C uptake by 8% for present-day conditions in response to increasing atmospheric CO_2 concentration and climate change. This result is consistent with previous global modelling studies (Thornton et al., 2007; Zaehle et al., 2010b), where also a reduction of land C uptake due to N limitation was found. The study by Zaehle et al. (2010b) showed that N limitation leads to a reduction of the land C uptake by 15%. In contrast, Jain et al. (2009) found in a similar global modeling study that approximately the same total global amount of land C uptake with and without land N cycle. For the 21st century, the present study shows that a lowering of total land C uptake by 16% due to N limitation. In comparison to these results, Zaehle et al. (2010c) found a reduction of the total land C uptake by 37%. However, Thornton et al. (2007) found a reduction of around 65%, which is much larger than any of the estimates so far in the literature. This larger difference can be explained by the higher N limitation obtained in the steady state by Thornton et al. (2007). In contrast, in the present study the steady state is assumed to be optimal with respect to N availability. Moreover, a consensus among the recent coupled C-N cycle models is the reduction of land C uptake due to the C-N interaction in the terrestrial biosphere in response to increasing atmospheric CO_2 concentration and climate change.

The results show that the global total land C uptake is reduced mostly in temperate and boreal regions of forests where N is known to be a limiting nutrient (Vitousek and Howarth, 1991; Tamm, 1992). In particular, grassland ecosystems indicate that they are predominately limited by N availability mostly in the temperate regions. These results are in line with the other experimental studies (Cech et al., 2008 and therein), where they reported that grasslands are limited by N or co-limited by N and P. Tropical and subtropical forests are not constrained by N availability except for some small regions. This is in line with the overwhelming evidence that N does not constrain tropical and subtropical forests but co-limited by P (Harrington et al., 2001; D'Antonio et al., 2006).

Mostly the soil C storage is limited by N availability as compared to the vegetation and litter C storage. The reduction of soil C storage is around 51 Pg C by the end of the 21st century and this is because N availability affects the turnover rate of litter C in the model.

Thus, N availability is considered as an important regulator of soil C. There is some evidence in the literature that nitrogen controls the rates of litter decomposition (Gosz, 1981; Fog, 1988; Taylor et al., 1989; O'Connell, 1994). However, a number of studies reported no significant change in the rates of decomposition as a consequence of N addition (Pastor et al. 1987, Theodorou and Bowen 1990, Prescott, 1995; Vitousek and Hobbie, 2000) and therefore N availability and its controls on rates of litter decomposition have been found inconclusive.

By ignoring the land N cycle, previous studies for example the C^4MIP inter-comparisons experiments (Friedlingstein et al., 2006) have been criticized for overestimating the potential future C balance and climate-C cycle feedback (Hungate et al., 2003; Thornton et al., 2007). As in the C^4MIP studies, the present model also simulates a positive climate-C cycle feedback. However, the inclusion of land N cycle in the model leads to a significant reduction of this positive climate-carbon cycle feedback by 21% under the A1B scenario until the end of the 21st century. In contrast, the extreme assumption "plant N uptake first" leads to a substantial larger positive climate-carbon cycle feedback by 33%, which is at first sight counter intuitive. But this can be explained by the larger N uptake for plant growth so that large amounts of N locked up in long-lived wood and SOM that thereby is missing for litter decomposition.

2.5.3. Progressive nitrogen limitation under climate change

Previous studies with respect to PNL occurrence are mostly carried out in short-term field experiments (Norby et al., 2006; De Graaff et al., 2006; Hungate et al., 2006; Reich et al., 2006). Some of these studies discussed that the results of CO_2 enrichment experiments are ambiguous with respect to the occurrence of PNL (Norby et al., 2006). Medlyn et al. (2000) addressed the importance of soil mineral N availability for forest ecosystems in response to elevated CO_2 and temperature. Several experimental studies inferred that low soil mineral N availability constraints the enhancement of NPP under elevated CO_2 as a direct consequence of enhanced plant N uptake from soils (Oren et al., 2001; Norby et al., 2005; De Graaff et al., 2006). Moreover, several studies discussed the availability of N in response to elevated CO_2, but findings are inconclusive, i.e. soil mineral N availability has been observed to decrease, remaining stable or increase (Reich et al., 2006). At a global

scale, so far there are no studies on PNL with a long-term perspective using model simulations for the large warming expected during the 21st century. The simulations performed in the present study show an increase in plant N demand for the 21st century with increasing CO_2 concentration in the atmosphere. Here, elevated CO_2 leads to enhanced sequestration of organic N in long-lived wood and SOM that subsequently leads to a lack of N availability. This in turn, reduces the soil mineral N availability and causes a PNL in a changing climate (Luo et al., 2004; Hu et al., 2006).

For forest ecosystems, the soil mineral N availability is reduced mostly during the first half of the 21st century (Like PNL) but recovers thereafter (Not PNL) under global warming. These results support the hypothesis that soil mineral N availability decreases under elevated CO_2 as N is locked in long-lived woody biomass and soil organic matter (Luo et al., 2004; De Graaff et al., 2006; Hungate et al., 2006). In a changing climate particularly after mid of 21st century, the present study results do not support the PNL hypothesis for regions where the soil mineral N availability progressively relaxes due to the increasing N mineralization rates under global warming. The occurrence of PNL caused the reduction of relative NPP difference (see section 2.4.7 for definition) by about 5% especially in the temperate and boreal forests. But when N scarcity is relaxed due to global warming the reduction of the relative NPP difference is lowering by the end of the 21st century. In general, the results of this study are consistent with observational (Yates et al., 1982; Gallardo and Schlesinger, 1992) as well as other modeling studies (Jain et al., 2009; Wang et al., 2010) which indicate that N limits NPP in shrubs, temperate and boreal forests including tundra (Jain et al., 2009).

The present study shows that grasslands ecosystem develop a deficiency of soil mineral N availability during the 21st century and thereby PNL causes a reduction of the relative NPP difference by about 20%. Nevertheless, the CN and CN-ct experiments suggest that an alleviation of PNL is likely under climate change by fastening the N mineralization (fast turnover). This process leads to an alleviation of PNL and causes a lowering of the reduction of the relative NPP difference from 35% (CN-ct) to 20% (CN) by the end of the 21st century. As compared to these results, Rütting et al. (2009) reported that the faster rates of internal cycling and enhanced N retention can potentially alleviate PNL in grazed temperate grassland at the New Zealand-FACE site. The study by Gill et al. (2006) found that the soil N availability is reduced (Like PNL) in Texas grassland under elevated CO_2

during 4 years field experiments. Similarly, Hovenden et al. (2008) reported a decline in the soil N availability (Like PNL) in Tasmanian perennial grassland under elevated CO_2 during 3-5 years field experiments. But, importantly it also shows that warming could prevent CO_2 induced decline in soil N availability.

Despite evidence from several FACE experiments on the occurrence of PNL (Luo et al., 2006b) there is a large uncertainty on soil N availability under global warming. Studies have suggested that increasing soil temperatures will increase the N availability in response to elevated CO_2 (Loiseau and Soussana, 2000). The results of the present study indicate that temperature is a sensitive parameter for PNL which can enhance the soil decomposition rates and thereby the availability of soil mineral N. In line to this, studies have demonstrated that the increased temperature stimulates soil N mineralization (Medlyn et al., 2000; Castaldi, 2000; Fenner et al., 2006). In addition, warming can enhance the soil mineral N availability under elevated CO_2 and thereby it may alleviate PNL (Hovenden et al., 2008).

The evidence of PNL under elevated CO_2 concentration is rather speculative and previous studies suggested that many ecosystems may have the ability to avoid PNL based on accumulation of exogenous N inputs (e.g., deposition, fixation) or lowered N losses (Hungate et al., 2003; Johnson et al., 2004; Luo et al., 2004, 2006a). Experiments performed in the present study show that by doubling biotic N fixation and without N losses through leaching, PNL cannot be completely avoided or delayed in grassland ecosystems. However, by doubling N fixation PNL occurrence is almost completely suppressed in forest ecosystems. In comparison to these results other studies reported that increased biotic N fixation and N deposition are not found to be significant for alleviating PNL under elevated CO_2 (Van Groenigen et al., 2006; Reich et al., 2006). Furthermore, there is no evidence in the experimental studies that N retention by less N leaching and gaseous losses of N is able to alleviate PNL (McKinley et al., 2009). The present study summarizes that since doubling of N fixation is quite unrealistic, this experiments show that the appearance of PNL for grasslands during the 21st century is a very robust simulation result, whereas occurrence of PNL in forests is much less robust.

2.6. Conclusions

In this study a simple scheme for the terrestrial N cycling has been incorporated into the existing land carbon cycle model (JSBACH). This newly developed model is based on only a small number of basic principles, namely mass conservation, a supply-demand ansatz, and fixed C-to-N ratios. Additional strength of this model is: It needs only a very limited number of additional state variables and model parameters as compared to the original JSBACH-C model (Section 2.2.2). This new model for the coupled nitrogen and carbon cycle is used to study their interactions by performing a series of simulations.

For today's conditions, the results from the C and CN experiments for the land carbon sink and land carbon stocks are well comparable with observational estimates. The N stocks and fluxes are also well comparable with those obtained by various other models and with published observational estimates.

Because of the tight coupling between the N and C cycle, a significant reduction of the land C uptake by 16% is found by the end of the 21st century in response to increasing CO_2 concentration and climate change under the A1B scenario. These results are qualitatively in agreement with previous global modeling studies (Thornton et al., 2007; Zaehle et al., 2010b. 2010c). Nevertheless, the magnitude of the consequences from the N cycle on the future global land C uptake is much less in this model than found in the study by Thornton et al. (2007). Besides, this study finds that the inclusion of land N cycle in the model leads to a reduction of 21% in the magnitude of positive climate-carbon cycle feedback. This result is qualitatively in agreement with the findings of Sokolov et al. (2008) and Thornton et al. (2009).

To check the robustness of certain model assumptions two sensitivity experiments are designed, assuming quite drastic modifications of the model. It turned out that even with these modifications today's land carbon sink is well within the uncertainty range from observational estimates so that from an observational point of view the particular model assumptions are cannot be discriminated. However, the assumption "plant N uptake first" turned out that it is unrealistic as mentioned in Section 2.5.1. The standard model setup where soil N is divided into the plant and microbial demand equally turned out to be the most appropriate setup.

In forest ecosystems, the simulated soil N availability decreases during the first half of the 21st century under increased CO_2 concentration and climate change. This shows the occurrence of PNL (Like PNL) as suggested by various authors (Luo et al., 2004; De Graaff et al., 2006; Hungate et al., 2006). But approximately mid of 21st century the PNL starts alleviating because of global warming. In grasslands the soil N availability decreases continuously (Like PNL) from the 19th century until the first half of the 21st century but recovers thereafter. Thus, the occurrence of PNL causes a substantial reduction in the relative NPP difference by 20%. However, an alleviation of PNL is also realized under global warming conditions mostly after mid of 21st century in grasslands ecosystem.

To study the robustness of occurrence of PNL additional sensitivity experiments have been performed. The results show that by doubling biotic N fixation PNL almost vanishes in forests but is only slightly alleviated for grasslands. By suppressing instead N losses through leaching and by reducing the nc–value of the slow soil pool the effect on alleviating PNL is very small. Since doubling of N fixation is quite unrealistic, these experiments show that the appearance of PNL for grasslands during the 21st century is a very robust simulation result, whereas occurrence of PNL in forests is much less robust.

Chapter 3

3. N_2O emissions from the terrestrial biosphere under climate change

Abstract

Nitrous oxide (N_2O) is produced in soils as a byproduct during nitrification and denitrification and contributes significantly to the annual N_2O budget. In this Chapter, the process controlling N_2O emissions have been incorporated in the JSBACH-CN model. The aims of this study are: To investigate N_2O emissions from natural soils under climate change and climate-N_2O feedback. To accomplish this simulations are performed.

For site-scale model evaluation, the data of simulated N_2O emissions is compared with that obtained from observations. The comparison shows a good correlation between simulated and observed N_2O emissions. The simulated N_2O emissions are largest for Southeast Asia, Amazon forest, and Central Africa. For present-day conditions globally, simulated N_2O emissions from natural soils are around 6 Tg N yr^{-1} and is consistent with the value reported in the IPCC. By the end of the 21st century, emissions increase up to 8 Tg N yr^{-1} (i.e. one-third increase) and contribute significantly to the global N_2O budget under the SRES A1B scenario. Furthermore, the simulated N_2O emissions from natural soils are combined with the other N_2O emission sources (e.g., ocean, fossil fuel, fertilizer, etc.) in order to construct atmospheric N_2O concentrations. The calculated rise in the atmospheric N_2O concentration is consistent with observations over the period 1860-2005 (a rise from 276 to 320 ppb). Under the A1B scenario they increase up to 469 ppb by the end of the 21st century. The global radiative forcing (RF) from N_2O emissions is around 0.14 Wm^{-2} in 2005 and is comparable with the value published in the IPCC AR4 report (ca. 0.16 Wm^{-2}). For the end of the 21st century, calculated RF is 0.6 Wm^{-2} and leads to a projected increase in temperature by 0.46^0C since 1860. The climate-N_2O feedback is found to be negligible because the value of feedback factor is very small (ca. 0.0003).

3.1. Introduction

Over the last two centuries, fossil fuels combustion and land use change (e.g., deforestation) have caused a substantial rise in the atmospheric CO_2 concentration and surface temperature (Prentice et al., 2001). The future global environmental change depends not only on temperature increase by CO_2 but also on non-CO_2 greenhouse gases (GHGs) such as nitrous oxide, methane, etc. Nitrous oxide (N_2O) is an important GHG that contributes significantly to global climate change. Its contribution to the anthropogenic greenhouse effect estimated to be 6-7% (IPCC, 1996a; Xu et al., 2008).

N_2O has a larger global warming potential (ca. 296 times) than CO_2 (Prather et al., 2001). Therefore, increase in N_2O emissions from the terrestrial biosphere (e.g., nitrification and denitrification) and anthropogenic sources (e.g., agriculture, deforestation) may have large effect on radiative forcing (RF) that is associated with climate change. Over the last few decades N_2O atmospheric concentration is increasing at the rate of about 0.6-0.9 ppb/yr (Albritton and Meira Filho, 2001). It has a life-time of about 114 years (Albritton and Meira Filho, 2001) and may play important role in global warming in the near future. It affects atmospheric chemistry and in the troposphere N_2O is chemically inert. But it rapidly diffuses to the stratosphere, where it initiates series of photochemical reactions that lead to the destruction of the ozone layer (Crutzen, 1981).

Over the last several decades, human activities have caused a substantial modification to the terrestrial N cycle (McElroy et al., 1977). As a consequence, N_2O atmospheric concentration has increased from pre-industrial value of 270 ppb to 320 ppb (Battle et al., 1996; Thompson et al., 2004). The modern N_2O concentration of 320 ppb exceeds by 18% than its pre-industrial values, which signifies a large-scale perturbation to the global N cycle. Since 1988, the rate of increase of N_2O concentration is 0.8 ppb yr^{-1} (IPCC, 2007).

N_2O is predominately produced in soils as a byproduct during bacterial nitrification (aerobic process) and denitrification (anaerobic process). Numerous factors that control the N_2O production are soil temperature, soil moisture, pH, oxygen concentration, ammonium and nitrate availability, etc (Silva et al., 2005; Cookson et al., 2006). Emissions produced from the above processes contribute about 70% of the annual N_2O budget worldwide (Mosier, 1998). Land and oceans are the principal natural sources of

N_2O emissions. The total annual emissions of N_2O are estimated at 16.2 Tg N in the late 1990s (IPCC, 2001). Soils are the largest contributors to N_2O emissions with 6.0 Tg N yr^{-1} (uncertainty range of 3.3 to 9.7) from natural soils and 4.2 Tg N yr^{-1} (uncertainty range of 0.6 to 14.8) from agricultural soils (IPCC, 2001).

In this study, the processes that produce N_2O are incorporated in the process-based JSBACH-CN model. The aims of this study are to investigate N_2O emissions from natural soils under climate change and climate-N_2O feedback. Further, using the simulated N_2O emissions data, this study aims to construct atmospheric N_2O concentration in combination with other N_2O emission sources (e.g., ocean, fossil fuel, fertilizer, etc.) over the period 1860-2100.

3.1.1. Modelling N_2O emissions in JSBACH-CN

The rate of N_2O emissions from soils due to nitrification and denitrification processes were documented previously in the literature. The N_2O emissions rate due to nitrification and denitrification varies from 0.1-0.2 % and 0.2%-4.7% (day^{-1}), respectively (Groffman et al., 2000; Breuer et al., 2002; Khalil et al., 2004; Well et al., 2003; Ambus, 2005; Stange et al., 2009). Furthermore, the denitrification rate reported by many experimental studies showed a wide range of values and therefore may have a larger uncertainty compared to the nitrification rate.

The most commonly used “Hole-in-the-pipe” model has implemented the nitrification and denitrification processes of N_2O emissions based on the N mineralization rate and soil water (Davidson and Verchot, 2000). In the CASA model, Potter et al. (1996) modelled N_2O emissions by considering a fixed fraction of N mineralization rate of about 2%. Xu-Ri et al. (2008) used the above mentioned literature values of nitrification and denitrification rate for modelling N_2O emissions in the process-based terrestrial ecosystem DyN model.

Here for the JSBACH-CN model, N_2O emissions are modeled based on the N mineralization processes (i.e. nitrification and dentrification). These processes are mainly affected by abiotic factors such as soil temperature and moisture. The detailed equations of N_2O emissions from the N mineralization processes are described as follows.

Table 3.1: Notations used for N_2O emission description in the JSBACH-CN model.

Abbreviations $X = N: nitrification; DN: denitrification; fix: fixation; depo: deposition$

Notation	Meaning
$NetN_m$	$Net\ N\ mineralization$
NH_4^+	$available\ ammonia\ in\ the\ soil$
NO_3^-	$available\ nitrate\ in\ the\ soil$
$f_{\rightarrow NH_4^+}$	$fraction\ of\ NH_4^+$
R_{N2ON}	$rate\ of\ nitrification$
R_{N2ODN}	$rate\ of\ denitrification$
EF	$emission\ factor$
$N_2O_{(X)}$	$N_2O\ emissions\ from\ X$
$F_{(X)}$	$Fluxes\ of\ X$

The equation for the net N mineralization flux ($NetN_m$) can be written as:

$$NetN_m = -f_{limit}\left((nc_S - nc_{LG})\, f_{LG\rightarrow S}\, R_{LG}^{pot} + (nc_S - nc_{LW})\, f_{LW\rightarrow S}\, R_{LW}^{pot}\right) + f_{limit}\left(nc_{LG}\, f_{LG\rightarrow A}\, R_{LG}^{pot} + nc_{LW}\, f_{LW\rightarrow A}\, R_{LW}^{pot}\right) + nc_S\, R_S \quad (1)$$

The details notations used in Eq.1 are described in Chapter 2 (Section 2.2). The first line of Eq. 1 represents the gross immobilization fluxes from the litter pools (i.e. litter green and wood), whereas the second line represents the mineralized fluxes associated with heterotrophic respiration by soil microorganisms. These mineralized fluxes are mostly from the litter pools as well as soil pool. The terms R_{LG}^{pot}, R_{LW}^{pot}, and R_S depend on soil temperature and moisture (for details see Chapter 2.2). In this study, soil pH is ignored because of its high spatial heterogeneity but it is an important factor that determines N_2O production.

$$NH_4^+ = f_{\rightarrow NH_4^+} NetN_m \quad (2)$$

$$NO_3^- = (1 - f_{\rightarrow NH_4^+}) NetN_m \quad (3)$$

The size of ammonia and nitrate availability in soils is derived from the $NetN_m$ flux (Eq. 2 and 3) by taking a fraction of NH_4^+ and NO_3^- availability. The fraction of NH_4^+ availability ($f_{\rightarrow NH_4^+}$) in soils is assumed to be 40% of $NetN_m$ flux. The remaining 60% of $NetN_m$ flux is assumed to be NO_3^- availability in soils. In general, NO_3^- availability is considered to be larger than the NH_4^+ availability (Mengel and Kirby, 2001; Xu-Ri et al., 2008). N_2O emissions are derived as:

$$N_2O_{(N)} = NH_4^+ R_{N2ON} \quad (4)$$

$$N_2O_{(DN)} = NO_3^- R_{N2ODN} \quad (5)$$

N_2O emissions due to nitrification and denitrification (Eq. 4 and 5) are determined by multiplying the substrate availability (i.e. ammonia and nitrate) with their corresponding nitrification rate (ca. 0.1%) or dentrification rate (ca. 0.2%). These rates are simply taken from the previous literatures values.

In particular, N_2O emissions from the N deposition and biotic N fixation are derived based on the IPCC methodology and can be written as:

$$N_2O_{(depo)} = F_{depo} EF \quad (6)$$

$$N_2O_{(fix)} = F_{fix} EF \quad (7)$$

$$N_2O_{(total)} = N_2O_{(N)} + N_2O_{(DN)} + N_2O_{(fix)} + N_2O_{(depo)} \quad (8)$$

According to the IPCC method, N_2O emissions are estimated by taking an emission factor of 1.0% of N deposition. Other studies showed emission factors of about 2-4% (Borken and Beese, 2005; Ernfors et al., 2007). Biologically fixed N also emits N_2O into the atmosphere during nitrification and denitrification (Minami, 1997; Mosier et al., 1998; Pathak, 1999), which has been ignored in most of the previous studies. From a top-down approach, Crutzen et al. (2008) estimated that about 4% of the biotic fixed N can be considered as the source of N_2O. However, Schmid et al. (2001) and Horak et al. (2006) used the IPCC emission factor of 1.25 (±1.0%) for estimating N_2O emissions due to biotic N fixation.

For the JSBACH-CN model, the IPCC methodology of N_2O emissions factor of 1% and 1.25% is used for the N deposition and biotic N fixation (Eq. 6 and 7), respectively. The total emissions are derived by summing all the emission sources (Eq. 8). Henceforth for shortness, N_2O emissions from the biotic N fixation and deposition are called as "open" sources of emissions.

3.1.2. Calculation: Emissions to concentration and temperature increases

(Emission → concentration → radiative forcing → temperature increase)

A box model calculation is applied to convert N_2O emissions (Tg N yr^{-1}) to atmospheric N_2O concentration (ppb). The resulting atmospheric N_2O concentration is converted to radiative forcing (RF) to derive the temperature increase due to the additional N_2O emissions since the pre-industrial level. For this calculation, the equations are adopted from Höhne and Blok, (2005) and modified accordingly by adding emissions from the other sources (e.g., fossil fuel, biomass burning, synthetic fertilizer, etc.). The equations for converting emissions to temperature increases are described in detail in Appendix 3.1.

N_2O emissions from natural soils and the so called emissions from "open" sources are obtained from the simulation results of JSBACH-CN model. However, N_2O emissions from the ocean are obtained from the published data of the study by Jungclaus et al. (2010).

In particular, N_2O emissions from the products of fossil fuels (e.g., nylon production, mobile and stationary), biomass burning, and synthetic N fertilizer (emission factor of 2.5%) are derived from the recent study by Davidson (2009). These data are used for the periods 1860 to 2005. For the future the SRES A1B scenario data is used (IPCC, 2001); this is especially valid for the fossil fuel emissions. However, emissions from biomass burning and synthetic N fertilizer are kept constant from 2005 until 2100.

3.2. Setup of model experiments and driving data

The experiments are designed by using the forcing data from Roeckner et al. (2011). The details about this data and the model setup were already described in Chapter 2.3. In the present study, the experiments differ from the previous experiments (Chapter 2.3) with respect to the inclusion of N_2O emissions in the JSBACH-CN model.

To address the main questions of this study, two transient experiments (named NE and NE1) are performed covering the years 1860-2100. The first transient experiment (called NE) is the main experiment in this study, which is performed with JSBACH-CN, where N_2O emissions are included as described in Section 3.1.1. The second transient experiment is called NE1, where the soil temperatures are kept at their pre-industrial values in order to isolate the effect of increasing CO_2.

3.3. Results

3.3.1. Comparison with site-scale observations

In this section the simulation results of N_2O emissions are compared with site-scale observations. These site-scale data are compiled from the available literature especially for forest and grassland ecosystems (see Appendix 3.2 for site description). Moreover, such a comparison of simulation results with site-scale (meters) observations for evaluating a global model is not straightforward. Because, the global model has been developed for a quite different scale, namely the scale of several grid boxes of Earth system models, which are hundreds of kilometres. Nevertheless, the simulated N_2O emissions are compared with observations in order to evaluate the order of magnitude of modeled N_2O emissions from the terrestrial biosphere.

The simulated N_2O emissions (i.e. natural plus open) used for comparison are the mean values from 1970 to 1999 obtained from the NE simulation. In Figure 3.1, the simulated N_2O emissions are compared with observations for forest and grassland ecosystems. Simulated N_2O emission correlates well ($r=0.89$, $n=18$, $p<0.01$) with observations for forest ecosystems (Figure 3.1a). A good correlation is also found ($r=0.83$, $n=7$, $p<0.05$) for grassland ecosystems despite the limited number of available observation sites (Figure

3.1b). These comparisons demonstrate that the simulated N_2O emissions are in the similar order of magnitude of observed N_2O emissions from terrestrial ecosystems.

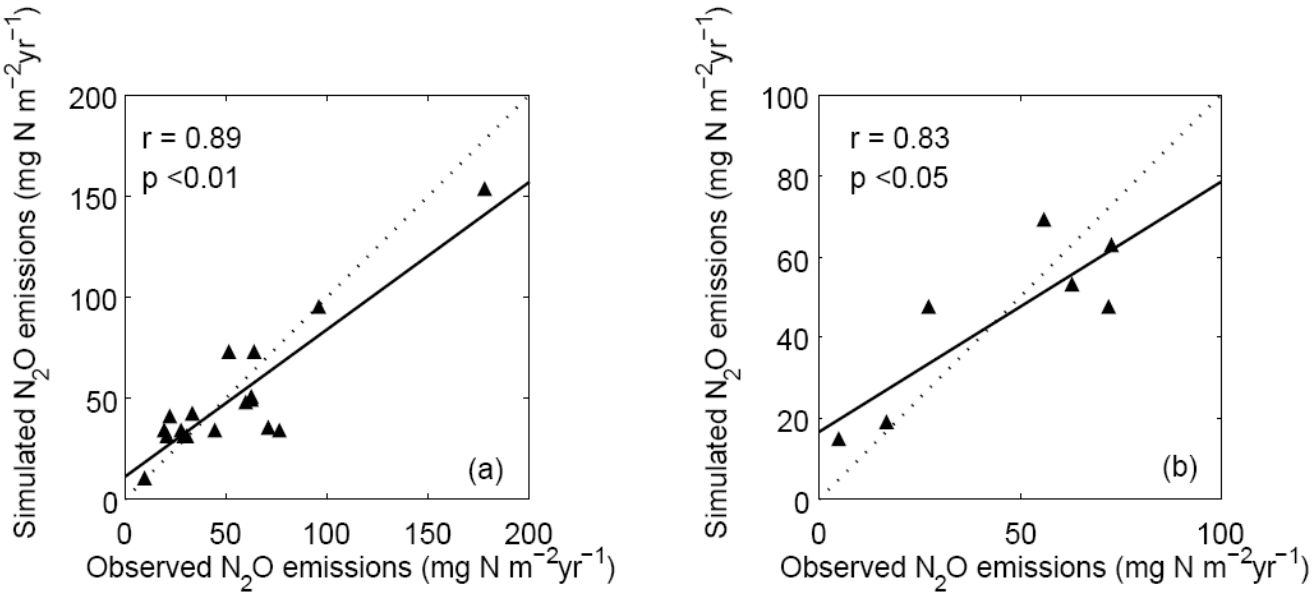

Figure 3.1: Comparison of simulated N_2O emissions with observed N_2O emissions in (a) forest and (b) grassland ecosystems. The diagonal dotted lines are the 1:1 line and the solid line depicts the least square regression line.

3.3.2. Spatial distribution of simulated N_2O emissions

Figure 3.2 shows the spatial distribution of simulated N_2O emissions from terrestrial ecosystems (i.e. natural plus open) obtained from the NE simulation. The simulation results show that higher N_2O emissions are found especially in Southeast Asia, Amazon forest, and Central Africa (>150 mg N m^{-2} yr^{-1}) as compared to the other regions. The reason for this is that the organic matter is decomposed at a faster rate because of higher temperatures. This accelerates the N mineralization processes (i.e. nitrification and denitrification). As a consequence, more mineral N is available for N_2O emissions. The results show that the tropical rainforests soils are the major source of N_2O emissions. They are in the range of about 100-250 mg N m^{-2} yr^{-1} and considered in the literature to be the largest natural terrestrial source for atmospheric N_2O. In comparison to these results, Melillo et al. (2001) reported the emissions to be in the range of 140-260 mg N m^{-2} yr^{-1}. However, Werner et al., (2007) found a wider range of emissions of 50-540 mg N m^{-2} yr^{-1}. Simulated emissions are found to be much lower in temperate and boreal regions (ca. <100 mg N m^{-2} yr^{-1}) because of lower temperatures and slow microbial processes. In

comparison to these results, other studies reported emissions to be in the range of 3-177 mg N m^{-2} yr^{-1} (mean value of about 78) from temperate regions of Europe (Pilegaard et al., 2006). These results are comparable with the previous reported emissions of <88 mg N m^{-2} yr^{-1} for North America (Venterea et al., 2003). The emissions of <100 mg N m^{-2} yr^{-1} are found in Oceania and Africa and are consistent with the results of Werner et al. (2007). Overall, the global distributions of simulated N_2O emissions are in the order of similar magnitude as in the CASA model (Potter et al., 1996). Also, the simulated N_2O emissions pattern are consistent with the statistical approach of Xu et al. (2008) where the emissions are mostly computed from observations.

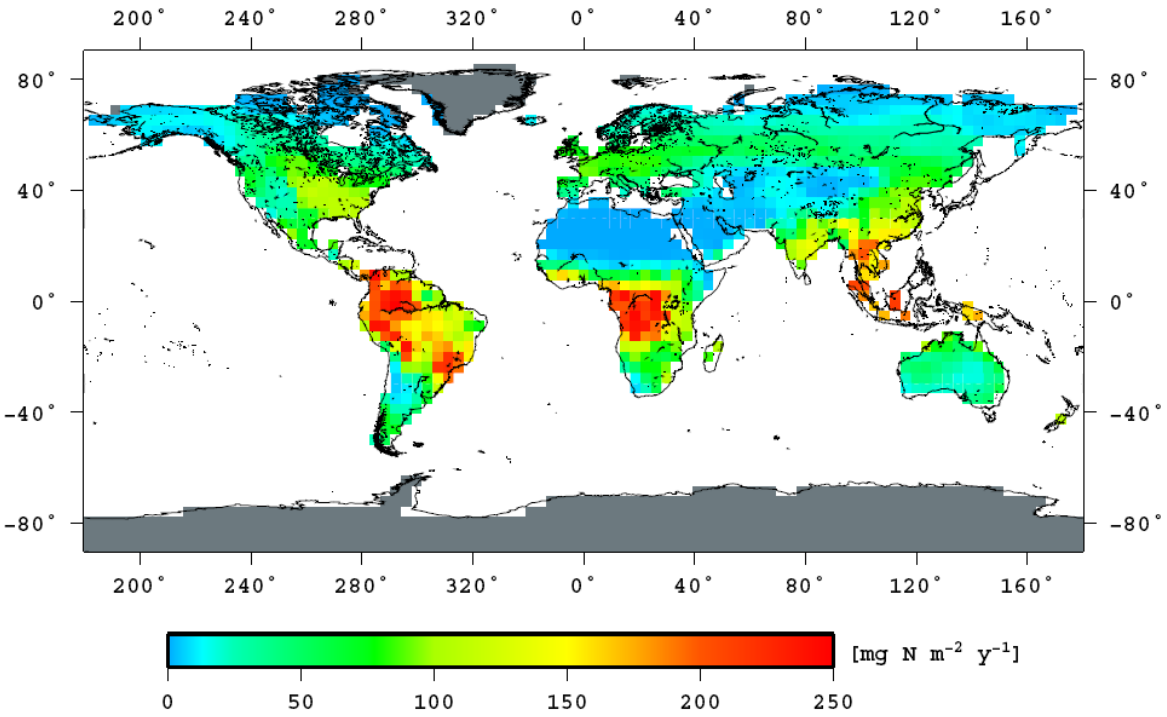

Figure 3.2: Simulated N_2O emissions from the terrestrial ecosystems (means for 1970-99) obtained from the NE simulation.

The emissions especially from the atmospheric N deposition and biotic N fixation are called as "open" sources of N_2O. The simulated open N_2O emissions are higher mostly in the regions with high N deposition and biotic fixation. Earlier studies have ignored biologically fixed N that contributes to emissions during nitrification and denitrification. The results show a significant amount of N_2O is released especially from the biologically fixed N. The simulated N_2O emissions both from the biotic N fixation and atmospheric N deposition are higher particularly in the tropics and sub tropics (ca. 40-70 mg N m^{-2} yr^{-1})

as compared to the temperate and boreal regions (ca. <40 mg N m^{-2} yr^{-1}). This is due to the fact that biotic N fixation is higher where the net primary productivity is high. Besides, the simulated emissions are higher in the regions with high atmospheric N deposition. These results are consistent with most of the previous studies that reported a significant positive relationship between the atmospheric N input and N_2O emissions (Butterbach-Bahl et al., 1998; Davidson et al., 2000; Skiba et al., 2004).

Table 3.2: Comparison of simulated N_2O emissions with various other models (means for 1970-99).

Tg N yr^{-1}	**Models**				**Empirical**	**IPCC AR4**
	JSBACH-CN	CASA	O-CN	DNDC	Xu et al., 2008	IPCC, 2007
Natural soils	5.9	6.12	7	11.33	13.3	3.3-9.9
Open sources	2.5	-	-	-		0.3-0.9
Total	**8.4**	**6.12**	**7**	**11.33**	**13.3**	

In Table 3.2, simulated global N_2O emissions as simulated by the JSBACH-CN model are compared with those obtained by various other models (Potter et al., 1996; Zaehle et al., 2010b) and also with the empirical model (Xu et al., 2008), which is based on observations. The simulated N_2O emissions especially from the open sources are 2.5 Tg N yr^{-1}, whereas the IPCC AR4 reported as 0.3-0.9 Tg N yr^{-1}. In comparison to the IPCC reported values, larger emissions are found from the open sources because it include emissions both from the N deposition and biotic N fixation, whereas the IPCC investigation ignored emissions from the biotic N fixation. N_2O emission from the N deposition accounts for 0.6 Tg N yr^{-1}. Indeed, this is consistent with the other reported values of about 0.8 Tg N yr^{-1} by Bouwman (1995). The global N_2O emissions from the terrestrial ecosystems (i.e. natural plus open) are around 8.4 Tg N yr^{-1}, which are also consistent with other model estimates of 6-13.3 Tg N yr^{-1} (Potter et al., 1996; Liu, 1996; Zaehle et al., 2010b). The IPCC AR4 reports a lower range of 3.3-9.0 Tg N yr^{-1}. However, in comparison to the statistical approach of Xu et al. (2008), all the models have underestimated the total terrestrial N_2O emissions. Besides, other sources reported a diverse estimates of N_2O emissions, for instance, 7-16 Tg N yr^{-1} (Bowden, 1986), 2.8-7.7

Tg N yr^{-1} (Watson et al., 1992), 4.6-15.9 Tg N yr^{-1} (Mosier et al., 1998, Kroeze et al., 1999).

3.3.3. Simulated N_2O emissions and temperature increase

The simulations results show that for present-day conditions, the simulated N_2O emissions from natural soils are nearly the same for both experiments (NE and NE1) (Figure 3.3). Globally, emissions from natural soils are around 6 Tg N yr^{-1} and are consistent with the value reported in the IPCC (IPCC, 2001). By the end of the 21st century, emissions increase to around 8 Tg N yr^{-1} (NE experiment) under increasing CO_2 concentration and climate change. This increase in emissions over the period 2000-2100 is about one-third that contributes significantly to the global N_2O budget.

Furthermore, the simulated N_2O emissions are higher by around 1.0 Tg N yr^{-1} in the NE experiment as compared to the NE1 experiment by the end of the 21st century. This is because higher temperature in the NE experiment causes faster N mineralization processes, which in turn lead to higher N_2O emissions from natural soils. The results obtained from the NE1 experiment also show an increase of emissions from natural soils. This is because of higher N substrate availability resulting from more litter fall through increased NPP in response to rising CO_2 concentration in the atmosphere.

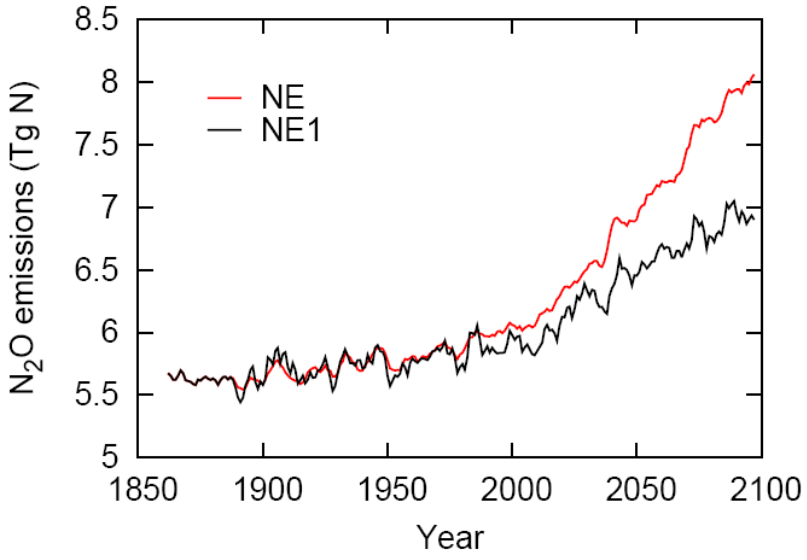

Figure 3.3: Comparison of simulated N_2O emissions from natural soils between NE and NE1 experiments over the period 1860-2100.

The linear relationship between surface temperature and N_2O emissions from natural soils shows that the emissions are increasing as surface temperature increases (R^2=0.93) (Figure 3.4). This indicates that under global warming conditions, the N_2O emissions will be enhanced significantly for the future climate. Furthermore, from this figure, the slope is about 0.69; this value is taken for Eq. B7 in the climate and N_2O feedback calculation (details in Appendix 3.1).

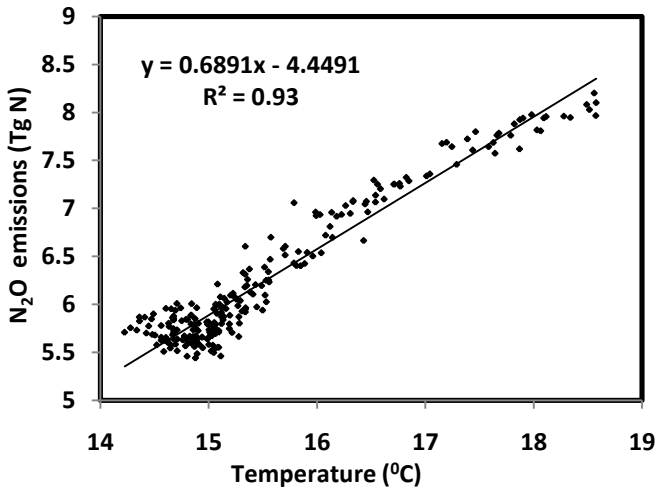

Figure 3.4: Linear regression between surface temperature and simulated N_2O emissions obtained from the NE simulation.

3.3.4. N_2O emission sources

The results show that the simulated N_2O emissions are predominantly larger for natural soils as compared to the other sources of N_2O (Figure 3.5, left panel). The emissions from natural soils increase from around 5.5 to 8 Tg N yr^{-1} over the period 1860-2100. Apart from natural soils emissions, larger emissions arise from open sources (i.e. N deposition and fixation) as well as from the ocean. The ocean emissions remain almost stable until the present-day conditions, found to be 2.2 Tg N yr^{-1}. However, it decline slowly after 2050 until end of the 21st century. The emissions from open sources are around 2 to 4.5 Tg N yr^{-1} over the period 1860-2100. This increase of about 2.5 Tg N can be explained by the high rates of both atmospheric N deposition and biotic N fixation.

N_2O emissions from synthetic N fertilizers are estimated by using the emission factor of 2.5%. The estimated N_2O emissions from synthetic N fertilizers show that the emissions

increased significantly during the agricultural revolution in 1960 (ca. 0.28 Tg N yr^{-1}) and continued up to present-day (ca. 2.2 Tg N yr^{-1}). This increased emission is about 8 times higher in 2005 as compared to the 1960. N_2O emissions from the fossil fuel increased also from 1960 (ca. 0.17 Tg N yr^{-1}) until 2005 (ca. 0.74 Tg N yr^{-1}). N_2O emissions from the biomass burning are lower than the other emission sources; they increase gradually from 1960 (ca. 0.3 Tg N yr^{-1}) until the present-day (ca. 0.5 Tg N yr^{-1}). As mentioned above, after 2005 biomass emissions are kept constant at the level of 2005 until the end of the 21st century.

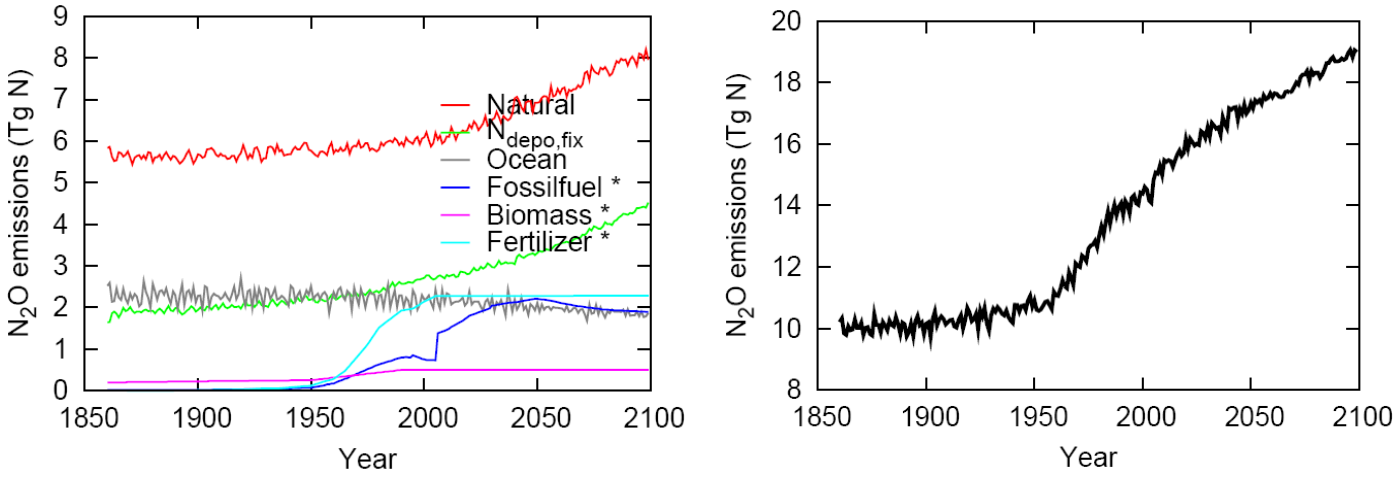

Figure 3.5: The simulated N_2O emissions from natural, open, and ocean sources are shown in the left panel. Emissions from the fossil fuel, biomass burning, and synthetic N fertilizer are marked by an asterisk. These data are obtained from Davidson (2009). The total emissions from all the sources are shown in the right panel.

The total N_2O emissions from all the above sources are around 14.4 Tg N yr^{-1} during 2000; these are estimated to increase to 19 Tg N yr^{-1} by the end of the 21st century (Figure 3.5, right panel). The sources of the increased emissions after the year 2000 are mostly from natural soils, open sources, and fossil fuel emissions; the increase in N_2O emissions over the period 2000-2100 is around 4.6 Tg N.

3.3.5. Atmospheric N_2O concentration and additional warming

Simulation results comprise the emissions mainly from the natural soils and open sources. However, only from the above two sources, calculated atmospheric N_2O concentration cannot be comparable with the historical observations trends until 2005 (Figure 3.6). Therefore, it is necessary to include other emission sources, for instance, emissions from the fossil fuel, biomass burning, and synthetic N fertilizer, which are taken from the data by Davidson (2009). By including above all emission sources, the results show that the calculated atmospheric N_2O concentrations are largely driven by natural soil emissions, ocean emissions, and open sources emission until 1960 (Figure 3.6). However after 1960, the atmospheric N_2O concentration rises sharply because a significant amount of N_2O is released from synthetic N fertilizers and fossil fuels. For the period 1860-2005, the results show that the calculated atmospheric N_2O concentration is well comparable with the historical observations by Machida et al. (1995) (i.e. ice core records), Battle et al. (1996) (i.e. firn data), and NOAA/ESRL flask (CATS data).

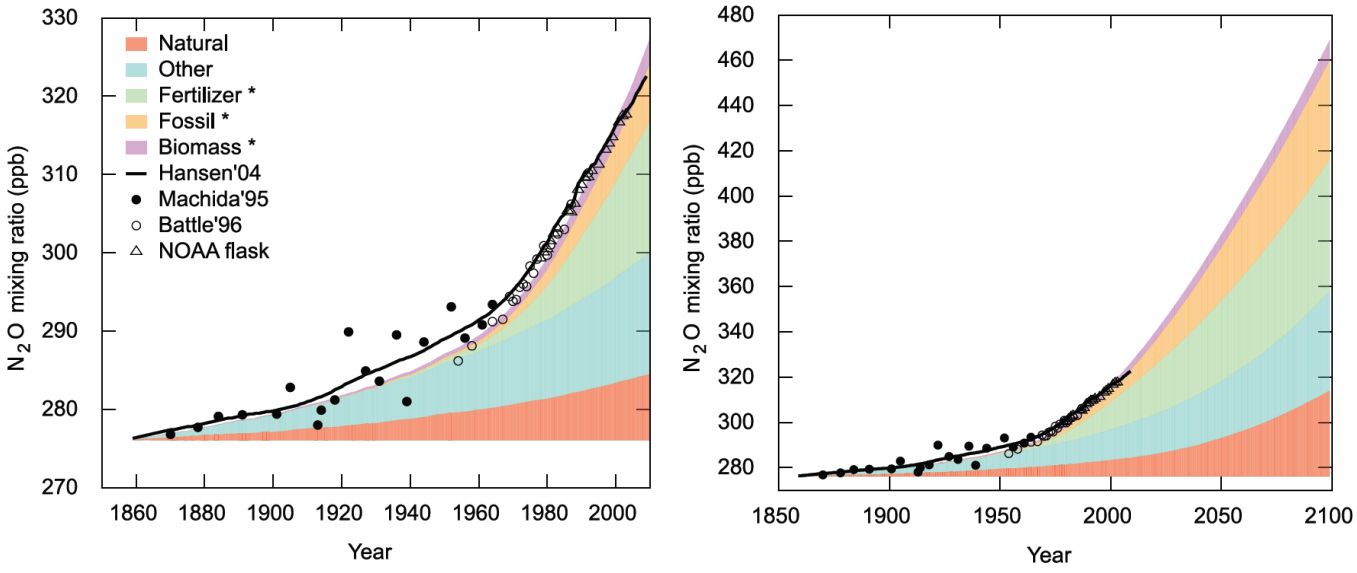

Figure 3.6: The calculated atmospheric N_2O concentration from 1860-2009 (left panel) and 1860-2100 (right panel). Emissions from the natural and other sources (ocean and open sources) are derived from the simulation results of the JSBACH-CN model. Emission sources marked by an asterisk are obtained from Davidson (2009). Measurements from ice core (Machida, 1995), firn (Battle, 1996), and NOAA flask are shown filled circle, open circle, and open triangle symbols, respectively. The black smooth

line shows the N_2O concentration (1860-2009) by Hansen and Sato, (2004) and NOAA/ESRL flask.

In particular for the year 2005, the calculated rise in atmospheric N_2O concentration is around 320 ppb. This is close to the observed value of 319 ppb by NOAA/ESRL flask data (Figure 3.6, left panel). The N_2O concentration increases rapidly up to 469 ppb by the end of the 21st century under the SRES A1B scenario. As compared to the year 2005, the N_2O concentration is higher by 149 ppb or 46% by the end of the 21st century.

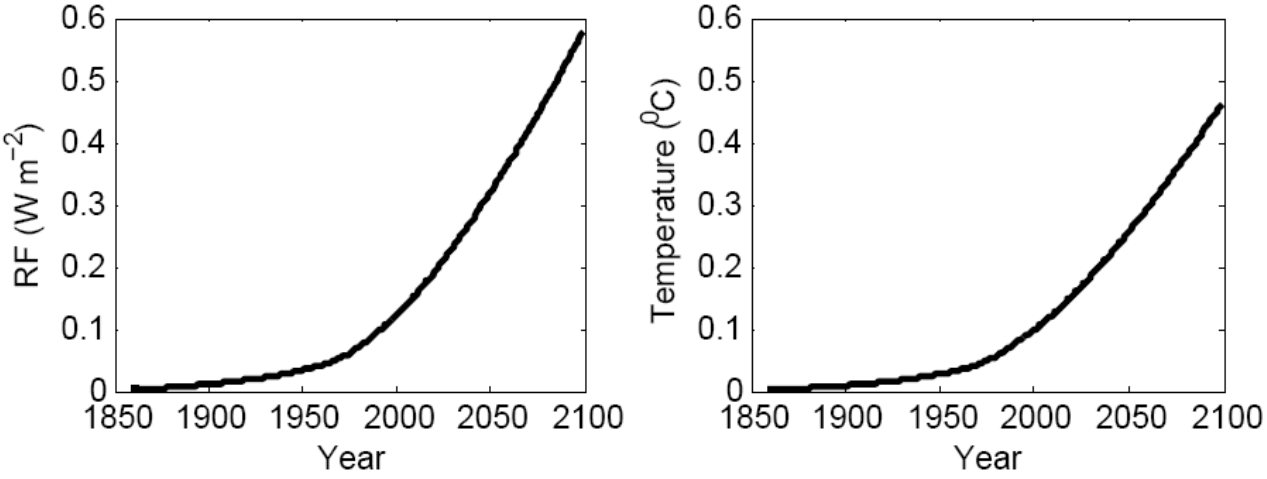

Figure 3.7: Radiative forcing (Wm^{-2}) and increase in temperature calculated from the global atmospheric N_2O concentration over the period 1860-2100.

The calculated global radiative forcing (RF) from N_2O emissions is around 0.14 Wm^{-2} in 2005 (Figure 3.7, left panel) and is in agreement with the value published in the IPCC AR4 report (ca. 0.16 Wm^{-2}) for present-day. The RF from N_2O is much less than from CO_2 (ca. 1.66 Wm^{-2}) because of lower mixing ratio of N_2O. The results also show that the calculated RF is increasing over the period 1860-2100 as the N_2O concentration increases in the atmosphere. By the end of the 21st century, the calculated RF reaches at 0.57 Wm^{-2} and leads to a projected increase in temperature by 0.46^0C since 1860 (Figure 3.7, right panel). In contrast, the temperature increase in relation to atmospheric CO_2 concentration usually ranges from 2 to 4.5°C (IPCC, 2007) following a doubling of CO_2 concentration.

As compared to CO_2, the temperature increases from atmospheric N_2O concentration is not significantly large because of its lower concentration in the atmosphere.

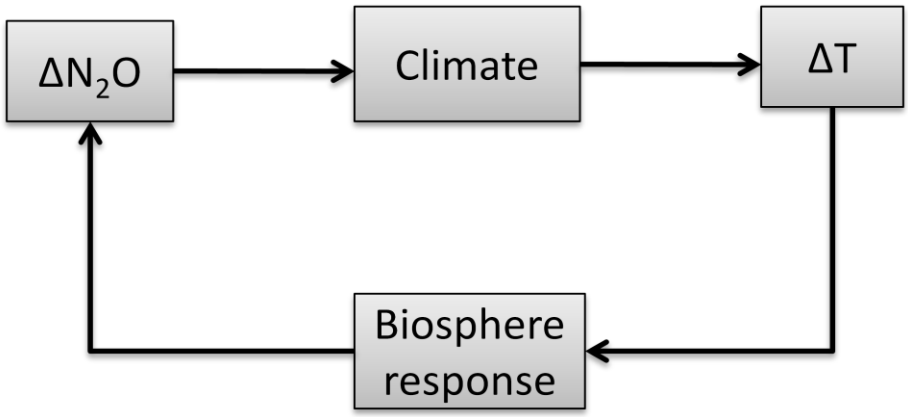

Figure 3.8: Schematic diagram depicts the climate-N_2O feedback. N_2O emissions from the terrestrial biosphere change the temperature. The increased temperature resulting from the emissions may in turn accelerate further the release of more N_2O emissions.

Figure 3.8 depicts the schematic diagram for climate-N_2O feedback. The results show a weak positive climate-N_2O feedback factor (0.0003) due to further release of N_2O emissions from the terrestrial biosphere at increased temperatures. Because of the weak positive climate-N_2O feedback gain factor, it is inferred that there would not be any further boosting of global warming arises particularly from the additional N_2O emissions related to temperature gain. Although, a weak positive climate-N_2O feedback factor is found between N_2O emissions and climate, the calculation and consideration of such effect is still very important in the context of global warming caused from the terrestrial N_2O emissions at increased temperatures.

3.4. Discussions

3.4.1. Effect of temperature and elevated CO_2 concentration on N_2O emissions

In the present study, temperature is found to be an important control for the microbial processes of N mineralization (i.e. nitrification and denitrification) and it induces the production of N_2O emissions from natural soils. Higher temperature causes an increase in N_2O emissions from natural soils by around 1 Tg N yr^{-1} by the end of the 21st century under the SRES A1B scenario (Figure 3.3). These results are consistent with the previous studies which reported that N_2O emissions are more sensitive to soil temperature (Prinn et al., 1999; Werner et al., 2007; Grant and Pattey, 2008; Szukics et al., 2010). However, Barnard et al. (2005) reported that the soil warming does not influence N_2O emissions, although these results are obtained where the emissions are predominately constrained by N availability. Additionally, the results show that the simulated N_2O emissions are positively correlated (e.g., slope around 0.69) with surface temperature (Figure 3.4). This result is in good agreement with other studies which reported a strong relationship between N_2O emissions and surface temperature (Dong et al., 2000; Lin et al., 2010; Zhang et al., 2010).

In particular, increased atmospheric CO_2 concentration generally leads to higher plant litter fall that induces N availability. This leads to increase in the simulated N_2O emissions and is consistent with the previous studies (Ineson et al., 1998; Baggs et al., 2003; Kammann et al., 2008). In contrast, some studies also reported that elevated CO_2 concentration does not increase N_2O emissions (Hungate et al., 1997; Ambus and Robertson, 1999; Billings et al., 2002; Mosier et al., 2002) because increase litter input leads to higher litter C:N ratio and increases microbial N demand by stimulating higher N immobilization flux (Hungate et al., 1997).

3.4.2. Atmospheric N_2O concentration and uncertainties

Microbial processes of nitrification and denitrification are the principal source of atmospheric N_2O and predominantly control N_2O evolution in the atmosphere (Bouwman et al., 1995; Kroeze et al., 1999; Flechard et al., 2007). However, N_2O from other sources, for example, the synthetic N fertilizer, biomass burning, transport and industrial process also contributes strongly to atmospheric N_2O concentration. The calculated rise in the

atmospheric N_2O concentrations from pre-industrial values of around 276 ppb to 320 ppb in 2005 is indeed a consequence of increased N_2O emissions from natural soils, driven by increased fertilizer use, fossil fuel combustion, biomass burning, biotic N fixation, and atmospheric N deposition. These results are consistent to observation by Hansen and Sato, (2004) and NOAA/ESRL, as mentioned previously above. Moreover, since 1960, the evolution of atmospheric N_2O concentrations is mainly determined by the N_2O emissions resulting from the use of synthetic N fertilizers (van Aardenne et al., 2001; Davidson, 2009) and fossil fuel emissions. By the end of the 21st century, the calculated atmospheric N_2O concentrations reach 469 ppb under the A1B scenario, which is quite close to estimate of 455 ppb by Höhne and Blok (2005).

The evolution of atmospheric N_2O concentrations may also differ probably due to the uncertainties in N_2O lifetime, as well as in the emission factors for various N_2O sources considered in the calculation. This study assumes not only the constant lifetime of N_2O (i.e. 114 years) but also the constant emission factor for the various N_2O sources. For instance, the emission factor for the synthetic N fertilizer is assumed to be 2.5% – also used by Davidson (2009) – for constructing the atmospheric N_2O concentration until 2005. Even so, this emission factor may vary from 1.25% (e.g., IPCC methodology) to 4% (Conrad et al., 1983; Bouwman, 1990; Houghton et al., 1990; Davidson, 2009). A top-down method by Crutzen et al. (2008) shows that in the IPCC method this emission factor is too low by factor of about two. Similarly, the constant emission factor from other N_2O emission sources, for instance, biotic N fixation and N deposition may be considered as an additional possible source of uncertainty in the calculation of atmospheric N_2O concentration.

3.4.3. N_2O emission and climate feedback

The direct effects of CO_2 on surface temperature are relatively well understood. However, the overall effect is complicated since it reflects the feedback of temperature and other GHG (Lashof et al., 1997; Scheffer et al., 2006). For instance, higher temperature may release more CO_2, CH_4, and N_2O from terrestrial ecosystems (Scheffer et al., 2006). In the C^4MIP studies, Friedlingstein et al. (2006) found consistently that all the models show the positive climate-carbon feedback and estimated the additional warming of about 0.1-1.5^{0}C. So far none of the studies have addressed the feedback resulting especially from

N_2O emissions of the terrestrial ecosystems. In the present study, a weak positive climate feedback gain factor of about 0.0003 is found due to the further release of N_2O emissions at increased temperatures from the terrestrial biosphere. Because of a weak climate feedback, it is inferred that the climate-N_2O feedback is negligible.

Furthermore, none of the other modeling studies have investigated the effect of climate feedback caused from the N_2O emissions. Moreover, process-based models of N trace gas emissions are still at an early stage, and only few studies have incorporated the N_2O emission into a process-based N cycle models (Sokolov et al., 2008; Xu-Ri and Prentice, 2008; Zeahle et al., 2010b). Nevertheless, most of these models so far do not attempt to compute atmospheric N_2O concentration from the terrestrial biosphere. Therefore, the climate-N_2O feedback factor derived from this study is an important step but at the same time it remains a high uncertainty especially due to uncertainty of emission factors.

3.5. Conclusions

In this study, the recently developed process-based JSBACH-CN model is used to investigate N_2O emissions from natural soils and climate-N_2O feedback. For site-scale model evaluation, the simulated N_2O emissions have been compared with the observations. The comparison shows a good correlation between simulated and observed N_2O emissions both for forest and grassland ecosystems (Section 3.3.1). The results show that the simulated N_2O emissions from the terrestrial ecosystems are higher in Southeast Asia, Amazon forest, and Central Africa when compared to the other regions. In particular, tropical rainforests soils are the major source of N_2O emissions and are in line with previous studies (Melillo et al., 2001; Werner et al., 2007).

Globally, the simulated N_2O emissions from natural soils are around 6 Tg N yr^{-1} for present-day conditions. By the end of the 21st century, emission increases to around 8 Tg N yr^{-1} (or one-third) under the A1B scenario and contributes significantly to the global N_2O budget. Furthermore, the results show that N_2O emissions from natural soils are sensitive to climate change. By the end of the 21st century, as temperature increases, N_2O emissions from natural soils also increase by about 1 Tg N yr^{-1}.

By including all N_2O emission sources (natural soils, ocean, open sources, fossil fuel, biomass burning, and synthetic N fertilizers) it is found that the rise in the atmospheric N_2O concentration is close to observations over the period 1860-2005 (a rise from 276 to 320 ppb). After 1960, the evolution of atmospheric N_2O concentrations is mainly determined by N_2O emissions resulting from the use of synthetic N fertilizers and fossil fuel emissions. By the end of the 21^{st} century, the calculated atmospheric N_2O concentrations reach 469 ppb under the A1B scenario. The calculated atmospheric N_2O concentrations may also differ due to uncertainties regarding the emission factors for various N_2O sources considered in the calculation.

The calculated RF from N_2O emissions is around 0.14 Wm^{-2} for 2005; this compares well with the value published in the IPCC AR4 report (i.e. 0.16 Wm^{-2}). For the end of the 21^{st} century, a RF of 0.6 Wm^{-2} is obtained. This leads to a projected increase in temperature by 0.46^0C since 1860. Additionally, a weakly positive climate-N_2O feedback gain factor is obtained because of the further release of N_2O emissions at increased temperatures from the terrestrial biosphere. However, the calculation results infer that this feedback is negligible.

Chapter 4

4. N_2O emissions in the presence of anthropogenic land cover change and wood products in mitigating climate change

Abstract

In the last several decades, increasing N inputs to agricultural soils through anthropogenic activity (e.g., use of synthetic N fertilizers) have led to an increase in N_2O emissions. Also the conversion of land for agricultural use (e.g., deforestation) has led to N_2O releases into the atmosphere. So far, only a few studies have estimated N_2O emissions from land use change based on the limited data or modeling. In the present study, N_2O emissions that arise from both anthropogenic land cover change and fertilized agricultural soils are addressed by performing several simulations. The conversion of forests also leads to carbon storage in the form of wood products (e.g., fuel wood, paper products, building, furniture, etc.) and thereby the present study discusses the role of long-lived wood products for climate change mitigation.

Simulation results show that the N_2O emissions from land use change are higher in the tropical regions where widespread deforestation over the last several decades has taken place. The associated global N_2O emissions for the 1990s are around 0.75 Tg N yr^{-1}; this accounts for about 5% of the global N_2O budget. Furthermore, the results show that fertilized agricultural soils emit substantially more N_2O into the atmosphere as a direct result of synthetic N fertilizer use. N_2O emissions from fertilized agricultural soils are around 4.9 Tg N yr^{-1} for the 2050s; the contribution of N fertilizers accounts for about 2.9 Tg N yr^{-1}, or 60%. Thus, synthetic N fertilizers are a significant source for N_2O emissions. Besides this, the results show that agricultural N_2O emissions are highest in Asia, followed by North America, and Europe, that is, 46, 18, and 14% of the fertilized agricultural soils emission, respectively.

Wood products from forests are important for climate change mitigation by curbing the land use emissions. The simulation results show that globally wood products cause a reduction of about 6% in land use carbon emissions over the period 1860-2000. This reduction is quite small as compared to the fossil fuel emissions. Therefore, this study found a minor role of wood products in mitigating climate change.

4.1. Introduction

Human-induced land cover change (e.g., deforestation) has a substantial effect on the environment. Over the last centuries to millennia, about one-third to one-half of the Earth's land surface has been modified by the transformation of natural ecosystems to agriculture areas (Vitousek et al., 1997). Such large-scale modifications of the land surface have an important consequences on the global N cycle (Conrad, 1996; Denman et al., 2007; Galloway et al., 2008) resulting in a change to the N_2O emissions from soils (Erickson and Keller, 1997; Skiba et al., 2000). For example, N_2O emissions are commonly high in newly deforested areas (Luizão et al., 1989) but after few years of disturbance less N_2O is emitted (Crutzen and Andreae, 1990; Bouwman et al., 1993; Van Amstel and Swart, 1994).

In tropical forests, the widespread human-induced land cover change leads to an increase in N_2O emissions (Erickson and Keller, 1997; Verchot et al., 1999). For example, in South and Central America, deforestation caused an increase in N_2O emissions by a factor of two (Keller et al., 1986). On the other hand, biomass burning is also substantial in the tropical countries. In the developing countries, a substantial amount of agricultural waste and fuel wood is combusted that further increases N_2O emissions into the atmosphere (Crutzen and Andreae, 1990).

N_2O emissions from anthropogenic sources (e.g. agriculture, N fertilizers use) account for about 65 to 80% of total emissions (Crutzen et al., 2008; IPCC, 2007). N inputs to agricultural soils through synthetic N fertilizers, atmospheric N deposition, and biotic N fixation are considered as the main contributors to global N_2O budget. However, emissions from the above mentioned sources are highly uncertain because they depend not only on various environmental factors but also on the amount of fertilizer applied (IPCC, 2001). Current estimates for global annual emissions from agricultural soils are about 4.2

Tg N yr^{-1}; the uncertainty range is 0.6-14.8 Tg N yr^{-1} (Mosier et al., 1998; Kroeze et al., 1999; IPCC, 2001). The IPCC method commonly estimates N_2O emissions from N inputs of fertilizers and N deposition by using a constant emissions factor of about 1.25% (IPCC, 1997). However, in comparison, field studies show an emissions factor in the range of about 0.2-4% (Conrad et al., 1983; Bouwman, 1990; Houghton et al., 1990).

The objectives of the present study are to study by simulations, N_2O emissions from anthropogenic land cover change and fertilized agricultural soils. To address N_2O emissions from anthropogenic land cover change, a relocation of both C and N pools are incorporated in the JSBACH-CN model. Additionally, N_2O emissions from agricultural soils are incorporated by including the data of synthetic N fertilizer application to agricultural ecosystems. The conversion of forests leads to carbon storage in the form of wood products (e.g., fuel wood, paper products, building, furniture, etc.) and thereby the present study also analyses the role of long-lived wood products for climate change mitigation.

4.1.1. Modelling N_2O emissions from anthropogenic land cover change

Worldwide deforestation releases not only CO_2 to the atmosphere but also other greenhouses gasses such as CH_4, N_2O, NO_x etc. In particular, N_2O is released into the atmosphere directly with biomass burning as well as with subsequent use of the land.

Land use emissions (i.e. CO_2) caused mainly by changes in land cover from the natural ecosystem to crop land and are modeled by Pongratz et al. (2009) in the JSBACH. However, this study incorporates a relocation of both carbon and nitrogen between the pools along with changes in the cover fractions. Three additional anthropogenic pools: annual (i.e. fuel wood, biomass burning), decadal (i.e. wood pulp, paper), and centennial (i.e. building, wood furniture) are incorporated according to the Grand Slam Protocol proposed by Houghton et al. (1983) with a turnover time of 1, 10, and 100 years, respectively.

The vegetation C and N are released to the atmosphere via the three anthropogenic pools. When forest is removed, 23% of the vegetation C is chosen to be stored in the annual pool,

which is released by burning of biomass or fuel wood within 1 year. About 20% and 7% of the vegetation C are chosen to be released to the atmosphere from the decadal and centennial pools, respectively. These fractions of C emitted to the atmosphere due to land use conversion are adopted from the Grand Slam Protocol (Houghton et al., 1983; Kato et al., 2009). The remaining C fraction is left on the litter pool as slash left on the ground. From the above three anthropogenic C pools, CO_2 releases to the atmosphere. In addition, anthropogenic C pools store some amount of carbon for certain period of time in the form of wood products (e.g., fuel wood, paper products, building, furniture), which in turn, delay carbon release to the atmosphere. Thus, the wood products may mitigate climate change by delaying carbon release to the atmosphere.

On the other hand, N trace gases in the form of N_2O and NO_x are also emitted into the atmosphere. N_2O emissions from land use change are calculated from anthropogenic N pools. The detail descriptions are as below.

Table 4.1: Notations used in description of anthropogenic pools in the JSBACH-CN model.

Abbreviations for anthropogenic pools: AA: annual; AD: decadal; AC: centennial
X, A: any of the foregoing pools, atmosphere. Throughout, fractions are denoted by f.
Notation G, R, M, and W represents green, reserve, mobile, and wood pools, respectively (see Chapter 2.1 for details about notation).

C_X	$size\ of\ C\ pool\ for\ type\ X\ [mol(C)/m^2]$
N_X	$size\ of\ N\ pool\ for\ type\ X\ [mol(N)/m^2]$
$f_{W \to X}$	$fraction\ of\ wood\ relocated\ to\ X$
$f_{G/M \to A}$	$fraction\ of\ N\ flux\ lost\ from\ G/M\ to\ A\ (i.e.\ 50\%)$
c_i^{old}	$old\ cover\ fraction\ of\ the\ i-th\ PFT$
c_i^{new}	$new\ cover\ fraction\ of\ the\ i-th\ PFT$
$a-$	$area\ lost\ due\ to\ land\ cover\ change$
τ_X	$turnover\ time\ of\ X$
EF	$emission\ factor$

The three anthropogenic C and N pools develop in time according to the following equation:

$$\frac{dC_X}{dt} = \sum_{i \in a-} r_i \, f_{W \to X} C_{W,i} - \frac{C_X}{\tau_X} \text{ , for pools X} = \text{AA, AD, and AC} \qquad (1)$$

$$\frac{dN_X}{dt} = \sum_{i \in a-} r_i \, f_{W \to X} N_{W,i} - \frac{N_X}{\tau_X} \text{ , for pools X} = \text{AA, AD, and AC} \qquad (2)$$

In Eq. 1 and 2, r_i denotes to the rate of change in cover fractions and this can be written as:

$$r_i = \frac{{c_i}^{old} - {c_i}^{new}}{1 \; year}$$

The term on the right hand side of the Eq. 1 and 2 is the losses of C or N to the atmosphere from anthropogenic pools. The green and reserve (mobile in case of N) pools also release C or N through biomass burning and are modelled as similar to the previous study by Pongratz et al. (2009).

N_2O emissions from anthropogenic land cover change can be written as:

$$N_2O_{(dir)} = \left(\frac{N_X}{\tau_X} + \sum_{i \in a-} r_i \, . \left(f_{G \to A} N_{G,i} + f_{M \to A} N_{M,i} \right) \right) * EF \qquad (3)$$

In Eq. 3, $N_2O_{(dir)}$ denotes direct N_2O emissions from anthropogenic land cover change. EF is the emission factor for the direct N_2O emissions and is assumed to be 1% of the biomass N release to atmosphere, which is close to the value of 0.7% (± 0.3%) obtained from Crutzen and Andreae (1990) and Jallow (1995). In the literature, this EF is in the range of 0.5 to 0.9% (Van Amstel and Swart, 1994). Additionally, this study assumes that the indirect emissions are 3% of the amount of biomass N exposed to destruction, which is quite close the study by Kroeze (1994).

4.1.2. Modelling N_2O emissions from fertilized agricultural soils

N_2O emissions from fertilized agricultural soils are modelled mainly by implementing synthetic N fertilizer application to agricultural ecosystems. The synthetic N fertilizer data is obtained from Bouwman et al. (2009) for the years 1970, 2000, 2030, and 2050. The synthetic N fertilizer data for the future years (2030 and 2050) is based on the Global Orchestration (GO) scenario, that was developed in the Millennium Ecosystem Assessment and the details can be found in Bouwman et al. (2009). To generate from all these snapshots yearly synthetic N fertilizer input data in time and space for the periods 1970-2050, the synthetic N fertilizer input maps are linearly interpolated.

The synthetic N fertilizer application to agricultural ecosystems is distributed equally into daily instead of split applications. Additionally, only 50% of synthetic N fertilizer to agricultural ecosystems is applied because this model does not have an explicit process, i.e. the so called "harvesting" from agricultural fields. Previous studies suggested that about 50% of the applied N is removed by crop harvesting and the remaining is prone to leaching or gaseous losses (Bouwman et al., 2005). Therefore, due to lack of a detailed process of crop harvesting in the JSBACH-CN model, this assumption of 50% of fertilizer application to agricultural ecosystems is quite reasonable. In particular, to obtain N_2O emissions from fertilized agricultural soils, this study assumes around 2.5% of synthetic N fertilizer that can be emitted to atmosphere as N_2O, which is quite close to study by Davidson (2009).

4.2. Setup of model experiments and driving data

In this study, the experiments are designed by using the forcing data from Roeckner et al. (2011). The details about this data and the model setup were already described in Chapter 2.3. In the present study, the experiments differ from the previous experiments (Chapter 2) with respect to the inclusion of N_2O emissions in the JSBACH-CN model. The experiments also differ with respect to additional forcing of the anthropogenic land cover change and synthetic N fertilizer. The anthropogenic land cover change maps are obtained from Pongratz et al. (2008); for the future, the land cover change maps are used under the SRES A1B scenario (for a description see Nakicenovic et al., 2000).

In order to address the main questions of this study, three transient simulation experiments are performed, i.e. CN-LC-AP, CN-LC, and CN-FL covering the years 1860-2100. The first transient experiment CN-LC-AP is the main experiment, which is performed with JSBACH-CN model, where the anthropogenic C and N pools are used as described in Section 4.1.1. In order to isolate the effect of anthropogenic C and N pools from the main experiment CN-LC-AP, the second experiment CN-LC is designed. In this case the anthropogenic C and N pools are not used, where 50% of the vegetation carbon and nitrogen are chosen as flux to the atmosphere (see Pongratz et al., 2009). In the above two experiments, the anthropogenic land cover change maps are used as an additional forcing variable. This study performs third experiment called CN-FL, where a constant land cover map of the year 1860 is used throughout the whole simulation. In all these experiments, an additional forcing of synthetic N fertilizer is used; however, a constant forcing of N fertilizer is kept from 2050 to 2100 by using the forcing data of year 2050.

The difference between two experiments, that is [CN-FL minus CN-LC-AP] and [CN-FL minus CN-LC] quantifies the net CO_2 emissions by considering the anthropogenic pools and without anthropogenic pools, respectively. The direct N_2O emissions are quantified by using the Eq. 1, which are obtained from the main experiment CN-LC-AP. The difference between CN-FL and CN-LC-AP experiments quantifies the indirect N_2O emissions from the amount of biomass N that is exposed to destruction.

4.3. Results

4.3.1. Land use change and wood products

In Figure 4.1, the simulated wood products for different regions obtained from the CN-LC-AP simulation are displayed. The results show that the simulated wood products are largest in Asia, South America, and Africa, found to be around 2.7, 2.0, and 1.15 Pg C, respectively. For North America and Europe, the simulated wood products are around 0.45 and 0.3 Pg C, respectively. Globally, the simulated wood products are around 7.2 Pg C. This is much larger than the estimate of 4.2 Pg C by SAR IPCC (IPCC, 1996b). However, the wood products stock is also reported in the range of about 10-20 Pg C (Sampson et al., 1993; Brown et al., 1996). For North America, the simulated wood products are quite

close to the lower end of the range of estimates of 0.4-1.3 Pg C (Churkina et al., 2010). For Europe, the simulated wood products are much lower than the estimates of about 0.7 Pg C by Eggers (2002).

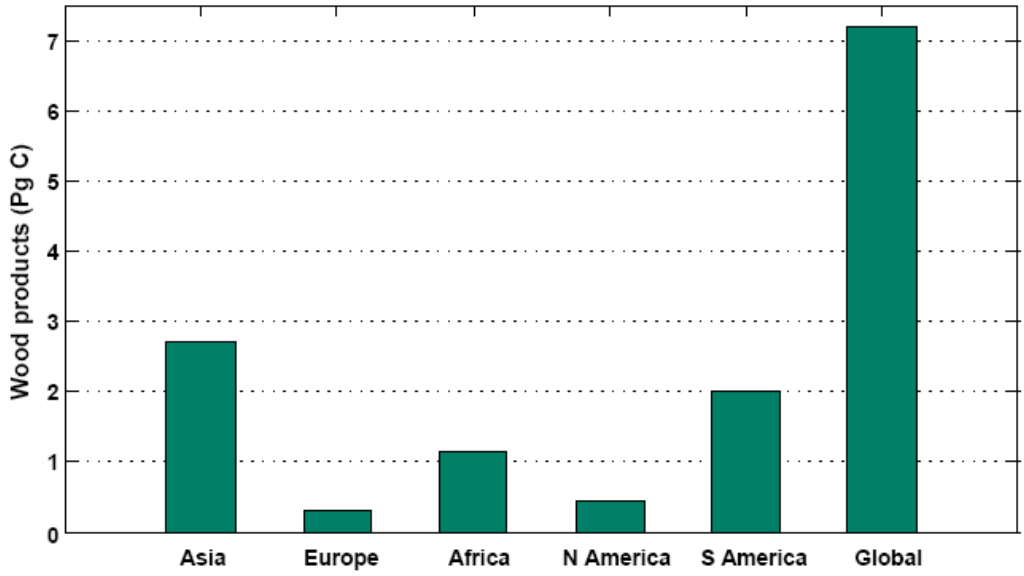

Figure 4.1: Simulated wood products (means for 1990-99) by region.

The results show that the wood products cause a global carbon sink of about 0.1 and 0.15 Pg C/yr for the 1980s and 1990s, respectively (Table 4.2). This result is consistent with the IPCC SAR estimates of 0.14 Pg C/yr. However, Houghton (1996) estimated the global carbon sink to be about 0.4 Pg C/yr, which seems to be an overestimation when taking the other results into consideration (Table 4.2).

Table 4.2: Comparison of simulated carbon sink (Pg C/yr) in wood products for 1980-89 and 1990-99.

study	1980s	1990s
CN-LC-AP	0.1	0.15
IPCC SAR	-	0.14
Houghton (1996)	0.4	0.5

The cumulated land use carbon emissions over the period 1860-2000 are 134 and 126 Pg C by the CN-LC and CN-LC-AP experiments, respectively (Table 4.3). These results are in line with previous estimates of 108-139 Pg C for the release to the atmosphere due to anthropogenic land cover change (Bolin et al., 2001; Gitz and Ciais, 2003; Pongratz et al., 2009). The results show that land use carbon emissions are reduced by 8 Pg C over the period 1860-2000 due to the inclusion of anthropogenic C pools. This equates to a reduction of about 6% of land use carbon emissions because the carbon stored in wood products is bound for a certain period of time and therefore not released immediately into the atmosphere.

Table 4.3: Cumulated land use carbon emissions over 1860-2000.

Study	Time Period	Emissions (Pg C)
CN-LC	1860-2000	134
CN-LC-AP	1860-2000	126
Pongratz et al. (2009)	1850-2000	108
Bolin et al. (2001)	1850-1998	136
Gitz and Ciais (2003)	1850-1998	139

4.3.2. Land use change and N_2O emissions

Figure 4.2 shows the spatial distribution of simulated N_2O emissions (i.e. direct plus indirect) obtained from the CN-LC-AP experiment. The results show that the deforested regions release higher N_2O emissions than the undisturbed regions. This is due to widespread burning of biomass and fuel wood. In addition, wood products with longer turnover time release small amounts of N_2O into the atmosphere through their decomposition.

The simulated N_2O emissions are particularly pronounced in Southeast Asia and South America. This is primarily due to the extensive conversion of natural forest to pasture or cropland. The simulated N_2O emissions are higher in the tropics and account in the range of 2-12 mg N m^{-2} yr^{-1}. In the temperate regions, the emissions are found to be lower, i.e. less than 2 mg N m^{-2} yr^{-1}.

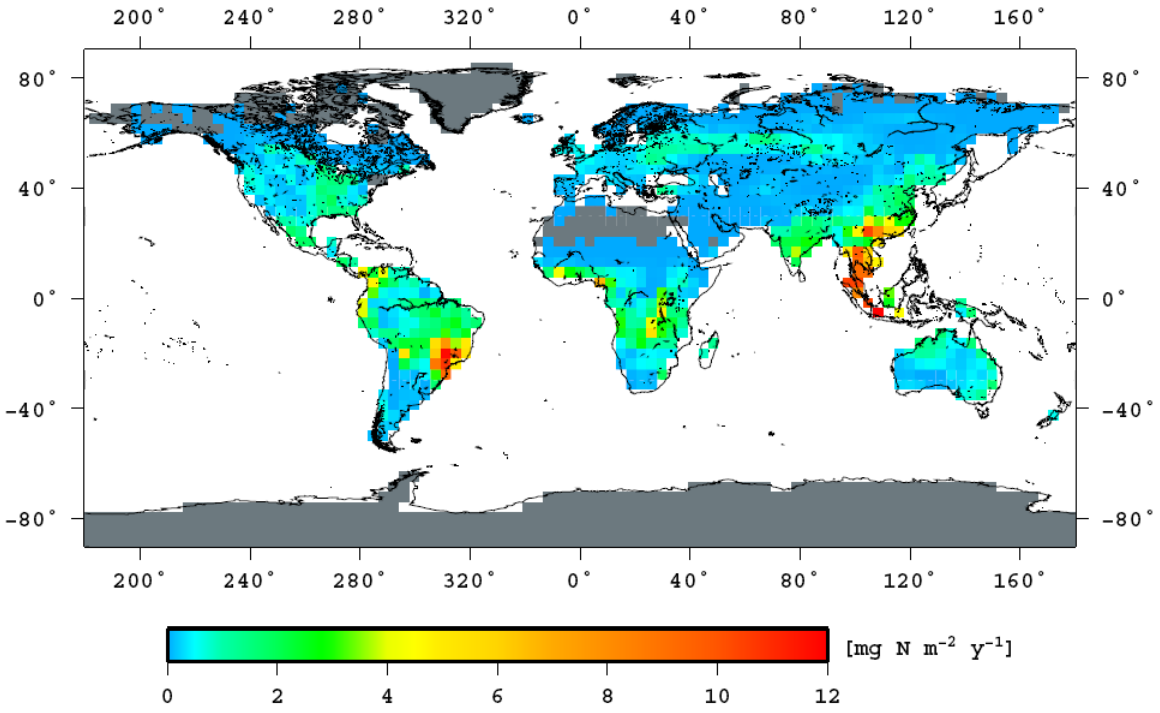

Figure 4.2: Simulated N_2O emission from anthropogenic land use change (means for 1970-99).

Globally, the simulated N_2O emissions due to land use change are around 0.6 and 0.75 Tg N yr^{-1} for the 1980s and 1990s, respectively. This result is consistent with the previous estimate of 0.5 Tg N yr^{-1} (Kroeze, 1994) but less than the 1.0 Tg N yr^{-1} obtained by Cofer et al. (1991). This result is also in agreement with the estimate of 0.2-1.0 Tg N yr^{-1} obtained by Houghton et al. (1992).

The results show that the simulated N_2O emissions increase from 0.2 to 0.8 Tg N yr^{-1} over the period 1860 to 1954 due to deforestation (Figure 4.3). However, the conversion of natural land to agriculture or pasture is reduced from the 1950s and thereby a sharp decline in N_2O emissions is seen in the next few decades. This decline is found to be around 0.4 Tg N. Since 1992, the results show that the simulated N_2O emissions are continuously declining because of the lower deforestation rate. The results also show that the simulated N_2O emissions are much smaller (ca. 0.1 Tg N yr^{-1}) for the end of the 21st century under the SRES A1B scenario.

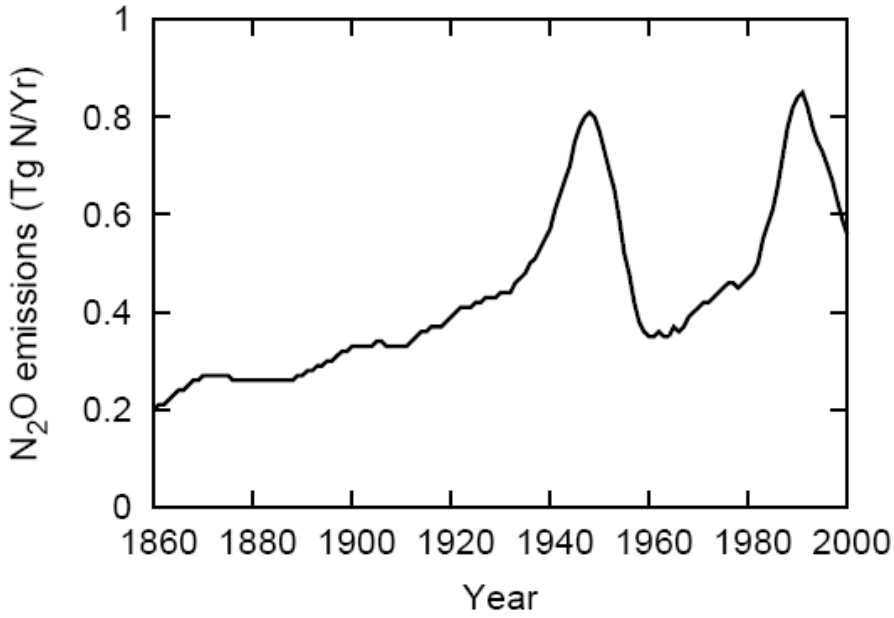

Figure 4.3: Simulated N_2O emissions over the period 1860-2000 from anthropogenic land use change.

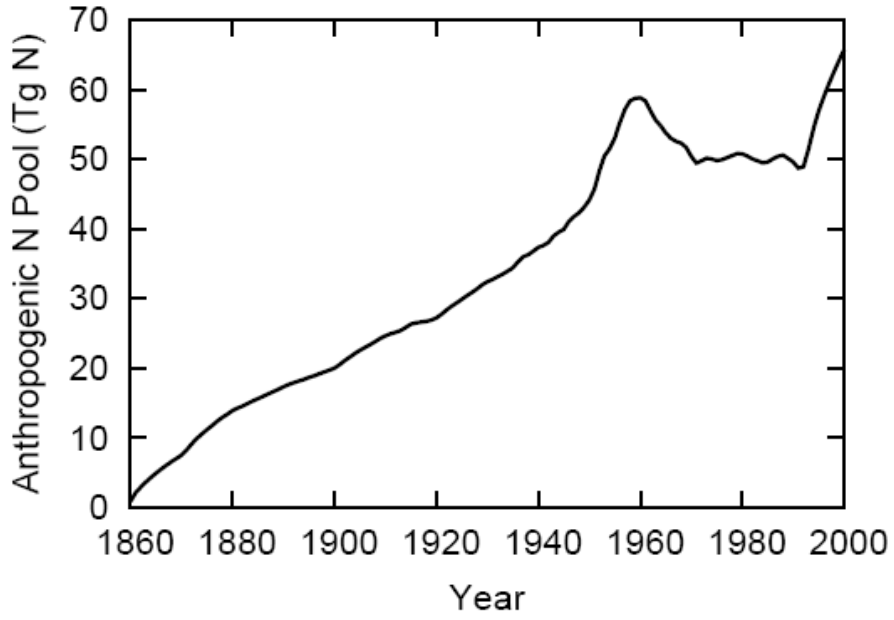

Figure 4.4: Simulated total anthropogenic N pool over the period 1860-2000.

The results of CN-LC-AP experiment show that the simulated total anthropogenic N pool size increased from 1860 to 1954 due to higher conversion rate of forest into agriculture or pasture (Figure 4.4). It's size is found to be around 50 Tg N during 1950s. Since the 1950s, a slight reduction of the anthropogenic N pool is obtained because of the lower plant material added to the anthropogenic pools from the converted natural vegetation. For the 1980s and 1990s, the size of the simulated anthropogenic N pool is around 50 and 55 Tg N, respectively. In particular, the centennial anthropogenic N pool shows a higher amount of N stock (ca. 40 Tg N) than the annual and decadal anthropogenic N pools and this is because of longer turnover time (ca. 100 years) of the pool. In contrast, the results show that less than 10 Tg N is stored in the annual and decadal pool and the reason for this is that N is converted to N_2O and other trace gases within 1 to 10 years. Therefore, the annual and decadal anthropogenic pool sizes are much smaller than the centennial anthropogenic N pool.

4.3.3. N_2O emissions from fertilized agricultural soils

The results show that the simulated N_2O emissions are pronounced in South East Asia, North America, and Europe (Figure 4.5). These regions show N_2O emissions which are typically more than 100 mg N m^{-2} yr^{-1} than for the other regions. The reason for high emissions is that these regions are dominated by agriculture with extensive synthetic N fertilizer application. The use of synthetic N fertilizer, furthermore, is now prevalent in both developing and developed countries. As a consequence, the simulated N_2O emissions are generally high for both. Additionally, atmospheric N deposition is found to be high in South East Asia, North America, and Europe. This aids the emission of N_2O from these regions. However, the simulated N_2O emissions are lower in South America, Africa, and Oceania, found to be less than 100 mg N m^{-2} yr^{-1}. The lower N_2O emissions from these regions are due to lower levels of N inputs to agricultural soils via N fertilizer as well as N deposition.

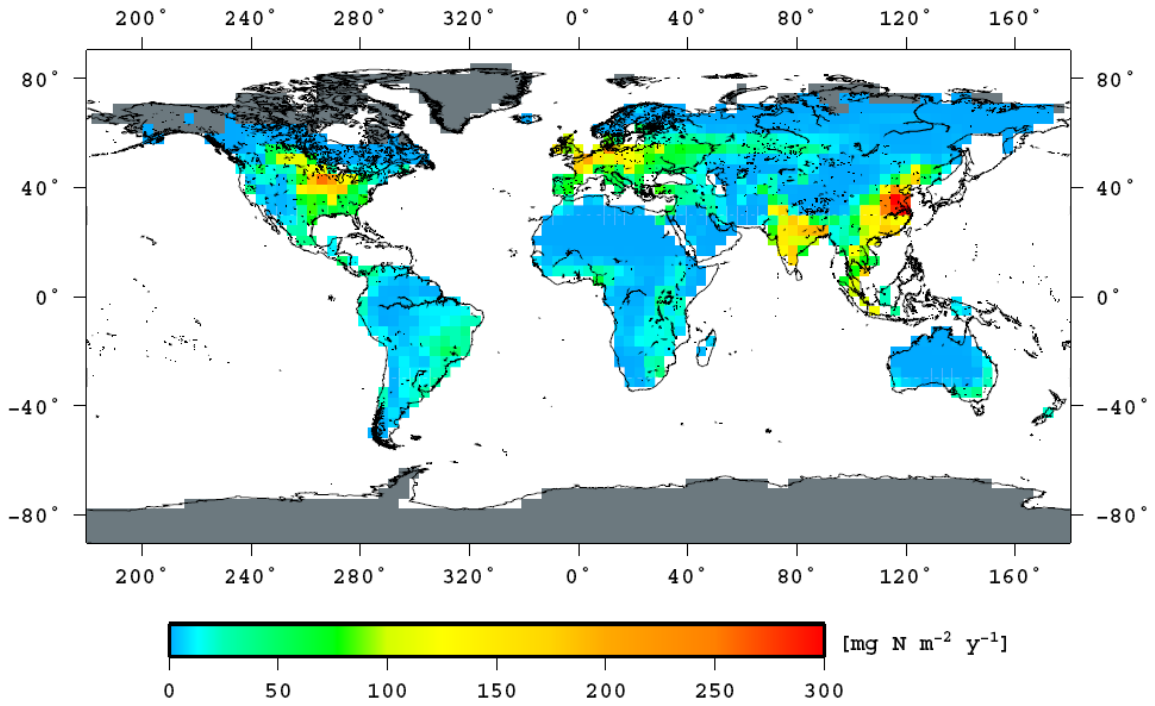

Figure 4.5: Simulated N_2O emissions from fertilized agricultural soils (means for 1990-99) obtained from the CN-LC-AP simulation.

The global N_2O emissions for the 1990s are around 1.73, 0.45, and 1.1 Tg N yr^{-1} from synthetic N fertilizer, open sources, and mineralization process (i.e. nitrification and denitrification), respectively. The global total N_2O emissions from fertilized agricultural soils are around 3.3 Tg N yr^{-1}, of which N_2O release from the application of nitrogenous fertilizer accounts for about 50%. These results are consistent with the other estimates of 1.9 to 4.2 Tg N yr^{-1} (Olivier et al., 1998; Mosier et al., 1998; Kroeze et al., 1999); the IPCC TAR shows a larger uncertainty range of 0.6-14.8 Tg N yr^{-1}. Furthermore, the results show that the global total N_2O emissions from fertilized agricultural soils increase to around 4.9 Tg N yr^{-1} by 2050s, of which N_2O release from the application of nitrogenous fertilizer accounts for about 60% (or 2.95 Tg N yr^{-1}). N_2O emissions from mineralization process and open sources account for about 26% and 14%, respectively.

Figure 4.6 depicts global N_2O emissions from fertilized agricultural soils for the different continents. The results show that during the 1860s, N_2O emissions from fertilized agricultural soils account for less than 0.3 Tg N yr^{-1} across all continents. Globally, N_2O

emissions are about 0.6 Tg N yr^{-1}. However, emissions increase rapidly from 1860s to 1990s due to the application of more amounts of synthetic N fertilizers and also by high N inputs from atmospheric N deposition and biotic N fixation.

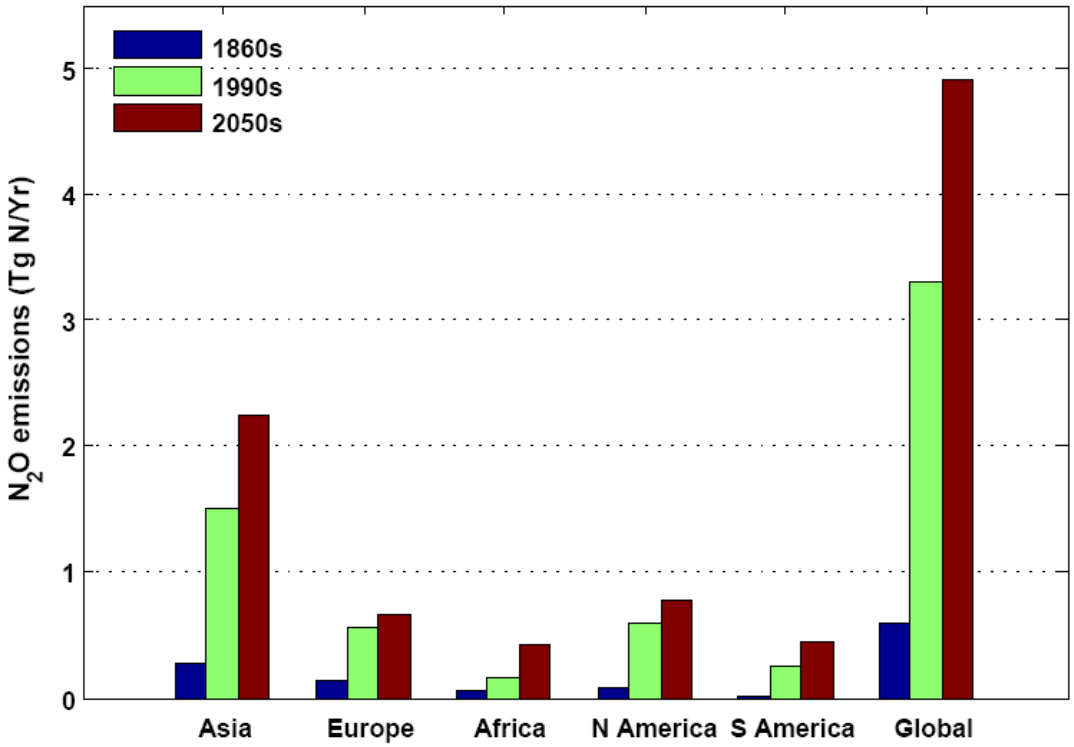

Figure 4.6: N_2O emissions by region from fertilized agricultural soils for the 1860s, 1990s, and 2050s.

During the 1990s, N_2O emissions from Asia are 1.5 Tg N yr^{-1}, which is the largest among the continents. This accounts for 45% of all global emissions (i.e. 3.3 Tg N yr^{-1}). The emissions from Asia reflect the high levels of N fertilizer applied to the agricultural ecosystems. The amount of N fertilizer applied in this region accounts for about 50% of the total amount of N fertilizer used globally (75.1 Tg N yr^{-1}, FAO, 1992). Second to Asia, N_2O emissions are high in North America (0.6 Tg N yr^{-1}), followed by Europe (0.55 Tg N yr^{-1}). Again, this also reflects the percentage of N fertilizer application, which for North America and Europe is 13.3 Tg N yr^{-1} (or 18%) and 12 Tg N yr^{-1} (or 16%), respectively (FAO, 1992). N_2O emissions from South America and Africa are around 0.24 and 0.16 Tg N yr^{-1}, respectively, which are generally lower than the other continents of the world.

During the 2050s, N_2O emissions from fertilized agricultural soils are around 4.9 Tg N yr^{-1}, of which Asia alone contribute 46% to global N_2O emissions. Next to Asia, North America and Europe account for 18% and 14% of fertilized agricultural soils emissions, respectively. Compared to the 1990s, N_2O emissions are increased by about 50% by 2050s in Asia. This is due to rapid increase in N fertilizer use as well as N inputs via N deposition and biotic N fixation. A similar rise in N_2O emissions also occur for North America, Europe, and South America by 2050s. The results also indicate that N_2O emissions in Africa jump by factor of 2.5 by 2050s, compared to 1990s levels. Again, this suggests that the continual rise in the use of synthetic N fertilizers in this region.

4.4. Discussions

4.4.1. Wood products for climate change mitigation

In several ways, forests are relevant in the context of climate change to limit the atmospheric CO_2 concentration that is rising continuously over the past century. One important aspect is the long-lived wood products, which delay carbon release to the atmosphere (Eggers, 2002). The carbon stored in wood products is bound for a certain period of time, because this is not released immediately to the atmosphere when the forest is cleared. However, after a certain period of time, wood products release carbon back to the atmosphere through decay and decomposition. Therefore, wood products storage is one way for the forest sector to mitigate climate change, along with carbon sequestration in the forest. Even so, there is a large uncertainty in the estimates of the amount of carbon stored in wood products (IPCC, 1996b). The simulation results show that globally about 7.2 Pg C is stored as wood products with a global carbon sink of 0.15 Pg C/yr. However, other studies reported a stock of 10-20 Pg C (Sampson et al., 1993; Brown et al., 1996) and a global sink of 0.14 Pg C/yr (Winjum et al., 1998). According to Houghton et al. (1996), the wood products may be higher by a factor two with a larger global sink of about 0.4 to 0.5 Pg C/yr. This indicates that the large accumulation of wood products may lead to a substantial reduction of land use carbon emissions. The simulated wood products cause a reduction of about 6% of land use carbon emissions over the period 1860-2000. As compared to fossil fuel emissions, wood products seem to be a minor role for long-lived wood products in helping to reduce land use carbon emissions. This study also inferred that anthropogenic C pools with a turnover time of 1 to 100 years do not change the land

use carbon emissions substantially as compared to the emissions that are without the inclusion of the anthropogenic C pools.

4.4.2. N_2O emissions from land use change and fertilized agricultural soils

The widespread deforestation that leads to N_2O emissions is mainly a consequence of human-caused modifications of land cover. Based on the limited data, Bouwman et al. (1995) reported that 0.4 Tg N yr^{-1} of N_2O is emitted from tropical forest. In contrast to Bouwman et al. (1995) results, the present simulation study shows that the global N_2O emissions resulting from widespread clearing of forests are 0.75 Tg N yr^{-1}. This is within the range of previous estimates of 0.2-1.0 Tg N yr^{-1} (Cofer et al., 1991; Houghton et al., 1992; Kroeze, 1994). These anthropogenic land use change emissions account for 5% of the global total N_2O budget (see Section 3.3.4 for total N_2O budget). This result is in line with the study of Kroeze (1994). Thus, N_2O emissions from anthropogenic land use change make up only a small portion of the global N_2O budget, suggesting that these may not cause a significant increase in atmospheric N_2O over the long term. The present study does not account N_2O emissions from agro-based biofuel production. However, a study by Crutzen et al. (2008) shows that biofuels especially from rapeseed with high plant N content can lead to a significant warming by N_2O emissions.

N_2O is primarily produced from fertilized agricultural soils by the microbial processes of nitrification and denitrification (Mosier, 1993). N_2O emissions also strongly depend on the level of mineral N availability in soil; further it is important to differentiate whether the mineral N availability is from synthetic N fertilizer, mineralization in the soil, atmospheric N deposition, or biotic N fixation (Duxbury and Mosier, 1993). N_2O emissions from fertilized agricultural soils are strongly influenced by direct changes in agricultural ecosystems that are affected by N input, i.e. the extent of synthetic N fertilizer application. The results show that the application of synthetic N fertilizers leads to a substantial N_2O emissions into the atmosphere, which are increasing at a faster rate since the agricultural revolution of the 1960s. The global N_2O emissions of fertilized agricultural soils are around 3.3 Tg N yr^{-1} for the 1990s; a significant amount, namely 1.73 Tg N yr^{-1}, or 50% of these emissions, are contributed by synthetic N fertilizers. These results are consistent with the estimate of 1.5 Tg yr^{-1} of N_2O from synthetic N fertilizers obtained in other studies (IPCC, 1992; Granli and Bøckman, 1994).

In particular, for present-day conditions this study finds that the largest N_2O emissions are from Asia, accounting for 45% of the global emissions resulting from fertilized agricultural soils. North America and Europe contribute around 18% and 16% to the global balance of N_2O emissions, respectively. These results match those of Bouwman et al. (2005), where a similar order of magnitude of N_2O emissions for fertilized agricultural soils from these three world regions was found. The results also show that the global N_2O emissions from fertilized agricultural soils increased rapidly between the 1860s and 1990s from 0.6 to 3.3 Tg N yr^{-1}. Further, the emissions rise to 4.9 Tg N yr^{-1} by 2050s; a significant amount, namely 60% of these emissions, are released from the application of nitrogenous fertilizer. The projected rise in N_2O emissions obtained from this study is quite close to the estimate of 4.2 Tg N yr^{-1} by Houghton et al. (1992). The results of this study also show that anthropogenic N_2O emissions from fertilized agricultural soils will continue to rise rapidly towards the end of the 21st century as N inputs via fertilizer, atmospheric deposition, and biotic fixation increase.

4.5. Conclusions

For the present study, the JSBACH-CN model is used to investigate by simulations, N_2O emissions both from anthropogenic land cover change and fertilized agricultural soils. The simulation results show that the N_2O emissions are higher in the tropical regions as a result of massive deforestation during the last several decades. Globally around 0.75 Tg N yr^{-1} of N_2O is emitted into the atmosphere as a result of the widespread clearing of forests. This constitutes about 5% of the total global N_2O budget, which seems to be only a minor contributing factor to the global atmospheric N_2O concentration.

This study finds that by 2050s N_2O emissions from fertilized agricultural soils are around 4.9 Tg N yr^{-1}, of which a significant amount, namely 60% of these emissions, are released from the application of nitrogenous fertilizer. Asia is the largest contributor to N_2O emissions and accounts for 46% of fertilized agricultural soils emission.

The wood products cause a global carbon sink of around 0.1 and 0.15 Pg C/yr for the 1980s and 1990s, respectively. This study finds that globally around 7.2 Pg C is stored in wood products. This amount of wood products stock reduces the land use carbon

emissions by 6% over the period 1860-2000. As compared to fossil fuel emissions, this reduction of the land use emissions is quite small. Thus, the present study infers that long-lived wood products have only a minor role to play in helping to mitigate the effects of climate change.

Chapter 5

5. Summary and Conclusion

5.1. Main findings of the interactions between C and N cycles

This thesis has addressed the interactions between the global C and N cycles in a changing climate. In order to study their interactions, this study describes a simple scheme for terrestrial N cycling that has been incorporated into the existing process-based land C cycle model (JSBACH). The newly developed C-N cycle model is based on only a small number of basic principles, namely mass conservation, a supply-demand ansatz, and fixed C-to-N ratios. Simulations have been performed for the period 1860-2100 by using this model and the main findings are:

- The tight coupling of C and N cycles in the terrestrial biosphere leads to a reduction of the global land C uptake by about 8% at the present-day condition. By the end of the 21st century, N limitation reduces the projected land C uptake by about 16% in response to increasing atmospheric CO_2 concentration and climate change under the A1B scenario. These results are qualitatively in agreement with previous global modeling studies (Thornton et al., 2007; Zaehle et al., 2010b. 2010c). But the consequences from the N cycle on the future global land C uptake are much less in this model than found in the study by Thornton et al. (2007).
- To check the robustness of certain model assumptions sensitivity experiments are performed, assuming quite drastic modifications of the model. The results show that the assumption “plant N uptake first” turned out to be unrealistic. From these sensitivity experiments, the present study infers that the standard model setup (i.e. equal competition between plants and soil microorganisms) is the most appropriate setup.
- The inclusion of the land N cycle in the model leads to a significant reduction of the positive climate-carbon cycle feedback by 21% under the A1B scenario until the end of the 21st century. These results are qualitatively in the same direction as found by Sokolov et al. (2008) and Thornton et al. (2009).

- A lowering of the land C storage due to N limitation is pronounced in grasslands than forests ecosystem. Moreover, N availability mostly affects carbon storage in soils (ca. 51 Pg C difference) as compared to vegetation and litter carbon storage. This is because N availability affects the turnover rate of litter carbon in the model. There is some evidence in the literature that N controls the rates of litter decomposition (Gosz, 1981; Fog, 1988; Taylor et al., 1989; O'Connell, 1994), however other studies found a contradictory results (Prescott, 1995; Vitousek and Hobbie, 2000) and therefore it remains inconclusive.
- In forest ecosystems, the soil N availability decreases during the first half of the 21st century under increased CO_2 concentration and climate change (Like PNL). These results support the hypothesis "PNL" as suggested by various authors (Luo et al., 2004; De Graaff et al., 2006; Hungate et al., 2006). But after mid of 21st century the PNL starts alleviating because of the relaxation of N scarcity due to global warming. The occurrence of PNL causes a reduction of the relative NPP difference more in temperate/boreal forests (ca. 5%) than tropical/subtropical forests (ca. 1%).
- In grassland ecosystems, the soil N availability decreases continuously (Like PNL) from the 19th century until the first half of the 21st century but recovers thereafter. Thus, the occurrence of PNL causes a substantial reduction of the relative NPP difference by 20%.
- To study the robustness of occurrence of PNL sensitivity experiments have been performed. These experiments show that by doubling biotic N fixation the appearance of PNL for grasslands during the 21st century is a very robust simulation result, whereas occurrence of PNL in forests is much less robust.

5.2. Main findings of N_2O emissions and climate change

In Chapter 3, N_2O emissions from natural soils under climate change and climate-N_2O feedback are investigated. To study this, the processes controlling N_2O emissions have been modelled in the JSBACH-CN model. Simulations have been performed for the period 1860-2100 and the main findings are:

- Globally, N_2O emissions from natural soils are around 6 Tg N yr^{-1} for present-day conditions. By the end of the 21st century, emissions increase up to 8 Tg N yr^{-1} (or one-third) and contribute significantly to the global N_2O budget under the SRES A1B scenario.
- Climate change increases emissions by 1.0 Tg N yr^{-1} by the end of the 21st century. In other words, N_2O emissions are sensitive to global warming.
- The rise in the atmospheric N_2O concentration is close to the observations for 1860-2005 (276-320 ppb). It increases up to 469 ppb by the end of the 21st century under the A1B scenario. This compares well with the estimate of 455 ppb by Höhne and Blok (2005).
- The calculated radiative forcing (RF) from N_2O emissions is around 0.14 Wm^{-2} in 2005 and is comparable with the value reported in the IPCC AR4. Further, this increases up to 0.6 Wm^{-2} by the end of the 21st century. The rise in RF from N_2O emissions leads to an increase in temperature by 0.46^0C under the A1B scenario.
- A weak positive climate-N_2O feedback gain factor is obtained due to the further release of N_2O emissions at increased temperatures from the terrestrial biosphere. Accordingly, it is inferred that the climate-N_2O feedback is negligible.

5.3. Main findings of N_2O emissions from land cover change

In Chapter 4, N_2O emissions from anthropogenic land cover change and fertilized agricultural soils are investigated. Due to large-scale deforestation, N_2O is emitted either directly by biomass burning or indirectly from the destructed biomass N. The conversion of forests also leads to carbon storage in the form of wood products and thereby the present study also discusses the role of long-lived wood products for climate change mitigation. The main findings from this Chapter are:

- The simulated global N_2O emissions from anthropogenic land cover change are around 0.75 Tg N yr^{-1} for the 1990s; this contributes around 5% of the global N_2O budget. As compared to these results, previous studies found in the range of 0.2-1.0 Tg N yr^{-1} (Cofer et al., 1991; Houghton et al., 1992; Kroeze, 1994).
- N_2O emissions from fertilized agricultural soils are around 4.9 Tg N yr^{-1} for the 2050s; a significant amount, namely 60% of these emissions is a direct consequence of the application of synthetic N fertilizers. The projected rise in N_2O emissions obtained from this study is comparable to the estimate of 4.2 Tg N yr^{-1} by Houghton et al. (1992).
- Agricultural N_2O emissions are higher in Asia, North America, and Europe than in the other regions. They account for 46, 18, and 14% of the total amount of fertilized agricultural soils emission, respectively.
- Long-lived wood products store about 7.2 Pg C. This carbon sink is responsible for a lowering of land use carbon emissions by 6% over the period 1860-2000. This reduction is quite small as compared to the fossil fuel emissions. Therefore, wood products play only a minor role to mitigate the climate change.

5.4. Next steps to be taken

This study has addressed the interactions between global C and N cycles and N_2O emissions by using a simple scheme of terrestrial N cycling in the JSBACH-CN model. For the present study, fixed C-to-N ratios across all PFTs are used. In addition, it does not distinguish explicitly the ammonia and nitrate pool for plant N uptake. These two simple approaches can be improved. This can be accomplished by including: (i) dynamic C-to-N ratios, and (ii) two distinct inorganic N pools. The dynamic C-to-N ratios could lead to future study, for instance, the plant adaptation in a changing climate by altering their N use efficiency (i.e. varying C-to-N ratios). The two distinct inorganic N pools could improve the approach of modeling N_2O emissions during nitrification and denitrifcation process.

In the present study, the biotic N fixation is computed based on net primary productivity and it does not account for the potential interactions with the phosphorus (P) cycle. The biotic N fixation can be improved by mechanistic model so that it can be linked to P

availability. In this context, the P cycle has to be added not only for improving the biotic N fixation in the model but also as an additional nutrient component in the JSBACH model. Many of the additional processes, for example, volatilization, split application of synthetic N fertilizers, or N harvesting along with the crop harvesting, are missing in the current model. Thus, in the future these missing processes could be taken into consideration in order to improve the N cycling in agricultural ecosystems as well as N_2O emissions from agricultural soils.

The present study can be expanded in the future with respect to the inclusion of the land C-N cycle dynamics with the fully-coupled MPI-ESM model so that the climate-carbon-nitrogen feedbacks can be analyzed. Other aspects of future study could be: to investigate the effect of N limitation on water cycle; the influence of disturbances (e.g., land use change, fire, etc.) on C-N cycle dynamics; and N_2O emissions from biofuel production.

6. Appendices

Appendix 2.1: Further details on C allocation in JSBACH

For better readability, in the main text a number of details on the JSBACH-C allocation scheme (Chapter 2.2) were omitted. These are provided by this appendix.

Allocation allometry

In JSBACH allometric relations are accounted for by distributing NPP at certain proportions to the different vegetation pools. The cases of positive and negative NPP have to be handled differently:

NPP > 0:

In this case NPP is distributed at fixed proportions to the three vegetation C pools (green, reserve, and wood) by the terms called NPP_G^{pot}, NPP_R, and NPP_W^{pot} (see equations (1)). In addition a certain part of NPP, called $F_{exudates}$, is reserved for root exudates. The respective equations are:

$$NPP_G^{pot} = f_{NPP \to G} * NPP^{pot} \qquad (A1)$$

$$NPP_R = f_{NPP \to R} * NPP^{pot} \qquad (A2)$$

$$NPP_W^{pot} = f_{NPP \to W} * NPP^{pot} \qquad (A3)$$

$$F_{exudates} = f_{NPP \to E} * NPP^{pot} \qquad (A4)$$

with

$$f_{NPP \to G} + f_{NPP \to R} + f_{NPP \to W} + f_{NPP \to E} = 1 \qquad (A5)$$

From these equations one easily finds equation (1). For the values of the allocation fractions $f_{NPP \to X}$ please see Table A1. These values lead to biomasses in different plant parts within observed ranges (Wolf et al., 2011).

NPP < 0:

In this case the respiration losses surmount the photosynthetic productivity. Accordingly, plants stop growing. For the model this means that no carbon can be allocated to the wood and green pool, and also there is no C available for exudates:

$$NPP_W^{pot} = NPP_G^{pot} = F_{exudates} = 0 \qquad (A6)$$

In this case plants activate sugars and starches to compensate the respiratory losses. In the model the C in the reserve pool is invested to replace missing productivity. For the model the only consequence is that the reserve pool is depleted by the negative NPP^{pot}. Within the framework of the rate equations from Section 2.2 this is achieved by setting

$$NPP_R = NPP^{pot} \qquad (A7)$$

In rare cases it happens that the reserve pool cannot fully compensate for the NPP deficit. In such cases the reserve pool is set to zero. In reality plants would let die part of the plants or even shed some leaves, as it is often observed during droughts. This process is not explicitly modelled in JSBACH, but taken implicitly into account by the shedding terms in equations (2) and (5) that are active even at negative NPP.

The foregoing presentation is in one respect incomplete: In reality plants actively prevent unhealthy growth by regulating dynamically the proportions of allocation to different organs, regulating down primary productivity, or increasing autotrophic respiration (Chambers et al., 2004). In JSBACH these processes are taken into account only in a very coarse way by limiting the size of the three vegetation C pools in such a way that plants cannot grow arbitrarily large: if the wood or reserve pool would exceed a prescribed maximum value, the excess C is used to fill the green pool. If the green pool thereby would its upper limit (this limit is closely linked to the leaf area index; see below) the surplus C is finally put into the reserve pool. Thereby the allocation fractions $f_{NPP \to X}$ are not as static as introduced above. This mechanism is actually an aposterior reduction of NPP^{pot} that mimics feedbacks from the carbon sinks (plant organs) to the carbon source (photosynthesis), a mechanism that is not well understood (Körner, 2003; Fourcaude et al., 2008; Körner, 2009).

Relation between green pool and leaf area index (LAI)

The LAI is computed in JSBACH at every time step taking the prevailing environmental conditions into account. The value of the LAI is an input variable for the carbon allocation model. It is clear that the leaf C content is directly related to the LAI. But in JSBACH there is no separate pool for leaf carbon. The reason is that not only leaves show an annual cycle, but also sapwood and fine roots. But the regulatory mechanisms how plants channel the carbon to these different plant compartments is not well known. Hence to prevent introducing additional unknown mechanisms, all these seasonally and to large extent synchronously varying compartments are lumped together in one pool, namely the green pool.

There are two aspects for the relation between the green pool and the LAI: First of all, as already mentioned, the LAI defines an upper bound for its carbon content $C_G^{\max}$. This relation is implemented as

$$C_G^{\max}(t) = \frac{f_{G/L}}{sla}\, LAI(t) \qquad A8$$

where the time t explicitly included into the formula to stress the fact that this relation is evaluated in every model time step. The quotient LAI/sla, where sla is the specific leaf area of the particular vegetation (leaf area per unit carbon mass), would be the carbon content of a fictive leaf pool, that does not exist in JSBACH. Here $f_{G/L}$ is a boost factor relates the amount of carbon in the green pools to leaf carbon (see Table A1). Please note that in JSBACH all pools have the units "mole carbon per square meter ground", and not, as one might think, "mole carbon". Accordingly, the units for $C_G^{\max}$ in (A8) are indeed those of the carbon pools.

The second aspect concerns leaf shedding, i.e. the determination of the term F_{litter} in equations (2) and (5). On first sight one may think that leaf litter appears only when the LAI drops. But especially in evergreen species the leaf turnover by aging is fully compensated by leaf growth so that for this case a constant shedding rate is assumed. The following relation implemented in JSBACH takes account of both cases:

$$F_{litter} = \frac{f_{G/L}}{sla}\begin{cases} r_{shed}\, LAI \;for\; \dfrac{dLAI}{dt} \geq 0 \\ \dfrac{dLAI}{dt} \quad otherwise \end{cases} \qquad A9$$

where $f_{G/L}$ is the boost factor from above relating green and leaf carbon, and r_{shed} is a shedding rate for green carbon.

C fluxes from grazing

Grazing by herbivores leads worldwide to significant losses of plant biomass. Particularly affected are grasslands. Conant (2003) estimates that grazing animals typically remove 30-50% of NPP usually, and occasionally as much as 80%. In JSBACH the rather coarse assumption is made that the grazing flux $F_{grazing}$ (compare Eq. (2) and (5)) is proportional to the size of the green pool:

$$F_{grazing} = r_{herbivory}\, C_G \qquad (A10)$$

where $r_{herbivory}$is the rate at which green carbon is consumed by herbivores. But only 30% of the biomass consumed stays in the ecosystem (Crush et al., 1992, Halliday et al., 2003), the remainder of the C is lost by oxidation to the atmosphere. This explains the additional factor $f_{grazing\rightarrow LG}$ in Eq. (5).

Carbon losses to the atmosphere

The total C flux to the atmosphere $F_{\rightarrow A}$ due to heterotrophic respiration and grazing ($F_{grazing\rightarrow A}$) is obtained from equations (2), (5), (6), and (7) as

$$F_{\rightarrow A} = f_{limit}\left[f_{LG\rightarrow A}\, R_{LG}^{pot} + f_{LW\rightarrow A}\, R_{LW}^{pot}\right] + R_S + F_{grazing\rightarrow A} \qquad (A11)$$

Table A1: PFTs specific parameters of JSBACH.

parameters	**trees**	**shrubs**	**grasses**	**crops**
$f_{NPP\rightarrow G}$	~ 50 %	~ 50 %	~ 70 %	~ 70 %
$f_{NPP\rightarrow W}$	~ 30 %	~ 30 %	-	-
$f_{NPP\rightarrow R}$	~ 15 %	~ 15 %	~ 25 %	~ 25 %
$f_{NPP\rightarrow E}$	5 %	5 %	5 %	5 %
$f_{G/L}$	4	4	4	4

~ means targeted $f_{NPP\rightarrow X}$.

Appendix 2.2: N exchange with the environment JSBACH-CN

In this appendix the N exchange fluxes with the environment that showed up in Eq. (18) are described in more detail.

Biotic N Fixation (F_{fix}):

Galloway et al. (1995) have reviewed the current understanding of the global distribution of biotic and anthropogenic N fixation. Here only biotic fixation is of interest. Pre-industrial biotic fixation is estimated in the range of 90–130 Tg N yr^{-1} and the global average is about 0.6–0.9 g m^{-2} yr^{-1} (Dickinson et al., 2002). In the CLM-CN model, F_{fix} (g N m^{-2} yr^{-1}) is formulated as a function of annual NPP (g C m^{-2} yr^{-1}), i.e. $F_{fix} = 1.8\ (1.0 - \exp(-0.003\ NPP)$. According to this formulation, F_{fix} is linked to the ecosystem productivity and at higher NPP there will be a smaller increase in biotic N fixation (Thornton et al., 2007). Thus, N fixation is hypothesized as it is limited by phosphorus (Vitousek and Howarth, 1991). Instead, in the Century model, Schimel et al. (1996) describe F_{fix} as a function of actual evapotranspiration (ET): $F_{fix} = 0.008\ (ET - 40)$. Here F_{fix} is set to zero if ET is less than 40 cm yr^{-1}. The fixation based on ET captures high fixation rates in moist and warm regions with relatively high ET.

For the JSBACH-CN model, F_{fix} (mole N m^{-2} yr^{-1}) is modelled as similar to the CLM-CN model (Thornton et al., 2007). But, the NPP is formulated as a function of weighted running mean of annual NPP. The slope value of 1.8 by Thornton et al. (2007) is modified to 0.7 in order to match the global total N fixation, i.e. close to the central value of 100-290 Tg N yr^{-1} as suggested by Cleveland et al. (1999). Here F_{fix} is formulated as: $F_{fix} = 0.7\ (1.0 - \exp(-0.003\ NPP)$. Moreover, in this study the NPP formulation is chosen because it gives a broad approximation of biotic fixation which relates to the ecosystem productivity whereas ET formulation may not capture the ecosystem productivity as it gives high fixation rates only in moist regions. The running mean of annual NPP is adopted to prevent the fast change of the symbiosis relation of microbes within the root nodules of plants for biotic fixation. In this formulation, as NPP increases in response to rising CO_2 and climate change, the fixation also increases.

In Section 2.4.8, the details about the CN-fd experiment are omitted with respect to biotic N fixation and this is accomplished here. In the CN experiment F_{fix} turned out to about be

148 Tg N/y for present-day conditions, which is close to the central value as suggested by Cleveland et al. (1999). Therefore in the CN-fd experiment, the N fixation rate is doubled by doubling the slope factor of 0.7 to 1.4.

Atmospheric N Deposition (F_{depo}):

For the N deposition flux F_{depo} this study used data from different sources. For present day and future N deposition this study took data generated by Dentener et al. (2006) that were obtained from the combination of results from 23 atmospheric chemistry transport models, calculating for current time and for the year 2030 deposition of reactive N (NO_y, NH_x) to land surfaces. In particular, this study used S1-B2000 (baseline) for present day N deposition and S4-A2 (pessimistic IPCC SRES-A2 Scenario) for future N deposition (see more on Dentener et al., 2006). For the pre-industrial N deposition flux this study took a pre-industrial N deposition map (ca. 1860) also generated by a global three dimensional chemistry-transport model (Jeuken et al., 2001; Lelieveld and Dentener, 2000). These data are available online at the DAAC website (ftp://daac.ornl.gov). To generate from all these snapshots yearly N deposition input data in time and space (i.e. 1860-2100), the two deposition maps for 1860, 2000, and 2030 were linearly interpolated/extrapolated (Eq. A12 and A13) proportionally to the atmospheric CO_2 concentration increase:

$$F_{depo}(t) = F_{depo(1860)} + (F_{depo(2000)} - F_{depo(1860)}) * \frac{CO_2(t) - CO_2(1860)}{CO_2(2000) - CO_2(1860)} \qquad 1860 < t \leq 2000 \qquad A12$$

$$F_{depo}(t) = F_{depo(2000)} + (F_{depo(2030)} - F_{depo(2000)}) * \frac{CO_2(t) - CO_2(2000)}{CO_2(2030) - CO_2(2000)} \qquad 2000 < t \leq 2099 \qquad A13$$

Leaching N losses (F_{leach}):

To describe N losses by leaching, this study takes over the model implemented in the CLM-CN (Thornton et al., 2007) and in the Century model (Meixner et al., 2002). In this approach it is assumed that soil mineral N is distributed homogeneously in the soil, and where the soil is wet a certain part is dissolved in the soil water (the soluble fraction sf). This dissolved part is then swept away with the runoff. This leads to the following flux for leaching of N:

$$F_{leach} = \frac{runoff}{\propto d_{soil}} \, sf \, N_{SM} \qquad (A14)$$

where $\propto$ is the relative soil humidity (volume water per volume soil), d_{soil} is the depth of the soil (equal to the depth of the soil water bucket in the model), and $runoff$ is the volume of water escaping per square meter ground and second. In the simulations $sf = 0.2$ yr^{-1} is chosen which is quite close to the other studies (Hedin et al., 1995; Wang et al., 2010). This formulation estimates globally about 58 Tg N yr^{-1} losses, which is comparable with the other estimates (Seitzinger et al., 2006; Jain et al., 2009; Zaehle et al., 2010b).

N losses by denitrification (F_{denit}):

Most of the terrestrial ecosystems models compute denitrification N losses (gaseous losses of N) by an empirical equation where denitrification is a function of soil mineral N (Meixner et al., 2002). In the model a simple linear approach is used:

$$F_{denit} = dnr \, N_{SM} \qquad (A15)$$

where dnr is the denitrification rate which is chosen as $dnr = 0.07$ yr^{-1}, a value quite close to 0.05 yr^{-1} (Parton et al., 1987; Wang et al., 2010). This formulation estimates globally about 88 Tg N yr^{-1} gaseous losses due to denitrification, which is comparable with the other estimates (Seitzinger et al., 2006; Zaehle et al., 2010b).

Appendix 2.3: Details of added processes: root exudates, grazing in JSBACH-CN

In this appendix the missing carbon cycle processes are described in more detail, which are omitted in Section 2.4.1. This study incorporates the additional missing carbon cycle processes such as root exudates and grazing into the JSBACH-CN model.

Root exudates in JSBACH:

In ecological modelling, knowledge of root exudates processes is still very limited and only few studies have estimated the root exudates flux that entering to the soil. A study based on the ^{14}C-labelling covering a wide range of plant species by Farrar et al. (2003) suggested that root exudates accounted for about 5–10% of net C assimilation. However, later it turns out to be an overestimation due to methodological bias and Jones et al. (2004) estimated that it is in the range of 2–4% of net C assimilation. Moreover, Pepper et al. (2007) allocated about 1% of NPP as root exudates in the G'DAY model, whereas an earlier study by Clark et al. (2001) allocated 3% of NPP as root exudates.

In general, previous literature and modelling studies indicate a range of about 1–5% of NPP which can be allocated as root exudates. Therefore, in the formulation of the JSBACH model, a fixed amount of NPP (ca. 5% NPP) is allocated to root exudates for all PFTs. This root exudates carbon is passed into the litter green pool, which is further assumed to be not constrained by N availability.

Grazing in JSBACH:

Grazers or herbivores (domesticated and wild animals) dominate many ecosystems covering the geographic regions from the tropics to the arctic (Conant, 2003). They consume a fraction of NPP and the rest NPP is accumulated as plant biomass (Cebrian et al., 1999). Grazers are capable of digesting cellulose and carbohydrates that are present in plant material. Several studies have investigated the fraction of NPP which is consumed by herbivores in grasslands, savannas, shrublands, and forests. For example, Conant (2003) suggests that grazing animals can remove significant amounts of NPP, typically in the range of 30–50%, occasionally up to 80%. However, in forest ecosystems, less than 10% of NPP is consumed by grazers (Whittaker, 1975; Sala et al., 1996; Scurlock et al., 1999).

Herbivorous consumption is largest mostly in grasslands. In this ecosystem, herbivorous consumption is in the range of about 25–50% of aboveground NPP (McNaughton, 1976, 1985; Lauenroth and Milchunas, 1992) and 25% of belowground productivity (Coleman, 1976; Ingham and Detling, 1984; Lauenroth and Milchunas, 1992). Milchunas and Lauenroth (1993) suggests based on the data that grazing intensity for grassland, shrub lands, and forest ecosystems is 44%, 55%, and 60% of aboveground NPP, respectively. In addition, Cebrian et al. (1999) compiled an extensive data set (> 200 published reports) on the percentage of NPP consumed by herbivores in grassland, forest, and shrub lands ecosystems. They found that in grassland ecosystems, 0–60% (mean ca. 30%) of NPP is consumed by herbivorous, whereas in forest and shrub lands, the consumption is 0–10% (mean ca. 3%).

In the JSBACH model, a rather coarse assumption is made that the grazing flux is proportional to the size of the green C pool. This approach leads to a grazing fluxes of about less than 10% of NPP for all PFTs except for grasslands (ca. 15%).

Appendix 2.4: Details of improved model parameters in JSBACH

In this appendix, the improved model parameters are described for the better carbon allocation in the model. In particular, this study improves the leaf longevity based on prior literature values for grassland ecosystems. This model parameter is described below in more detail.

Leaf longevity of grassland ecosystems:

Leaf longevity is an important plant trait that linked to leaf ecophysiology (e.g., photosynthetic rate, leaf N content), plant growth (e.g., carbon gain), and ecosystem processes (e.g., litter turnover, nutrient cycling) (Craine et al., 1999). This determines generally the litterfall, standing biomass, and NPP. However, so far only a few studies quantified the longevity for grasses (Sydes, 1984; Cornelissen and Thompson, 1997). Craine et al. (1999) measured the leaf longevity of 14 species of grasses and forbs and found that average leaf longevity for the 14 species was around 2 months. Tjoelker et al. (2005) measurements show that mean leaf longevity of the species usually ranged from 1–3 months.

Based on the above literature values, C_3 and C_4 grasses are parameterised as 4–6 months of leaf longevity in the JSBACH model. Thus, this parameterisation maximises the carbon allocation of grasslands in the JSBACH-CN model.

Appendix 2.5: Observation sites for cycling of nitrogen.

Table A2: Nitrogen observation sites from Raich et al. (1991) and McGuire et al. (1992) used for model evaluation.

Site number	Vegetation Type	Site name	Country	Latitude	Longitude
1	Boreal Woodland	Schefferville, Quebec	Canada	54.72	-66.70
2	Boreal Forest	Bonanza Creek Experimental Forest, Alaska	USA	64.75	-148.25
3	Temperate Coniferous Forest	Andrews Experimental Forest Watershed 10, Oregon	USA	44.25	-122.33
4	Arid Shrubland	Curlew Valley, Utah	USA	41.08	-113.08
5	Short Grassland	Central Plains Experimental Range, Colorado	USA	40.82	-104.77
6	Tall Grassland	Osage prairie, Oklahoma	USA	36.95	-96.55
7	Temperate mixed Forest	Harvard Forest, Massachusetts	USA	42.53	-72.17
8	Temperate Broadleaved Evergreen Forest	Taita Experimental Station, North Island	New Zealand	-41.18	174.97
9	Tropical Deciduous Forest	Chakia	India	25.33	83.00
10	Tropical Evergreen Forest	Ducke Forest, Manaus	Brazil	-2.83	-59.95
11	Tropical Broadleaved Evergreen Forest	Pasoh	Malaysia	3.0	102.5
12	Tropical Broadleaved Evergreen Forest	San Carlos	Venezuela	2.0	-67.0

Appendix 2.6: Comparison of simulated global N pools obtained in different simulation studies.

Table A3: Comparison of global N pools (vegetation N, litter N, soil N, soil mineral N in Pg N) simulated by different models (means for 1970-99).

Pool size	JSBACH-CN	CASA*	O-CN**	DyN-LPJ¶	Other sources	Range
Vegetation	green 0.68 mobile 0.07 wood 4.2					
	total 4.9	6.6	3.8	5.3	10¶¶	10-16$
Litter	litter green 0.92 litter wood 0.28					
	total 1.2	1.3		4.6	10†	
Soil	139.5	126	101	67	140 (1 m)††	70-820$
Soil mineral	1.2	0.5	0.3	0.94	17#	25$

* Wang et al., 2010

** Zaehle et al., 2010b

¶ Xu-Ri and Prentice, 2008

¶¶ McElroy et al., 1976, 1983

† Davidson, 1994

†† Batjes, 1996

Esser et al., 2011

$ Lin et al., 2000

Here simulated global N storages as simulated by the JSBACH-CN model are compared with those obtained by various other models (Lin et al., 2000; Xu-Ri and Prentice, 2008; Wang et al., 2010; Zaehle et al., 2010b) and also with published observational estimates (Batjes, 1996) (Table A3). For present-day condition, the vegetation and the litter N are simulated to be 4.9 and 1.2 Pg N, respectively. Overall, the vegetation N accounts for about 3.4% (ca. 5% by Wang et al., 2010) of the total N. Overall, the simulated vegetation N is of similar magnitude as those reported from other model simulations (Xu-Ri and Prentice, 2008; Wang et al., 2010; Zaehle et al., 2010b). Only a few studies estimated the global litter N this study estimates that the simulated litter N is to be about 1.2 Pg N, which is quite close to the estimates of 1.3 Pg N by Wang et al. (2010) and 1.5 Pg N by

Esser et al. (2011). But it is much less than the estimates of 4.6 Pg N by Xu-Ri et al. (2008).

The largest pool of N in the terrestrial biosphere is organic soil N, which accounts for more than 90% of total soil N (Xu-Ri et al., 2008; Wang et al., 2010). The simulated soil organic N storage is about 139.5 Pg N (95%), which is consistent with observations (Batjes, 1996, 1997) and also quite close to the CASA-CNP model estimates of 126 Pg N (ca. 94%). As compared to the JSBACH-CN model, the DyN and ISAM-CN model show a lower organic soil N storage of 56.8 and 65 Pg N, respectively (Xu-Ri et al., 2008; Yang et al., 2009). The observed soil N storage is to be 92-117 Pg N (Zinke et al., 1984), 95 Pg N (Post et al., 1985), 63-67 Pg N (30 cm soil depth) and 133-140 Pg N (100 cm) (Batjes, 1996, 1997). However, the range varies to a larger extent (ca. 70-820 Pg N) because various estimates consider different soil depth (Lin et al., 2000). Moreover, all studies estimate that more than 90% of the soil N is organic which is similar to the field measurements by Brady (1998).

Globally soil inorganic N (N_{SM}) is a small pool and comprising only 0.9% of the soil N (139.5 Pg N) and is consistent with the DyN model (Xu-Ri et al., 2008) which accounts 1.4% of the global soil N. However, Lin et al. (2000) estimated that inorganic N accounts about 10% of the global soil N – this seems to be an overestimation.

Appendix 3.1: Calculation: Emissions to concentration and temperature increases

In this study, a 1-dimensional box model is applied for calculating atmospheric N_2O concentration from the different emission sources, that is, natural soils, open fluxes, fossil fuel, biomass burning, and synthetic N fertilizer. The initial pre-industrial atmospheric N_2O concentration is assumed to be 276 ppb (i.e. 1860). This study also assumes a constant life time (i.e. 114 years) of N_2O in the atmosphere.

To calculate the additional concentration induced by N_2O emissions since pre-industrial times, the following equations are used:

$$\frac{d\Delta N_2O(t)}{dt} = cf * \left(EN(t) + EO(t) + EO_c(t) + EF_s(t) + EB(t) + EF_z(t)\right) - \frac{1}{\tau}\Delta N_2O(t) \quad (B1)$$

t: Time in years

$\Delta N_2O(t)$: Additional concentration (ppb) due to N_2O emissions as a function of time

$EN(t)$: Natural emission (Tg N) as a function of time

$EO(t)$: Open emission (Tg N) as a function of time

$EO_c(t)$: Ocean emission (Tg N) as a function of time

$EF_s(t)$: Fossil fuel emission (Tg N) as a function of time

$EB(t)$: Biomass emission (Tg N) as a function of time

$EF_z(t)$: Fertilizer emission (Tg N) as a function of time

τ: Lifetime in years (i.e. 114 years adopted from IPCC, 2001)

cf: Conversion factor of emission to concentration (i.e. 0.209 ppb/Tg N)

In Eq. B2, the total atmospheric N_2O concentration is computed as:

$$N_2O(t+1) = N_2O(t) + \Delta N_2O(t) \quad (B2)$$

$N_2O(t)$: Concentration at pre-industrial state 1860 (i.e. 276 ppb)

The radiative forcing (RF) due to emissions is computed by a simple linear relationship between additional concentrations and a radiative efficiency constant (Eq. B3). The radiative efficiency constant (α) is adopted from the IPCC (2001, see p. 388).

$$\Delta F(t) = \alpha * \Delta N_2O(t) \quad (B3)$$

$\Delta F(t)$: Additional RF due to the additional concentration (Wm^{-2})

α: Constant (i.e. 0.003 Wm^{-2}/ppb)

The temperature increase due to the additional RF is calculated as (IPCC, 2001):

$$\Delta T(t) = \lambda\, \Delta F(t) \quad (B4)$$

$\Delta T(t)$: Increase in global average surface temperature (°C)

λ: Climate sensitivity parameter (°C/Wm^{-2}). The value adopted for λ is 0.8°C/(Wm^{-2}) (Lenton and Vaughan, 2009). It can be range from 0.6 -1.2 °C/(Wm^{-2}) (IPCC, 2007).

$\Delta T(t)$ can be written as:

$$\Delta T(t) = \lambda * \Delta N_2O(t) * \alpha \quad \text{(B5)}$$

The natural N_2O emissions from soil due to nitrification and denitrificaion processes are sensitive to global warming. To include the additional N_2O emissions as a result of warming, this study incorporates climate feedback into the natural soil emissions. The climate feedback to the natural soil emissions is represented as:

$$EN^f(t) = EN(t) + slope * \Delta T(t) \quad \text{(B6)}$$

$EN^f(t)$: Natural emissions (Tg N) as a function of time

The slope is derived from a linear relationship between N_2O emissions from soil and surface temperature. This slope is used to calculate the climate feedback in Eq. B7. For this calculation, the slope value is 0.69. More details about the slope are given in Section 3.3.3 and Figure 3.4.

The climate feedback is incorporated into the natural soil emissions (i.e. Eq. B7 and B8). This can be obtained as:

$$\frac{\Delta N_2O(t+1) - \Delta N_2O(t)}{1\ year} = cf * (EN(t) + slope * \Delta T(t) + EO(t) + EO_c(t) + EF_s(t) + EB(t) + EF_z(t)) - \frac{1}{\tau} \Delta N_2O(t) \quad (B7)$$

In Eq. B8, the term ΔT can be replaced by Eq. B5 and can be written as:

$$\frac{\Delta N_2O(t+1) - \Delta N_2O(t)}{1\ year} = cf * (EN(t) + slope * \lambda * \Delta N_2O(t) * \alpha + EO(t) + EO_c(t) + EF_s(t) + EB(t) + EF_z(t)) - \frac{1}{\tau}\Delta N_2O(t) \quad (B8)$$

The Eq. B9 can be derived from Eq. B1, which does not consider climate feedback, unlike Eq. B8. So, it can be written as:

$$\frac{\Delta N_2O(t+1) - \Delta N_2O(t)}{1\ year} = cf * \left(EN(t) + EO(t) + EO_c(t) + EF_s(t) + EB(t) + EF_z(t)\right) - \frac{1}{\tau}\Delta N_2O(t) \quad (B9)$$

Furthermore, N_2O emissions from the terrestrial biosphere affect global surface temperature due to their radiative properties. At the same time, temperature affects the N_2O emissions. To calculate these effects, climate-N_2O feedback gain factor (Eq. B11) is obtained from the equation of Torn and Harte (2006):

$$\frac{T^f_{2100} - T^f_{1860}}{T^0_{2100} - T^0_{1860}} = \frac{\Delta T^f}{\Delta T^0} = \frac{1}{1-f} \quad (B10)$$

$$f = 1 - \frac{\Delta T^0}{\Delta T^f} \quad (B11)$$

$\Delta T^f(t)$: Increase in global average surface temperature (°C) with feedback

$\Delta T^0(t)$: Increase in global average surface temperature (°C) without feedback

f: Feedback gain factor

Appendix 3.2: Observation sites for forest and grassland ecosystems.

Table A4: N_2O emissions observation sites used for model evaluation.

Site name	Vegetation Type	Latitude	Longitude	N_2O emissions (mg N m^{-2} yr^{-1})	References
Xishuangbanna, China	Tropical forest	21.52	101.27	63.9	Werner et al., 2006
SW China	Tropical forest	21.96	101.2	51.1	Werner et al., 2007
Brazil	Tropical forest	- 10.5	- 62.5	178	Werner et al., 2007
China	Birch forest	41.38	126.91	61.6	Chen et al., 2000
Brazil	Tropical forest	- 20.4	-47.51	96.3	Cattaneo et al., 2002
Wyoming, US	Alpine Tundra	41.33	-106.33	8.6	Sommerfeld et al, 1993
Southern Sweden	Temperate forest	57.13	14.75	44.5	Arnold et al, 2005b
Southern Sweden	Tundra	57.13	14.75	27.9	Arnold et al, 2005a
Austria	Temperate forest	48.11	15.25	59.7	Kitzler et al, 2006
Eastern Finland	Tundra	62.67	31.38	29	Nykänen et al, 1995
Finland	Tundra	61.8	24.33	30	Laine et al, 1996; Martikainen et al, 1995
Ach, Austria	Spruce	47	11	75.74	Kesik et al., 2005
Soro, Denmark	Beech	55	12	71.18	Kesik et al., 2005
UK	Birch	55	-3.0	18.25	Kesik et al., 2005
Wildbahn, Germany	Pine	53	11	62	Kesik et al., 2005
Parco, Italy	Hard woods	45	9	32.85	Kesik et al., 2005
San, Italy	Pine	43	10	20.08	Kesik et al., 2005
Speu, Netherland	Douglas Fir	52	5	21.9	Kesik et al., 2005
Songnen plain, China	Temperate grassland	123.01-119.15	123.01-119.15	72	Huang et al., 2003
Inner Mongolia, China	Temperate grassland	43.5	116.66	73	Du et al., 2006
Inner Mongolia, China	Temperate grassland	43.5-45	116-117	56	Dong et al., 2000
Qinghai, China	Montane grassland	35.22	93.83	5	Pei et al., 2003; 2004
Wyoming, US	Montane grassland	41.33	-106.33	17	Mosier et al., 1993
Calabozo, Venezuela	Tropical savanna & grassland	-8.86	-67.33	63	Sanhueza et al., 1994
Brazil	Tropical savanna & grassland	-15.93	47.85	27.3	Poth et al., 1995

List of Figures

List of Tables

7. Bibliography

Albritton, D. L., and L. G. Meira Filho (2001), Technical Summary of Working Group I, in *Climate Change 2001: The Scientific Basis. Contribution of Working Group I to the Third Assessment Report of the Intergovernmental Panel on Climate Change*, edited by F. Joos et al., pp. 21–83, Cambridge Univ. Press, Cambridge, U. K. and New York.

Ambus, P. (2005), Relationship between gross nitrogen cycling and nitrous oxide emission in grass clover pasture, *Nutr. Cycl. Agroecosys.*, *72*, 189–199.

Ambus, P., G. P. Robertson (1999), Fluxes of CH_4 and N_2O in aspen stands grown under ambient and twice-ambient CO_2, *Plant Soil*, *209*, 1–8.

Anderson, J. (1973), The breakdown and decomposition of sweet chestnut (Castanea sativa Mill.) and beech (Fagus sylvatica L.) leaf litter in two deciduous woodland soils: II. Changes in the carbon, nitrogen and polyphenol content, *Oecologia*, *12*, 275–288.

Arnold, K., M. Nilsson, B. Hanell, P. Weslien, L. Klemedtsson (2005b), Fluxes of CO_2, CH_4 and N_2O from drained organic soils in deciduous forests, *Soil Biol. Biochem.*, *37*, 1059–1071.

Arnold, K., P. Weslien, M. Nilsson, B. Svensson, L. Klemedtsson (2005a), Fluxes of CO_2, CH_4 and N_2O from drained coniferous forests on organic soils, *For. Ecol. Manage.*, *210*, 239–254.

Baggs, E. M., M, Richter, G. Cadisch, U. A. Hartwig (2003), Denitrification in grass swards is increased under elevated atmospheric CO_2, *Soil Biol. Biochem.*, *35*, 729–732.

Barnard, R., L. Barthes, P. W. Leadley (2006), Short-term uptake of ^{15}N by a grass and soil micro-organisms after long-term exposure to elevated CO_2, *Plant Soil*, *280*(1-2), 91–99.

Barnard, R., P. W. Leadley, B. A. Hungate (2005), Global change, nitrification, and denitrification: a review, *Global Biogeochem. Cycles*, *19*, GB1007.

Batjes, N. (1996), Total carbon and nitrogen in the soils of the world, *Eur. J. Soil Sci*, *47*(2), 151–163.

Batjes, N. H. (1997), A world dataset of derived soil properties by FAO–UNESCO soil unit for global modelling, *Soil Use and Manage.*, *13*, 9–16.

Battle, M., et al. (1996), Atmospheric gas concentrations over the past century measured in air from firn at the South Pole, *Nature*, *383*, 231-235.

Billings, S. A., S. M. Schaeffer, R. D. Evans (2002), Trace N gas losses and N mineralization in Mojave desert soils exposed to elevated CO_2, *Soil Biol. Biochem.*, *34*, 1777–1784.

Bolin, B., R. Sukumar, P. Ciais, W. Cramer, P. Jarvis, H. Kheshgi, C. A. Nobre, S. Semenov, and W. Steffen (2001), Global perspective, in *Land Use, Land-Use Change, and Forestry - A Special Report of the IPCC*, edited by R. T. Watson et al., pp. 23–52, Cambridge Univ. Press, Cambridge, U. K.

Borken, W., and F. Beese (2005), Control of nitrous oxide emissions in European beech, Norway spruce and Scots pine forests, *Biogeochemistry*, *76*, 141–159.

Bouwman, A. F. (1990), *Exchange of greenhouse gases between terrestrial ecosystems and the atmosphere. In: Bouwman, A. F. (Ed.) Soils and the Greenhouse Effect*, J. Wiley & Sons Ltd., Chichester, pp 61-127.

Bouwman, A. F., A. H. W. Beusen, and G. Billen (2009), Human alteration of the global nitrogen and phosphorus soil balances for the period 1970–2050, *Global Biogeochem. Cycles*, *23*, GB0A04.

Bouwman, A. F., G. Van Drecht, and K. W. Van der Hoek (2005), Nitrogen surface balances in intensive agricultural production systems in different world regions for the period 1970–2030, *Pedosphere*, *15*, 137–155.

Bouwman, A. F., I. Fung, E. Matthews, and J. John (1993), Global analysis of the potential for N_2O production in natural soils, *Global Biogeochem. Cycles*, *7*(3), 557–597.

Bouwman, A. F., K. W. Vanderhoek, and J. G. J. Olivier (1995), Uncertainties in the global source distribution of nitrous oxide, *J. Geophys. Res.*, *100(D2)*, 2785–2800.

Bowden, W. B. (1986), Gaseous nitrogen emissions from undisturbed terrestrial ecosystems: an assessment of their impacts on local and global nitrogen budgets, *Biogeochemistry*, *2*, 249–279.

Brady, N. C. (1998), *Nitrogen and sulfur economy of soils. In: Brady, N.C., Weil, R.R. (Eds.), The Nature and Properties of Soils*, 12th edn. Elsevier, New York, pp. 492–522.

Breuer, L., R. Kiese, K. Butterbach-Bahl (2002), Temperature and moisture effects on nitrification rates in tropical rain-forest soils, *Soil Sci. Soc. Am. J.*, *66*, 834–844.

Brown, S., J. Sathaye, M. Cannell, and P. E. Kauppi (1996), Management of forests for mitigation of greenhouse gas emissions, in *Climate Change 1995 - Impacts, Adaptations and Mitigation of Climate Change: Scientific-Technical Analyses. Contribution of Working Group II to the Second Assessment Report of the Intergovernmental Panel on Climate Change*, edited by R. T. Watson et al., pp. 773-797, Cambridge Univ. Press, Cambridge, U.K.

Butterbach-Bahl, K., et al. (1998), Inpact of N-input by wet deposition on N-trace gas fluxes and CH_4-oxidation in spruce forest ecosystems of the temperate zone in Europe, *Atmos. Environ.*, *32*(3), 559–564.

Castaldi, S. (2000), Responses of nitrous oxide, dinitrogen and carbon dioxide production and oxygen consumption to temperature in forest and agricultural light-textured soils determined by model experiment, *Biol. and Fertility of Soils*, *32*, 67–72.

Cattaneo, A. (2002), *Balancing Agricultural Development and Deforestation in the Brazilian Amazon*, Research Report 129, International Food Policy Research Institute,Washington D.C., USA. Online at: http://www.ifpri.org/pubs/abstract/129/rr129.pdf.

Cebrian, J. (1999), Patterns in the fate of production in plant communities, *American Naturalist*, *154*, 449-468.

Cech, P. G., T. Kuster, P. J. Edwards, H. O. Venterink (2008), Effects of herbivory, fire and N_2-fixation on nutrient limitation in a humid African savanna, *Ecosystems*, *11*(6), 991–1004.

Chambers, J. Q., et al. (2004), Respiration from a tropical forest ecosystem: partitioning of sources and low carbon use efficiency, *Ecol. Appl.*, *14*, 72–88.

Chen, G. X., et al. (2000), Nitrous oxide emissions from terrestrial ecosystems in China, *Chemosphere Global Change Sci.*, *2*, 373–378.

Chen, J. L., J. F. Reynolds, P. C. Harley, J. D. Tenhunen (1993), Coordination theory of leaf nitrogen distribution in a canopy, *Oecologia*, *93*(1), 63-69.

Churkina, G., D. G. Brown, and G. Keoleian (2010), Carbon stored in human settlements: the conterminous United States, *Global Change Biol.*, *16*, 135–143.

Clark, D. A., S. Brown, D. W. Kicklighter, J. Q. Chambers, J. R. Thomlinson, and J. Ni (2001), Measuring net primary production in forests: Concepts and field methods, *Ecol. Appl.*, *11*, 356–370.

Cleveland, C., and D. Liptzin (2007), C:N:P stoichiometry in soil: is there a Redfield ratio for the microbial biomass, *Biogeochemistry*, *85*, 235–252.

Cleveland, C. C., A. R. Townsend, D. S. Schimel, H. Fisher, R. W. Howarth, L. O. Hedin, S. S. Perakis, E. F. Latty, J. C. Von Fischer, and A. Elseroad (1999), Global patterns of terrestrial biological nitrogen (N_2) fixation in natural ecosystems, *Global Biogeochem. Cycles*, *13*(2), 623–645.

Cofer, W. R., J. S. Levine, E. L. Winstead, and B. J. Stocks (1991), New estimates of nitrous oxide emissions from biomass burning, *Nature*, *349*, 689–691.

Cole, D. W., and M. Rapp (1981), Elemental cycling in forest ecosystems, in *Dynamic Properties of Forest Ecosystems*, edited by D. E. Reichle, pp 341–409, Cambridge Univ. Press, London.

Coleman, D. C. (1976), A review of root production processes and their influence on soil biota in terrestrial ecosystems, in *The Role of Terrestrial and Aquatic Organisms in Decomposition Processes*, edited by J. M. Anderson and A. Macfadyem, pp. 417–434, Blackwell Scientific, Oxford, England.

Collatz, G. J., M. Ribas-Carbo, and J. A. Berry (1992), Coupled photosynthesis-stomatal conductance model for leaves of C_4 plants, *Aust. J. Plant Physiol.*, *19*, 519-538.

Conant, R. T. (1993), Grazer-dominated Ecosystems, *Encyclopedia of Life Sciences*.

Conrad, R. (1996), Soil microorganisms as controllers of atmospheric trace gases (H_2, CO, CH_4, OCS, N_2O, and NO), *Microbiol. Rev.*, *60*, 609-640.

Conrad, R., W. Seiler, G. Bunse (1983), Factors influencing the loss of fertilizer nitrogen in the atmosphere as N_2O, *J. Geophys. Res.*, *88*, 6709-6718.

Cookson, W. R., et al. (2006), The influence of season, agricultural management, and soil properties on gross nitrogen transformations and bacterial community structure, *Aust. J. Soil Res.*, *44*, 453–465.

Cornelissen, J. H. C., and K. Thompson (1997), Functional leaf attributes predict litter decomposition rate in herbaceous plants, *New Phytologist*, *135*, 109-114.

Craine, J. M., D. M. Berin, P. B. Reich, D. G. Tilman, J. M. H. Knops (1999), Measurement of leaf longevity of 14 species of grasses and forbs using a novel approach, *New Phytologist*, *142*, 475-481.

Crush, J. R., G. C. Waghorn, M. P. Rolston (1992), Greenhouse gas emissions from pasture and arable crops grown on a Kairanga soil in the Manawatu, North Island, New Zealand, *New Zealand J. Agri. Res.*, *35*, 253-257.

Crutzen, P. J. (1981), Atmospheric chemical processes of the oxides of nitrogen including nitrous oxide, in *Denitrification, Nitrification and Atmospheric Nitrous Oxide*, edited by C. C. Delwiche, pp 17-44, John Wiley and Sons, New York.

Crutzen, P. J., A.R. Mosier, K. A. Smith, and W. Winiwarter (2008), N_2O release from agro-biofuel production negates global warming reduction by replacing fossil fuels, *Atmos. Chem. Phys.*, *8*, 389-395.

Crutzen, P. J., and M. O. Andreae (1990), Biomass burning in the tropics: Impact on atmospheric chemistry and biogeochemical cycles, *Science*, *250*, 1669–1678.

D'Antonio, C. M., and M. C. Mack (2006), Nutrient Limitation in a Fire-derived, Nitrogen-rich Hawaiian Grassland, *Biotropica*, *38*, 458-467.

Davidson, E. A. (1994), *Climate change and soil microbial processes: secondary effects are hypothesized from better known interacting effects, In: Soil Responses to Climate Change.*, NATO ASI Series (eds RounsevellMDA, LovelendPJ), Springer, Heidelberg, pp. 155–168.

Davidson, E. A., M. Keller, H. E. Erickson, L. V. Verchot, and E. Veldkamp (2000), Testing a conceptual model of soil emissions of nitrous and nitric oxides, *BioScience*, *50*, 667-680.

Davidson, E. A., and L.V. Verchot (2000), Testing the hole-in-the-pipe model of nitric and nitrous oxide emissions from soils using the TRAGNET database, *Global Biogeochem. Cycles*, *14*(4), 1035-1043.

Davidson, E. A. (2009), The contribution of manure and fertilizer nitrogen to atmospheric nitrous oxide since 1860, *Nat. Geosci.*, *2*, 659–662.

Dickinson, R. E., et al. (2002), Nitrogen controls on climate model evapotranspiration, *J. Clim.*, *15*(3), 278-295.

De Graaff, M. A., C. Van Kessel, and J. Six (2009), Rhizodeposition-induced decomposition increases N availability to wild and cultivated wheat genotypes under elevated CO_2, *Soil Biol. Biochem.*, *41*, 1094-1103.

De Graaff, M. A., K. J. van Groeningen, J. Six, B. A. Hungate, and C. van Kessel (2006), Interactions between plant growth and nutrient dynamics under elevated CO_2: a meta analysis, *Global Change Biol.*, *12*, 1-15.

Denman, K. L., et al. (2007), Couplings between changes in the climate system and biogeochemistry, in *Climate Change 2007: The Physical Science Basis: Contribution of Working Group I to the Fourth Assessment Report of the Intergovernmental Panel on Climate Change*, edited by S. Solomon et al., pp. 499–587, Cambridge Univ. Press, Cambridge, U.K. and NY, USA.

Dentener, F., et al. (2006), Nitrogen and sulfur deposition on regional and global scales: A multimodel evaluation, *Global Biogeochem. Cycles*, *20*, GB4003.

Dong, Y. S., S. Zhang, Y. C. Qi, Z. Z. Chen, and Y. B. Geng (2000), Fluxes of CO_2, N_2O and CH_4 from a typical temperate grassland in Inner Mongolia and its daily variation, *Chin. Sci. Bull.*, *45*, 1590–1594.

Du, R., D. Lu, and G. Wang (2006), Diurnal, seasonal, and inter-annual variations of N_2O fluxes from native semi-arid grassland soils of inner Mongolia, *Soil Biol. Biochem.*, *38*, 3474–3482.

Duxbury, J. M., and A. R. Mosier (1993), *Status and issues concerning agricultural emissions of greenhouse gases. In: Kaiser, H.M., and T.E. Drennen (eds.) Agricultural Dimensions of Global Climate Change*, St. Lucie Press, Delray Beach, FL, pp. 229-258.

Eggers, T. (2002), *The Impacts of Manufacturing and Utilisation of Wood Products on the European Carbon Budget*, European Forest Institute, Joensuu, Finland, Internal Report 9, pp 90.

Epstein, E., and A. J. Bloom (2005), *Mineral Nutrition of Plants: Principles and Perspectives*, (Sinauer Associates, Sunderland, MA, ed. 2).

Erickson, H. E., and M. Keller (1997), Tropical land use change and soil emissions of nitrogen oxides, *Soil Use and Manage.*, *13*, 278–287.

Ernfors, M., K. von Arnold, J. Stendahl, M. Olsson, L. Klemedtsson (2007), Nitrous oxide emissions from drained organic forest soils-an up-scaling based on C:N ratios, *Biogeochemistry*, *84*, 219–231.

Esser, G., J, Kattge, A, Sakalli (2011), Feedback of carbon and nitrogen cycles enhances carbon sequestration in the terrestrial biosphere, *Global Change Biol.*, *17*, 819–842.

Falkengren-Grerup, U. (1995), Interspecies differences in the preference of ammonium and nitrate in vascular plants, *Oecologia*, *102*(3), 305–311.

FAO (1992), FAO Yearbook, Fertilizer, Vol. 42, and earlier issues.

Farquhar, G. D., S. von Caemmerer, and J. A. Berry (1980), A biochemical model of photosynthetic CO_2 as simulation in leaves of C_3 species, *Planta*, *149*, 78-90.

Farquharson, R., and J. Baldock (2008), Concepts in modelling N_2O emissions from land use, *Plant Soil*, *309*, 147–167.

Farrar, J., M. Hawes, D. Jones, S. Lindow (2003), How roots control the flux of carbon to the rhizosphere, *Ecology*, *84*, 827–837.

Fenner, N., D. J. Dowrick, M. A. Lock, C. R. Rafarel, C. Freeman (2006), A novel approach to studying the effects of temperature on soil biogeochemistry using a thermal gradient bar, *Soil Use and Manage.*, *22*, 267–273.

Finzi, A. C., E. H. DeLucia, J. G. Hamilton, D. D. Richter, and W. H. Schlesinger (2002), The nitrogen budget of a pine forest under free-air CO_2 enrichment, *Oecologia*, *132*(4), 67–578.

Finzi, A. C., et al. (2006), Progressive nitrogen limitation of ecosystem processes under elevated CO_2 in a warm-temperate forest, *Ecology*, *87*(1), 15–25.

Finzi, A. C., et al. (2007), Increases in nitrogen uptake rather than nitrogen-use efficiency support higher rates of temperate forest productivity under elevated CO_2, *Proc. Natl. Acad. Sci. U. S. A.*, *104*(35), 14014-14019.

Finzi, A. C., W. H. Schlesinger (2002), Species control variation in litter decomposition in a pine forest exposed to elevated CO_2, *Global Change Biol.*, *8*, 1217–1229.

Flanagan, P., and K. van Cleve (1983), Nutrient cycling in relation to decomposition and organic matter quality in taiga ecosystems, *Can. J. For. Res.*, *13*, 795–817.

Flechard, C. R., et al. (2007), Effects of climate and management intensity on nitrous oxide emissions in grassland systems across Europe, *Agric. Ecosyst. Environ.*, *121*, 135–152.

Fog, K. (1988), The effect of added nitrogen on the rate of decomposition of organic matter, *Biol. Rev.*, *63*, 433-462.

Fourcaud, T., X. Zhang, A. Stokes, H. Lambers, C. Körner (2008), Plant growth modelling and applications: The increasing importance of plant architecture in growth models, *Ann. Bot.*, *101*, 1053–1063.

Friedlingstein, P., et al. (2006), Climate-carbon cycle feedback analysis: Results from the C^4MIP model intercomparison, *J. Clim.*, *19*, 3337–3353.

Gallardo, A., and W. H. Schlesinger (1992), Carbon and nitrogen limitation of soils microbial biomass in desert ecosystems, *Biogeochemistry*, *18*, 1-17.

Galloway, J. N., et al. (2004), Nitrogen cycles: Past, present and future, *Biogeochemistry*, *70*, 153–226.

Galloway, J. N., et al. (2008), Transformation of the Nitrogen Cycle: Recent Trends, Questions, and Potential Solutions, *Science*, *320*, 889-892.

Galloway, J. N., W. H. Schlesinger, H. Levy II, A. Michaels, and J. L. Schnoor (1995), Nitrogen fixation: Anthropogenic enhancement-environmental response, *Global Biogeochem. Cycles*, *9*(2), 235–252.

Gärdenäs, A. I., et al. (2011), Knowledge gaps in soil carbon and nitrogen interactions –From molecular to global scale, *Soil Biol. Biochem.*, 43(4), 702-717.

Gill, R. A., L. J. Anderson, H. W. Polley, H. B. Johnson, and R. B. Jackson (2006), Potential nitrogen constraints on soil carbon sequestration under low and elevated atmospheric CO_2, *Ecology*, *87*, 41–52.

Gitz, V., and P. Ciais (2003), Amplifying effects of land-use change on future atmospheric CO_2 levels, *Global Biogeochem. Cycles*, *17*(1), 1024.

Gosz, J. R. (1981), *Nitrogen cycling in coniferous ecosystems. In Terrestrial Nitrogen Cycles, Eds. F E Clark and T Rosswall*, Ecol. Bull. (Stockholm) 33, pp 405-426.

Granli, T., and O. C. Bøckman (1994), Nitrous oxide from agriculture, *Nor. J. Ag.Sci.*, Supplement No. 12, 128.

Grant, R. F., and E. Pattey (2008), Temperature sensitivity of N_2O emissions from fertilized agricultural soils: Mathematical modeling in ecosys, *Global Biogeochem. Cycles*, *22*, GB4019.

Grassi, G., E. Vicinelli, F. Ponti, L. Cantoni, and F. Magnani (2005), Seasonal and interannual variability of photosynthetic capacity in relation to leaf nitrogen in a deciduous forest plantation in northern Italy, *Tree Physiol.*, *25*, 349–360.

Groffman, P. M., A. J. Gold, K. Addy (2000), Nitrous oxide production in riparian zones and its importance to national emission inventories, *Chemosphere Global Change Sci.*, *2*, 291–299.

Halliday, J. C., K. R. Tate, R. E. McMurtrie, and N. A. Scott (2003), Mechanisms for changes in soil carbon storage with pasture to Pinus radiata land-use change, *Global Change Biol.*, *9*, 1294-1308.

Hansen, J. E., and M. Sato (2004), Greenhouse gas growth rates, *Proc. Natl. Acad. Sci. U. S. A.*, *101*, 16109-16114.

Harrington, R. A., J. H. Fownes, and P. M. Vitousek (2001), Production and resource-use efficiencies in N- and P-limited tropical forest ecosystems, *Ecosystems*, *4*, 646–657.

Hedin, L. O., J. J. Armesto, and A. H. Johnson (1995), Patterns of nutrient loss from unpolluted, old-growth temperate forests: evaluation of biogeochemical theory, *Ecology*, *76*, 493–509.

Hodge, A., D. Robinson, A. Fitter (2000), Are microorganisms more effective than plants at competing for nitrogen?, *Trends Plant Sci.*, *5*(7), 304-308.

Höhne N., and K. Blok (2005), Calculating historical contributions to climate change-discussing the 'Brazilian proposal', *Clim. Change*, *71*(1), 141–173.

Horak, J., and B. Siska (2006), Evaluation of N_2O emissions by DNDC model from sandy loam soils of Danubian Lowland, *J. Environ. Eng. and Landscape Manage.*, *XIV*, 165-171.

Houghton, J. T., B. A. Callander, and S. K. Varney (eds.) (1992), *Climate Change 1992: The supplementary report to the IPCC scientific assessment*, pp. 1-200, Cambridge Univ. Press, Cambridge.

Houghton, J. T., G. J. Jenkins, J. J. Ephraums (1990), *Climate Change: The IPCC scientific assessment*, Cambridge Univ. Press, Cambridge.

Houghton, R. A. (1996), Converting terrestrial ecosystems from sources to sinks of carbon, *Ambio*, *25*(4), 267-272.

Houghton, R. A., et al. (1983), Changes in the carbon content of terrestrial biota and soils between 1860 and 1980: a net release of CO_2 to the atmosphere, *Ecol. Monogr.*, *53*, 235–262.

Hovenden, M. J., et al. (2008), Warming prevents the elevated CO_2-induced reduction in available soil nitrogen in a temperate, perennial grassland, *Global Change Biol.*, *14*, 1018–1024.

Hu, S., F. S. Chapin III, M. K. Firestone, C. B. Field, and N. R. Chiariello (2001), Nitrogen limitation of microbial decomposition in a grassland under elevated CO_2, *Nature*, *409*, 88-191.

Hu, S. J., C. Tu, X. Chen, J. B. Gruver (2006), Progressive N limitation of plant response to elevated CO_2: a microbiological perspective, *Plant Soil*, *289*, 47–58.

Huang, B., G. Chen, G. Huang, and T. Hauro (2003), Nitrous oxide emission from temperate meadow grassland and emission estimation for temperate grassland of China, *Nutr. Cycl. Agroecosys.*, *67*, 31–36.

Hungate, B. A., C. P. Lund, H. L. Pearson, F. S. III Chapin (1997), Elevated CO_2 and nutrient addition alter soil N cycling and N trace gas fluxes with early season wet-up in a California annual grassland, *Biogeochemistry*, *37*, 89-109.

Hungate, B. A., et al. (2006), Nitrogen cycling during seven years of atmospheric CO_2 enrichment in a scrub oak woodland, *Ecology*, *87*, 26–40.

Hungate, B. A., J. S. Dukes, M. R. Shaw, Y. Luo, and C. B. Field (2003), Nitrogen and climate change, *Science*, *302*, 1512–1513.

Hungate, B. A., P. Dijkstra, D. W. Johnson, C. R. Hinkle, B. G, Drake (1999), Elevated CO_2 increases nitrogen fixation and decreases soil nitrogen mineralization in Florida scrub oak, *Global Change Biol.*, *5*, 781–789.

Ineson, P., P. A. Coward, U. A. Hartwig (1998), Soil gas fluxes of N_2O, CH_4 and CO_2 beneath Lolium perenne under elevated CO_2: The Swiss free air carbon dioxide enrichment experiment, *Plant Soil*, *198*, 89–95.

Ingham, R. E., and J. K. Detling (1984), Plant-herbivore interactions in a North American mixed-grass prairie, *Oecologia*, *63*, 307–313.

IPCC (1992), Greenhouse gases: Sources and sinks, in *Climate Change 1992: The supplementary report to the IPCC Scientific Assessment*, edited by R. T. Watson, L. G. Meira Filho, E. Sanhueza, and A. Janetos, pp. 25-46, Cambridge Univ. Press, Cambridge.

IPCC (1996a), *Climate Change 1995: The Science of Climate Change. Contribution of Working Group I to the Second Assessment Report of the Intergovernmental Panel on Climate Change [Houghton, J. T., L. G. Meira Filho, B. A. Callander, N. Harris, A. Kattenberg, and K. Maskell (eds.)]*, pp. 572, Cambridge Univ.Press, Cambridge, U.K. and NY, USA.

IPCC (1996b), *Climate Change 1995: Impacts, Adaptations and Mitigation of Climate Change: Scientific-Technical Analyses. Contribution of working group II to the Second Assessment Report of the Intergovernmental Panel on Climate Change [R. Watson, M.C. Zinyowera, and R. Moss (eds.)]*, pp. 880, Cambridge Univ. Press, Cambridge, U.K.

IPCC (2001), *Climate Change 2001: The Scientific Basis. Contribution of Working Group I to the Third Assessment Report of the Intergovernmental Panel on Climate Change [Houghton, J.T., Y. Ding, D.J. Griggs, M. Noguer, P.J. van der Linden, X. Dai, K. Maskell, and C.A. Johnson (eds.)]*, pp. 881, Cambridge Univ. Press, Cambridge, U.K. and NY, USA.

IPCC (2007), *Climate Change 2007: The Physical Science Basis. Contribution of Working Group I to the Fourth Assessment Report of the Intergovernmental Panel on Climate Change [Solomon, S., D. Qin, M. Manning (eds.)]*, Cambridge Univ. Press, Cambridge, U.K. and NY, USA.

Jain, A. K., X. Yang, H. Kheshgi, A. D. McGuire, W. Post, and D. Kicklighter (2009), Nitrogen attenuation of terrestrial carbon cycle response to global environmental factors, *Global Biogeochem. Cycles*, *23*, GB4028.

Jallow, B. P. (1995), Emissions of greenhouse gases from agriculture, land-use change, and forestry in the Gambia, *Environ. Monito. and Assess.*, *38*, 301-312.

Jenkinson, D. S., R. H. Fox, and J. H. Rayner (1985), Interactions between fertilizer nitrogen and soil nitrogen -the so-called "priming" effect, *J. Soil Sci.*, *36*, 425-444.

Jensen, R. G. (2000), Activation of Rubisco regulates photosynthesis at high temperature and CO_2, *Proc. Natl. Acad. Sci. U. S. A.*, *97*(24), 12937–12938.

Jeuken, A., J. P. Veefkind, F. Dentener, S. Metzger, and C. R. Gonzalez (2001), Simulation of the aerosol optical depth over Europe for August 1997 and a comparison with observations, *J. Geophys. Res.*, *106*(28), 295–311.

Johnson, D. W., B. A. Hungate, P. Dijkstra, G. Hymus, C. R. Hinkle, P. Stiling, and B. G. Drake (2003), The effects of elevated CO_2 on nutrient distribution in a fire-adapted scrub oak forest, *Ecol. Appl.*, *13*, 1388–1399.

Johnson, D. W., et al. (2004), Effects of elevated CO_2 on nutrient cycling in a sweetgum plantation, *Biogeochemistry*, *69*, 379–403.

Jones, D. L., A. Hodge, and Y. Kuzyakov (2004), Plant and mycorrhizal regulation of rhizodeposition, *New Phytologist*, *163*, 459–480.

Jones, D. L., J. R. Healey, V. B. Willett, J. F. Farrar, A. Hodge (2005), Dissolved organic nitrogen uptake by plants - an important N uptake pathway?, *Soil Biol. Biochem.*, *37*(3), 413-423.

Jungclaus, J. H., et al. (2006), Ocean circulation and tropical variability in the coupled model ECHAM5/MPI-OM, *J. Clim.*, *19*(16), 3952–3972.

Jungclaus, J. H., et al. (2010), Climate and carbon-cycle variability over the last millennium, *Clim. Past*, *6*, 723-737.

Kammann, C., C. Müller, L. Grünhage, H-J. Jäger (2008), Elevated CO_2 stimulates N_2O emissions in permanent grassland, *Soil Biol. Biochem.*, *40*, 2194–2205.

Kato, T., A. Ito, and M. Kawamiya (2009), Multiple temporal scale variability during the twentieth century in global carbon dynamics simulated by a coupled climate-terrestrial carbon cycle model, *Clim. Dyn*, *32*, 901–923.

Kaye, J. P., and S. C. Hart (1997), Competition for nitrogen between plants and soil microorganisms, *Trends Ecol. Evol.*, *12*(4), 139-143.

Keller, M., W. A. Kaplan, and S. C. Wofsy (1986), Emissions of N_2O, CH_4 and CO_2 from tropical forest soils, *J. Geophys. Res.*, *91*, 11791-11802.

Kesik, M., et al. (1995), Inventories of N_2O and NO emissions from European forest soils, *Biogeosciences*, *2*, 353-375.

Khalil, K., B. Mary, P. Renault (2004), Nitrous oxide production by nitrification and denitrification in soil aggregates as affected by O_2 concentration, *Soil Biol. Biochem.*, *36*, 687–699.

Kirschbaum, M. U. F., and K. I. Paul (2002), Modelling C and N dynamics in forest soils with a modified version of the CENTURY model, *Soil Biol. Biochem.*, *34*, 341–354.

Kitzler, B., et al. (2006), Controls over N_2O, NO_x and CO_2 fluxes in a calcareous mountain forest soil, *Biogeosciences*, *3*, 383-395.

Knops, J. M. H., and D. Tilman (2000), Dynamics of soil carbon and nitrogen accumulation for 61 years after agricultural abandonment, *Ecology*, *81*, 88–98.

Knops, J. M. H., and K. L. Bradley (2009), Soil carbon and nitrogen accumulation and vertical distribution across a 74-year chronosequence, *Soil Sci. Soc. Am. J.*, *73*, 2096-2104.

Knorr, W. (2000), Annual and interannual CO_2 exchanges of the terrestrial biosphere: process-based simulations and uncertainties, *Global Ecol. Biogeo.*, *9*, 225–252.

Körner, C. (2000), Biosphere responses to CO_2 enrichment, *Ecol. Appl.*, *10*(6), 1590–1619.

Körner, C. (2003), Carbon limitation in trees, *J. Ecol.*, *91*, 4–17.

Körner, C., and J. A. Arnone (1992), Responses to elevated carbon dioxide in artificial tropical ecosystems, *Nature*, *257*, 1672-1675.

Körrner, C. (2009), Responses of humid tropical trees to rising CO_2, *Annu. Rev. Ecol.*, *40*, 61–79.

Kroeze, C. (1994), Nitrous oxide and global warming, *Sci. Total Environ.*, *143*, 193-209.

Kroeze, C., A. Mosier, and L. Bouwman (1999), Closing the Global N_2O Budget: a Retrospective Analysis 1500 - 1994, *Global Biogeochem. Cycles*, *13*(1), 1-8.

Laine, J., et al. (1996), Effect of water level drawdown in northern peatlands on the global climatic warming, *Ambio*, *25*, 179–184.

Lashof, D. A., B. J. DeAngelo, S. R. Saleska, and J. Harte (1997), Terrestrial ecosystem feedbacks to global climate change, *Annu. Rev. Energy Environ.*, *22*, 75–118.

Lauenroth, W. K., and D. G. Milchunas (1992), *Short-grass steppe. In: R.T. Coupland, Editor, Ecosystems of the World 8A, Natural Grasslands, Introduction and Western Hemisphere*, Elsevier, New York, 183–226 (Chapter II).

Lelieveld, J., and F. J. Dentener (2000), What controls tropospheric ozone?, *J. Geophys. Res.*, *105*(D3), 3531-3551.

Lenton, T. M., and N. E. Vaughan (2009), The radiative forcing potential of different climate geoengineering options, *Atmos. Chem. Phys.*, *9*, 5539-5561.

Li, C. S., J. Aber, F. Stange, K. Butterbach-Bahl, and H. Papen (2000), A process-oriented model of N_2O and NO emissions from forest soils: 1. Model development, *J. Geophys. Res.*, *105*, 4369–4384.

Lin, B. L., A. Sakoda, R. Shibasaki, N. Goto, M. Suzuki (2000), Modelling a global biogeochemical nitrogen cycle in terrestrial ecosystems, *Ecol. Model.*, *145*, 89–110.

Lin, S., J. Iqbal, R. Hu, and M. L. Feng (2010), N_2O emissions from different land uses in mid-subtropical China, *Agri. Ecosyst. Environ.*, *136*, 40–48.

Liu, Y. (1996), *Modeling the emissions of nitrous oxide (N_2O) and methane (CH_4) from the terrestrial biosphere to the atmosphere*, Massachusetts Institute of Technology, Dept. of Earth, Atmospheric, and Planetary Sciences, Report No.10.

Loiseau, P., J. F. Soussana (2000), Effects of elevated CO_2, temperature and N fertilization on nitrogen fluxes in a temperate grassland ecosystem, *Global Change Biol.*, *6*, 953–965.

Lu, C., and J. Zhang (2000), Photosynthetic CO_2 assimilation, chlorophyll fluorescence and photo inhibition as affected by nitrogen deficiency in maize plants, *Plant Sci.*, *151*(2), 135–143.

Luizão, F., P. Matson, G. Livingston, R. Luizão, and P. Vitousek (1989), Nitrous oxide flux following tropical land clearing, *Global Biogeochem. Cycles*, *3*(3), 281–285.

Luo, Y., C. B. Field, and R. B. Jackson (2006b), Does nitrogen constrain carbon cycling, or does carbon input stimulate nitrogen cycling?, *Ecology*, *87*, 3-4.

Luo, Y., D. Hui, and D. Zhang (2006a), Elevated CO_2 stimulates net accumulations of carbon and nitrogen in land ecosystems: A meta-analysis, *Ecology*, *87*, 53–63.

Luo, Y., et al. (2004), Progressive nitrogen limitation of ecosystem responses to rising atmospheric CO_2 concentration, *BioScience*, *54*, 731–739.

Machida, T., T. Nakazawa, Y. Fujii, S. Aoki, and O. Watanabe (1995), Increase in the atmospheric nitrous oxide concentration during the last 250 years, *Geophys. Res. Lett.*, *22*(21), 2921–2924.

Martikainen, P., H. Nykänen, J. Alm, J. Silvola (1995), Change in fluxes of carbon dioxide, methane and nitrous oxide due to forest drainage of mire sites of different trophy, *Plant Soil*, *168/169*, 571–577.

Matthews, E. (1997), Global litter production, pools, and turnover times: Estimates from measurement data and regression models, *J. Geophys. Res.*, *102*(D15), 18771-18800.

McElroy, M. B. (1983), *Global Change: A Biogeochemical Perspective*, JPL-Publishers, Pasadena, CA, USA.

McElroy, M. B., J. W. Elkins, S. C. Wofsy, Y. L. Yung (1976), Sources and sinks for atmospheric N_2O, *Rev. Geophy. Space Phy.*, *14*, 143–150.

McElroy, M. B., S. C. Wofsy, and Y. L. Yung (1977), Nitrogen Cycle - Perturbations Due to Man and Their Impact on Atmospheric N_2O and O_3, *Philosophical Transactions of the Royal Society of London Series B-Biological Sciences*, *227*, 159-181.

McGuire, A. D., J. M. Melillo, D. W. Kicklighter, Y. Pan, X. Xiao, J. Helfrich, B. Moore III, C. J. Vorosmarty, and A. L. Schloss (1997), Equilibrium responses of global net primary production and carbon storage to doubled atmospheric carbon dioxide: Sensitivity to changes in vegetation nitrogen concentration, *Global Biogeochem. Cycles*, *11*, 173–189.

McGuire, A. D., J. Melillo, L. Joyce, D. Kicklighter, A. Grace, B. Moore III, and C. Vorosmarty (1992), Interactions between carbon and nitrogen dynamics in estimating net primary productivity for potential vegetation in North America, *Global Biogeochem. Cycles*, *6*(2), 101-124.

McKinley, D. C., J. C. Romero, B. A. Hungate, B. G. Drake, and J. P. Megonigal (2009), Deep soil N availability sustain long-term ecosystem responses to elevated CO_2?, *Global Change Biol.*, *15*, 2035–2048.

McNaughton, S. J. (1976), Serengeti migratory wildbeest: facilitation of energy flow by grazing, *Science*, *191*, 92–94.

McNaughton, S. J. (1985), Ecology of a grazing system: the Serengeti, *Ecol. Monogr.*, *55*, 259–294.

Medlyn, B. E., R. E. McMurtrie, R. C. Dewar, and M. P. Jeffreys (2000), Soil processes dominate the long-term response of forest net primary productivity to increased temperature and atmospheric CO_2 concentration, *Can. J. For. Res.*, *30*, 873–888.

Meixner, T., and R. C. Bales (2003), Hydrochemical Modeling of Coupled C and N Cycling in High-Elevation Catchments: Importance of Snow Cover, *Biogeochemistry*, *62*, 289-308.

Melillo, J. M., A. D. McGuire, D. W. Kicklighter, B. Moore, C. J. Vorosmarty, and A. L. Schloss (1993), Global climate change and terrestrial net primary production, *Nature*, *363*, 234–240.

Melillo, J. M., et al. (2001), Nitrous oxide emissions from forests and pastures of various ages in the Brazilian Amazon, *J. Geophys. Res.*, *106*(34), 179-188.

Melillo, J. M., et al. (2002), Soil warming and carbon cycle feedbacks to the climate system, *Science*, *298*, 2173–2176.

Mengel, K., and E. A. Kirkby (2001), *Principles of Plant Nutrition*, pp. 864, 5th edn. Kluwer Academic Publishers.

Milchunas, D. G., and W. K. Lauenroth (1993), Quantitative effects of grazing on vegetation and soils over a global range of environment, *Ecol. Monogr.*, *63*(4), 327–366.

Minami, K. (1997), Atmospheric methane and nitrous oxide: sources, sinks and strategies for reducing agricultural emissions, *Nutr. Cycl. Agroecosys.*, *49*, 203-211.

Mosier, A. R. (1993), Nitrous Oxide Emissions from Agricultural Soils, *Proceedings: Methane and Nitrous Oxide, "Methods in National Emissions Inventories and Options for Control", RIVM, Netherlands*.

Mosier, A. R. (1998), Soil processes and global change, *Biol. and Fertility of Soils*, *27*, 221–229.

Mosier, A. R., J. A. Morgan, J. Y. King, D. LeCain, D. G. Milchunas (2002), Soil-atmosphere exchange of CH_4, CO_2, NO_x, and N_2O in the Colorado shortgrass steppe under elevated CO_2, *Plant Soil*, *240*, 201–211.

Mosier, A. R., J. M. Duxbury, J. R. Freney, O. Heinemeier, and K. Minami (1996), Nitrous oxide emissions from agricultural fields: assessment, measurement and mitigation, *Plant Soil*, *181*, 95 – 108.

Müller, C., et al. (2009), Effect of elevated CO_2 on soil N dynamics in a temperate grassland soil, *Soil Biol. Biochem.*, *41*, 1996–2001.

Nakicenovic, N., et al. (2000), *Special Report on Emissions Scenarios: A Special Report of Working Group III of the Intergovernmental Panel on Climate Change*, pp. 612, Cambridge Univ. Press, Cambridge, U.K.

Näsholm, T., A. Ekblad, A. Nordin, R. Giesler, M. Hogberg, and P. Hogberg (1998), Boreal forest plants take up organic nitrogen, *Nature*, *392*, 914-916.

Newton, P. C. D., V. Allard, R. A. Carran, M. Lieffering (2006), Impacts of elevated CO_2 on a grassland grazed by sheep: the New Zealand FACE experiment. In: Managed Ecosystems and CO_2. Case Studies, Processes, and Perspectives, Vol. 187 (eds NösbergerJ, LongSP, NorbyRJ, StittM, HendreyGR, BlumH), pp. 157–171, Springer, Berlin-Heidelberg.

NOAA/ESRL, Nitrous Oxide data from the NOAA/ESRL halocarbons in situ program, ftp://ftp.cmdl.noaa.gov/hats/n2o/insituGCs/CATS/global.

Norby, R. J., C. M. Iversen (2006), Nitrogen uptake, distribution, turnover, and efficiency of use in a CO_2-enriched sweetgum forest, *Ecology*, *87*, 5–14.

Norby, R. J., et al. (2005), Forest response to elevated CO_2 is conserved across a broad range of productivity, *Proc. Natl. Acad. Sci. U. S. A.*, *102*(50), 1852–1856.

Nordin, A., P. Högberg, T. Näsholm (2001), Soil nitrogen form and plant nitrogen uptake along a boreal forest productivity gradient, *Oecologia*, *129*(1), 125-132.

Nykänen, H., J. Alm, K. Lång, J. Silvola, and P. J. Martikainen (1995), Emissions of CH_4, N_2O and CO_2 from a virgin fen and a fen drained for grassland in Finland, *J. Biogeography*, *22*, 351–357.

O'Connell, A. M. (1994), Decomposition and nutrient content of litter in a fertilized eucalypt forest, *Biol. and Fertility of Soils*, *17*, 159-166.

Oliver, J. G. J., A. F. Bouman, K. W. Van der Hoek, J. J. M. Berdowski (1998), Global air emission inventories for anthropogenic sources of NO_x, NH_3 and N_2O in 1990, *Environ. Pollut.*, *102*, 135–148.

Oren, R., et al. (2001), Soil fertility limits carbon sequestration by forest ecosystems in a CO_2-enriched atmosphere, *Nature*, *411*, 469–472.

Parton, W. J., A. R. Mosier, D. S. Ojima, D. W. Valentine, D. S. Schimel, K. Weier, and A. E. Kulmala (1996), Generalized model for N_2 and N_2O production from nitrification and denitrification, *Global Biogeochem. Cycles*, *10*(3), 401–412.

Parton, W. J., D. S. Schimel, C. V. Cole, and D. S. Ojima (1987), Analysis of factors controlling soil organic matter levels in Great Plains grasslands, *Soil Sci. Soc. Am. J.*, *51*, 1173–1179.

Parton, W. J., et al. (2001), Generalized model for NO_x and N_2O emissions from soils, *J. Geophys. Res.*, *106*(17), 403–419.

Pastor, J., M. A. Stillwell, and D. Tilman (1987), Little bluestem litter dynamics in Minnesota old fields, *Oecologia*, *72*, 327-330.

Pathak, H. (1999), Emissions of nitrous oxide from soil, *Curr. Sci.*, *77*, 359−369.

Pei, Z., H. Ouyang, C. Zhou, and X. Xu (2003), Fluxes of CO_2, CH_4 and N_2O from alpine grassland in the Tibetan Plateau, *J. Geog. Sci.*, *13*, 27–34.

Pei, Z. Y., H. Ouyang, C. Zhou, and X. Xu (2004), N_2O exchange within a soil and atmosphere profile in alpine grasslands on the Qinghai-Xizang Plateau, *Acta Bot. Sin.*, *46*, 20–28.

Pepper, D. A., et al. (2007), Simulated mechanisms of soil N feedback on the forest CO_2 response, *Global Change Biol.*, *13*, 1265–1281.

Pidwirny, M. J. (2006). The Nitrogen Cycle, *Fundamentals of Physical Geography*, 2nd Edition.

Pilegaard, K., et al. (2006), Nitrogen load and forest type determine the soil emission of nitrogen oxides (NO and N_2O), *Biogeosc. Discuss.*, *3*, 837-869.

Pongratz, J., C. H. Reick, T. Raddatz, and M. Claussen (2009), Effects of anthropogenic land cover change on the carbon cycle of the last millennium, *Global Biogeochem. Cycles*, *23*, GB4001.

Pongratz, J., C. Reick, T. Raddatz, and M. Claussen (2008), A reconstruction of global agricultural areas and land cover for the last millennium, *Global Biogeochem. Cycles*, *22*, GB3018.

Post, W. M., J. Pastor, P. J. Zinke, and A. G. Stangenberger (1985), Global patterns of soil nitrogen storage, *Nature*, *317*, 613–616.

Post, W. M., W. R. Emanuel, P. J. Zinke, and A. G. Stangenberger (1982), Soil carbon pools and world life zones, *Nature*, *298*, 156–159.

Poth, M., I. C. Anderson, H. S. Miranda, A. C. Miranda, and P. J. Riggan (1995), The magnitude and persistence of soil NO, N_2O, CH_4, and CO_2 fluxes from burned tropical savanna in Brazil, *Global Biogeochem. Cycles*, *9*(4), 503–513.

Potter, C. S., P. A. Matson, P. M. Vitousek, and E. A. Davidson (1996), Process modeling of controls on nitrogen trace gas emissions from soils worldwide, *J. Geophys. Res.*, *101*(D1), 1361–1377.

Prather, M., et al. (2001), Atmospheric chemistry and greenhouse gases, in *Climate Change 2001: The Scientific Basis*, edited by J. T. Houghton et al., pp. 239–287, Cambridge Univ. Press, Cambridge, U. K.

Pregitzer, K. S., D. R. Zak, J. Maziasz, J. DeForest, P. S. Curtis (2000), Interactive effects of atmospheric CO_2 and soil-N availability on fine roots of Populus tremuloides, *Ecol. Appl.*, *10*, 18–33.

Prentice, I. C., et al. (2001), The carbon cycle and atmospheric carbon dioxide, in *Climate Change 2001: The Scientific Basis. Contribution of Working Group I to the Third Assessment of the Intergovernmental Panel on Climate Change*, edited by J. Houghton et al., pp. 183–237, Cambridge Univ. Press, New York.

Prescott, C. E. (1995), Does nitrogen availability control rates of litter decomposition in forests?, *Plant Soil*, *168/169*, 83-88.

Prinn, R., et al. (1999), Integrated global system model for climate policy assessment: feedbacks and sensitivity studies, *Clim. Change*, *41*, 469–546.

Raddatz, T. J., C. H. Reick, W. Knorr, J. Kattge, E. Roeckner, R. Schnur, K.G. Schnitzler, P. Wetzel, and J. Jungclaus (2007), Will the tropical land biosphere dominate the climate-carbon cycle feedback during the twenty-first century?, *Clim. Dyn*, *29*, 565–574.

Raich, J., E. Rastetter, J. Melillo, D. W. Kicklighter, P. A. Steudler, B. Peterson, A. Grace, B. Moore III, and C. Vorosmarty (1991), Potential net primary productivity in South America: Application of a global model, *Ecol. Appl.*, *1*(4), 399–429.

Raich, J. W., C. S. Potter (1995), Global patterns of carbon dioxide emissions from soils, *Global Biogeochem. Cycles*, *9*, 23–36.

Read, D. J. (1996), The structure and function of the ericoid mycorrhizal root, *Ann. Bot.*, *77*(4), 365–374.

Reich, P. B., B. A. Hungate, and Y. Luo (2006), Carbon-nitrogen interactions in terrestrial ecosystems in response to rising atmospheric carbon dioxide, *Annu. Rev. Ecol. Evol. Syst.*, *37*, 611–636.

Reich, P. B., D. S. Ellsworth, M. B. Walters, J. M. Vose, C. Gresham, J. C. Volin, W. D. Bowmann (1999), Generality of leaf trait relationships: a test across six biomes, *Ecology*, *80*, 1955–1969.

Roeckner, E. (2009), ENSEMBLES STREAM2 ECHAM5C-MPI-OM SRA1B run3, daily values. World Data Center for Climate. CERA-DB "ENSEMBLES2_MPEH5C_SRA1B_3_D" http://cera-www.dkrz.de/WDCC/ui/Compact.jsp?acronym=ENSEMBLES2_MPEH5C_SRA1B_3_D.

Roeckner, E., et al. (2003), The atmospheric general circulation model ECHAM5. Part I: Model description, Rep. 349, Max Planck Inst. for Meteorol., Hamburg, Germany.

Roeckner, E., M. A. Giorgetta, T. Crueger, M. Esch, and J. Pongratz (2011), Historical and future anthropogenic emission pathways derived from coupled climate-carbon cycle simulations, *Clim. Change*,*105*, 91-108.

Roedenbeck, C., S. Houweling, M. Gloor, M. Heimann (2003), CO_2 flux history 1982–2001 inferred from atmospheric data using a global inversion of atmospheric transport, *Atmos. Chem. Phys. Discuss.*, *3*, 2575–2659.

Rosswall, T. (1982), Microbiological regulation of the biogeochemical nitrogen cycle, *Plant Soil*, *67*, 15–34.

Rütting, T., T. J. Clough, C. Müller, M. Lieffering, and P. C. D. Newton (2010), Ten years of elevated atmospheric carbon dioxide alters soil nitrogen transformations in a sheep-grazed pasture, *Global Change Biol.*, *16*, 2530–2542.

Sala, O. E., W. K. Lauenroth, and I. C. Burke (1996), Carbon budgets of temperate grasslands and the effects of global change, In: A. I. Breymeyer, D. O. Hall, J. M. Melillo and G. I. Ågren, Editors, Global Change: Effects on Coniferous Forests and Grasslands, John Wiley & Sons Ltd., Chichester, pp. 101–120.

Sampson, R. N., et al. (1993), Workshop Summary Statement - Terrestrial Biospheric Carbon Fluxes - Quantification of Sinks and Sources of CO_2, *Water Air and Soil Pollution*, *70*, 3-15.

Sanhueza, E., L. Cárdenas, L. Donoso, and M. Santana (1994), Effect of plowing on CO_2, CO, CH_4, N_2O, and NO fluxes from tropical savannah soils, *J. Geophys. Res.*, *99*(D8), 16429–16434.

Saugier, B., and J. Roy (2001), Estimations of global terrestrial productivity: Converging towards a single number?, in *Global Terrestrial Productivity: Past, Present and Future*, edited by H. Mooney, J. Roy, and B. Saugier, Academic, San Diego, Calif.

Scheffer, M., V. Brovkin, and P. M. Cox (2006), Positive feedback between global warming and atmospheric CO_2 concentration inferred from past climate change, *J. Geophys. Res.*, *33*, L10702.

Schimel, D. S., B. Braswell, R. McKeown, D. Ojima, W. Parton, and W. Pulliam (1996), Climate and nitrogen controls on the geography and timescales of terrestrial biogeochemical cycling, *Global Biogeochem. Cycles*, *10*, 677–692.

Schimel, J. P., and J. Bennett (2004), Nitrogen mineralization: Challenges of a changing paradigm, *Ecology*, *85*, 591–602.

Schmid, M., A. Neftel, M. Riedo, and J. Fuhrer (2001), Process-based modelling of nitrous oxide emissions from different nitrogen sources in mown grassland, *Nutr. Cycl. Agroecosys.*, *60*, 177–187.

Schulze, E. D. (2000), *Carbon and Nitrogen Cycling in European Forest Ecosystems*, 500 pp., Springer, Berlin.

Scurlock, J. M. O., W. Cramer, R. J. Olson, W. J. Parton, and S. D. Prince (1999), Terrestrial NPP: Toward a consistent data set for global model evaluation, *Ecol. Appl.*, *9*, 913–919.

Seitzinger, S., et al. (2006), Denitrification across landscapes and waterscapes: a synthesis, *Ecol. Appl.*, *16*, 2064–2090.

Silva, R. G., E. E. Jorgensen, S. M. Holub, and M. E. Gonsoulin (2005), Relationships between culturable soil microbial populations and gross nitrogen transformation processes in a clay loam soil across ecosystems, *Nutr. Cycl. Agroecosys.*, *71*, 259–270.

Skiba, U., and K. A. Smith (2000), The control of nitrous oxide emissions from agricultural and natural soils, *Chemosphere*, *2*, 379-386.

Skiba, U., C. Pitcairn, L. Sheppard, V. Kennedy, and D. Fowler (2004), The influence of atmospheric N deposition on nitrous oxide and nitric oxide fluxes and soil ammonium and nitrate concentrations, Water, Air and Soil Pollution, *Focus*, *4*, 37–43.

Smith, S. E., and D. J. Read (1997), *Mycorrhizal symbiosis*, 605 pp, Academic press, San Diego.

Sokolov, A. P., D. W. Kicklighter, J. M. Melillo, B. S. Felzer, C. A. Schlosser, and T. W. Cronin (2008), Consequences of considering carbon-nitrogen interactions on the feedbacks between climate and the terrestrial carbon cycle, *J. Clim.*, *21*, 3776–3796.

Sommerfeld, R., A. Mosier, R. Musselman (1993), CO_2, CH_4 and N_2O flux through a Wyoming snowpack and implications for global budgets, *Nature*, *361*, 140–142.

Sprugel, D. G., M. G. Ryan, J. R. Brooks, K. A. Vogt, and T. A. Martin (1996), Respiration from the organ level to the stand, in *Resource Physiology of Conifers*, edited by K. Smith and T. M. Hinckley, pp. 255–299, Academic, San Diego, Calif.

Stange, C. F., and H.U. Neue (2009), Seasonal variation of gross nitrification rates at three differently treated long-term fertilisations sites, *Biogeosc. Discuss.*, *6*, 1565-1598.

Stover, D. B., et al. (2007), Effect of elevated CO_2 on coarse-root biomass in Florida scrub detected by ground-penetrating radar, *Ecology*, *88*, 1328–1334.

Sydes, C. L. (1984), A comparative study of leaf demography in limestone grassland, *J. Ecol.*, *72*, 331-345.

Szukics, U., et al. (2010), Nitrifiers and denitrifiers respond rapidly to changed moisture and increasing temperature in a pristine forest soil, *FEMS Microbiol. Ecol.*, *72*, 395–406.

Tamm, C. O. (1992), *Nitrogen in terrestrial ecosystems*, Ecological Studies 81, 115, Springer, New York.

Tanner, E. V. J., P. M. Vitousek, and E. Cuevas (1998), Experimental investigation of nutrient limitation of forest growth on wet tropical mountains, *Ecology*, *79*, 10–22.

Taylor, B. R., D. Parkinson, and W. F. J. Parsons (1989), Nitrogen and lignin content as predictors of litter decay rates: a microcosm test, *Ecology*, *70*, 97-104.

Theodorou, C., and G. D. Bowen (1990), Effects of fertilizer on litterfall and nitrogen and phosphorus release from decomposing litter in a Pinus radiata plantation, *For. Ecol. Manage.*, *32*, 87-102.

Thompson, T. M., et al. (2004), Halocarbons and other atmospheric trace species, in *Climate Monitoring Diagnostics Lab. Summary Rep. 27, 2002-2003*, edited by R. C. Schnell, A. M. Buggle, and R. M. Rosson, pp. 115-135, U.S. Dept. of Commerce., Boulder, Colo.

Thornton, P. E., et al. (2009), Carbon-nitrogen interactions regulate climate–carbon cycle feedbacks: Results from an atmosphere-ocean general circulation model, *Biogeosc. Discuss.*, *6*, 3303–3354.

Thornton, P. E., J. F. Lamarque, N. A. Rosenbloom, and N. M. Mahowald (2007), Inclusion of carbon-nitrogen cycle coupling on land model response to CO_2 fertilization and climate variability, *Global Biogeochem. Cycles*, *21*, GB4018.

Tjoelker, M. G., J. M. Craine, D. Wedin, P. B. Reich, D. Tilman (2005), Linking leaf and root trait syndromes among 39 grassland and savannah species, *New Phytologist*, *167*, 493–508.

Torn, M. S., and J. Harte (2006), Missing feedbacks, asymmetric uncertainties, and the underestimation of future warming, *Geophys. Res. Lett.*, *33*, L10703.

van Aardenne, J. A., F. J. Dentener, J. G. J. Olivier, C. G. M. K. Goldewijk, and J. Lelieveld (2001), A 1°×1° resolution data set of historical anthropogenic trace gas emissions for the period 1890–1990, *Global Biogeochem. Cycles*, *15*(4), 909–928.

Van Amstel, A. R., and R. J. Swart (1994), Methane and nitrous oxide emissions: an introduction, *Fertilizer Res.*, *37*, 213-225.

Van Groenigen, K.-J., M-A. De Graaff, J. Six, D. Harris, P. Kuikman, C. Van Kessel (2006), *The impact of elevated atmospheric [CO_2] on soil C and N dyanamics: a meta-analysis. In: Managed Ecosystems and CO_2 Case Studies, Processes, and Perspectives, Vol. 187* (eds Nösberger J, Long SP, Norby RJ, Stitt M, Hendrey GR, Blum H), pp. 373–391. Springer, Berlin-Heidelberg.

Venterea, R. T., et al. (2003), Nitrogen oxide gas emissions from temperate forest soils receiving long-term nitrogen inputs, *Global Change Biol.*, *9*, 346–357.

Verchot, L. V., E. A. Davidson, H. Cattânio, I. L. Ackerman, H. E. Erickson, and M. Keller (1999), Land use change and biogeochemical controls of nitrogen oxide emissions from soils in eastern Amazonia, *Global Biogeochem. Cycles*, *13*(1), 31–46.

Vitousek, P. M., and R. W. Howarth (1991), Nitrogen limitation on land and in the sea: How it can occur, *Biogeochemistry*, *13*, 87–115.

Vitousek, P. M., and S, Hobbie (2000), Heterotrophic nitrogen fixation in decomposing litter: patterns and regulation, *Ecology*, *81*, 2366–2376.

Vitousek, P. M., H. A. Mooney, J. Lubchenco, and J. M. Melillo (1997), Human domination of earth's ecosystems, *Science*, *277*, 494–499.

Vitousek, P. M., T. Fahey, D. W. Johnson, and M. J. Swift (1988), Element interactions in forest ecosystems: Succession, allometry and input-output budgets, *Biogeochemistry*, *5*, 7–34.

Wallenda, T., and D. J. Read (1999), Kinetics of amino acids uptake by ectomycorrhizal roots, *Plant cell Envrion.*, *22*, 179-187.

Wang, J. G., and L. R. Bakken (1997), Competition for nitrogen during mineralization of plant residues in soil: Microbial response to C and N, *Soil Biol. Biochem.*, *29*(2), 163-170.

Wang, Y. P., R. M. Law, and B. Pak (2010), A global model of carbon, nitrogen and phosphorus cycles for the terrestrial biosphere, *Biogeosciences*, *7*, 2261-2282.

Warren, C. R., E. Dreyer, M. A. Adams (2003), Photosynthesis-Rubisco relationships in foliage of Pinus sylvestris in response to nitrogen supply and the proposed role of Rubisco and amino acids as nitrogen stores, *Trees Struct. Funct.*, *17*(4), 359-366.

Watson, R. T., et al. (1992), Sources and sinks, in *Climate Change 1992, The Supplementary Report to the IPCC Scientific Assessment*, edited by J. T. Houghton, et al., pp. 25–46, Cambridge Univ. Press, Cambridge.

Wedin, D. A., and D. Tilman (1996), Influence of nitrogen loading and species composition on the carbon balance of grasslands, *Science*, *274*, 1720–1723.

Well, R., J. Augustin, K. Meyer, D. D. Myrold (2003), Comparison of field and laboratory measurement of denitrification and N_2O production in the saturated zone of hydromorphic soils, *Soil Biol. Biochem.*, *35*, 783–799.

Werner, C., et al. (2006), N_2O, CH_4 and CO_2 emissions from seasonal tropical rain forests and a rubber plantation in Southwest China, *Plant Soil*, *289*, 335–353.

Werner, C., K. Butterbach-Bahl, E. Haas, T. Hickler, and R. Kiese (2007), A global inventory of N_2O emissions from tropical rainforest soils using a detailed biogeochemical model, *Global Biogeochem. Cycles*, *21*, GB3010.

White, M. A., P. E. Thornton, S. W. Running, and R. R. Nemani (2000), Parameterization and sensitivity analysis of the BIOME–BGC terrestrial ecosystem model: Net primary production controls, *Earth Interact.*, *4*, 1-85.

Winjum, J. K., S. Brown, and B. Schlamadinger (1998), Forest harvests and wood products: sources and sinks of atmospheric carbon dioxide, *Forest Sci.*, *44*(2), 272-284.

Wolf, A., et al. (2011), Forest biomass allometry in global surface models, *in press*.

Wright, I. J., P. B. Reich, M. Westoby, D. D. Ackerly, Z. Baruch, F. Bongers (2004), The worldwide leaf economics spectrum, *Nature*, *428*, 821-827.

Xu-Ri, and I. C. Prentice (2008), Terrestrial nitrogen cycle simulation with a dynamic global vegetation model, *Global Biogeochem. Cycles*, *14*, 1745–1764.

Xu, X., H. Tian, and D. Hui (2008), Convergence in the relationship of CO_2 and N_2O exchanges between soil and atmosphere within terrestrial ecosystems, *Global Change Biol.*, *14*, 1651–1660.

Yang, X., V. Wittig, A. K. Jain, and W. M. Post (2009), Integration of nitrogen cycle dynamics into the Integrated Science Assessment Model for the study of terrestrial ecosystem responses to global change, *Global Biogeochem. Cycles*, *23*, GB4029.

Yates, L. R., P. W. Rundel, R. Sylvester-Bradely, and R. E. Cisternas (1982), Report of the work group on savannas and shrublands, *Plant Soil*, *67*, 409–413.

Zaehle, S., A. D. Friend, P. Friedlingstein, F. Dentener, P. Peylin, M. Schulz (2010b), Carbon and nitrogen cycle dynamics in the O-CN land surface model: 2. The role of the nitrogen cycle in the historical terrestrial C balance, *Global Biogeochem. Cycles*, *24*, GB1006.

Zaehle, S., and A. D. Friend (2010a), Carbon and nitrogen cycle dynamics in the O-CN land surface model: 1. Model description, site-scale evaluation, and sensitivity to parameter estimates, *Global Biogeochem. Cycles*, *24*, GB1005.

Zaehle, S., P. Friedlingstein, and A. D. Friend (2010c), Terrestrial nitrogen feedbacks may accelerate future climate change, *Geophys. Res. Lett.*, *37*, L01401.

Zak, D. R., K. S. Pregitzer, J. S. King, W. E. Holmes (2000), Elevated atmospheric CO_2, fine roots and the response of soil microorganisms: a review and hypothesis, *New Phytologist*, *147*, 201-222.

Zhang, F., J. Qi, F. M. Li, C. S. Li, and C. B. Li (2010), Quantifying nitrous oxide emissions from Chinese grasslands with a process-based model, *Biogeosc. Discuss.*, *7*, 1675-1706.

Zinke, P. J., A. G. Stangenberger, W. M. Post, W. R. Emanuel, and J. S. Olson (1984), *Worldwide Organic Soil Carbon and Nitrogen Data*, ORNL/TM–8857, Oak Ridge National Laboratory, Oak Ridge, TN, USA.

Acknowledgements

I would like to express my gratitude to my supervisors, Prof. Dr. Martin Claussen, Dr. Christian Reick, and Dr. Jens Kattege for their scientific advice, guidance, critical comments, and the continuous support throughout the years. I am very grateful to Dr. Victor Brovkin for the scientific discussions of this work, for his time, interest, and fruitful input. I am also thankful to Dr. Thomas Raddatz for helping me to understand the JSBACH model and for answering all the basic questions and sharing with me his ideas. Special thanks go to Veronika Gayler and Reiner Schnur for the technical support during my work. I am grateful to Katharina Six for providing the N_2O data for the Ocean.

I am glad to be a member of the International Max Planck Research School on Earth System Modelling (IMPRS-ESM). I am thankful to Antje Weitz, Cornelia Kampmann, and Barbara Zinecker for their continuous support, both administratively and morally. It was an immense experience to be part of the IMPRS-ESM PhD program!

I would like to thank all my colleagues Robert, Daniel, Helge, Julia, Juliane, Swati, Anne, Sebastian, Sajjad, Freja, Armelle, and Natalia for their cooperation throughout the years. Special thanks go to my friends Bakim and Brijesh for their continuous moral support.

I am also thankful to my parents for their support, and encouragement all these years. Last but not least, I would like to thank to my wife Nandita for her motivations and inspirations.



ISSN 1614-1199